

THE ROLE OF BDNF IN THE SURVIVAL AND MORPHOLOGICAL
DEVELOPMENT OF ADULT-BORN OLFACTORY NEURONS

by

Brittnee McDole

A Dissertation Submitted to the Faculty of

The Charles E. Schmidt College of Science

In Partial Fulfillment of the Requirements for the Degree of

Doctor of Philosophy

Florida Atlantic University

Boca Raton, FL

December 2018

Copyright 2018 by Brittnee McDole

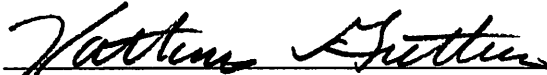
THE ROLE OF BDNF IN THE SURVIVAL AND MORPHOLOGICAL
DEVELOPMENT OF ADULT-BORN OLFACTORY NEURONS

by

Brittnee McDole

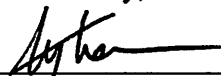
This dissertation was prepared under the direction of the candidate's dissertation advisor, Dr. Kathleen Guthrie, Department of Biomedical Sciences, and has been approved by the members of her supervisory committee. It was submitted to the faculty of the Charles E. Schmidt College of Science and was accepted in partial fulfillment of the requirements for the degree of Doctor of Philosophy.


SUPERVISORY COMMITTEE:

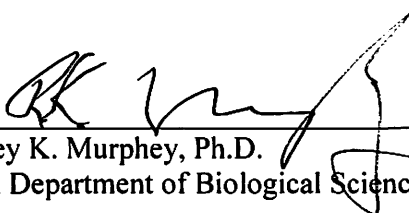

Kathleen Guthrie, Ph.D.


Dissertation Advisor



Ken Dawson-Scully, Ph.D.



Ceylan Isgor, Ph.D.


Robert W. Stackman, Ph.D.


Rodney K. Murphey, Ph.D.
Chair, Department of Biological Sciences


Ata Sarajedini, Ph.D.
Dean, Charles E. Schmidt College of
Science


Khaled Sobhan, Ph.D.
Interim Dean, Graduate College


Date

ACKNOWLEDGEMENTS

I would like to thank my committee members, Dr. Ken Dawson-Scully, Dr. Ceylan Isgor, and Dr. Robert W. Stackman for their guidance and invaluable input in the preparation of this dissertation. I would also like to acknowledge my adviser, Dr. Kathleen Guthrie for her mentorship and support through graduate school. Thank you!

I would like to thank all my past and current colleagues in our lab for always being willing to help, and especially Crystal Gilkes for her countless attendance at 6am surgeries and her selflessness in providing me with any help I needed that allowed me to complete my project. I am forever in your debt!

I would like to thank my family and friends for their overwhelming support and understanding. I would especially like to acknowledge my mother, thank you for believing in me and providing me with the strength and encouragement I needed to succeed.

I would like to thank the National Institutes of Health for the support provided by grant NIH: DC012425

ABSTRACT

Author: Brittnee McDole

Title: The role of BDNF in the survival and morphological development of adult-born olfactory neurons

Institution: Florida Atlantic University

Dissertation Advisor: Dr. Kathleen Guthrie

Degree: Doctor of Philosophy

Year: 2018

Olfactory Granule cells (GCs) are a population of inhibitory interneurons responsible for maintaining normal olfactory bulb (OB) function and circuitry. Through dendrodendritic synapses with the OBs projection neurons, the GCs regulate information sent to the olfactory cortices. Throughout adulthood, GCs continue to integrate into the OB and contribute to olfactory circuitry. However, only ~50% will integrate and survive long-term. Factors aiding in the survival and morphological development of these neurons are still being explored. The neurotrophin brain-derived neurotrophic factor (BDNF) aids in the survival and dendritic spine maturation/maintenance in several populations of CNS neurons. Investigators show that increasing BDNF in the adult-rodent SVZ stimulates proliferation and increases numbers of new OB GCs. However, attempts to replicate these experiments failed to find that BDNF affects proliferation or survival of adult-born granule cells (abGCs). BDNFs regulation of dendritic spines in the CNS is well characterized. In the OB, absence of BDNF's receptor on abGCs hinders normal spine development and

demonstrates a role for BDNF /TrkB signaling in abGCs development. In this study, we use transgenic mice over-expressing endogenous BDNF in the OB (TgBDNF) to determine how sustained increased in BDNF affect the morphology of olfactory GCs and the survival and development of abGCs. Using protein assays, we discovered that TgBDNF mice have higher BDNF protein levels in their OB. We employed a Golgi-cox staining technique to show that increased BDNF expression leads to an increase in dendritic spines, mainly the mature, headed-type spine on OB GCs. With cell birth-dating using 5-bromo-2'-deoxyuridine (BrdU), immunofluorescent cell markers, TUNEL staining and confocal microscopy, we demonstrate that over-expression of BDNF in the OB does not increase survival of abGCs or reduce cell death in the GC population. Using virally labeled abGCs, we concluded that abGCs in TgBDNF mice had similar integration patterns compared to wild-type (WT) mice, but maintained increases in apical headed-type spine density from 12 to 60 days PI. The evidence combined demonstrates that although increased BDNF does not promote cell survival, BDNF modifies GC morphology and abGC development through its regulation of dendritic spine development, maturation and maintenance *in vivo*.

DEDICATION

This manuscript is dedicated to my best-friend and mother, Pamela McDole.

THE ROLE OF BDNF IN THE SURVIVAL AND MORPHOLOGICAL DEVELOPMENT OF ADULT-BORN OLFACTORY NEURONS

FIGURES	xiii
ABBREVIATIONS	xv
PART I: INTRODUCTION.....	1
1.1 Olfactory Bulb Anatomy and Circuitry	1
1.2 Adult Neurogenesis.....	4
1.2.1 Subventricular zone	5
1.3 Integration of adult born olfactory granule cells.....	6
1.4 Neurotrophic Factors	10
1.4.1 Brain-Derived Neurotrophic Factor in the CNS	11
1.5 BDNF's role in adult neurogenesis.....	14
1.7 BDNF's role in dendrite and spine morphology.....	16
1.9 Mouse background.....	19
1.8 Dissertation aims and objectives.....	19
1.9.1 Chapter 2.....	20
1.9.2 Chapter 3	21
1.9.3 Chapter 4.....	21

PART II: BDNF OVER-EXPRESSION INCREASES OLFACTORY BULB GRANULE CELL DENDRITIC SPINE IN VIVO.....	23
2.1 Abstract	23
2.2 Introduction.....	24
2.3 Materials Methods	28
2.3.1 Animals	28
2.3.2 BDNF Enzyme-Linked Immunosorbent Assay (ELISA)	29
2.3.3 Western blotting.....	30
2.3.4 Golgi–Cox staining	31
2.3.5 Analyses of dendritic morphology.....	32
2.3.6 Analyses of dendritic spines	34
2.4 Results.....	35
2.4.1 BDNF protein levels are increased in the transgenic olfactory bulb	35
2.4.2 GC dendritic lengths and branch complexity.....	36
2.4.3 Over-expression of BDNF by GCs increases their dendritic spine number and density	37
2.4.4 BDNF-mediated changes in spine density occur in proximal and distal dendritic domains.....	38
2.5 Discussion	39
PART III: OVER-EXPRESSION OF BDNF IN THE OLFACTORY BULB DOES NOT INCREASE ADULT-BORN GRANULE CELL SURVIVAL	46

3.1 Abstract	46
3.2 Introduction.....	47
3.3 Materials and methods	50
3.3.1 Animals	50
3.3.2 BrdU injections	51
3.3.3 Immunofluorescence.....	52
3.3.4 Imaging	52
3.3.5 Terminal deoxynucleotidyl transferase dUTP nick end labeling (TUNEL).....	53
3.4 Results.....	54
3.5 Discussion	55
 PART IV- VIRAL-MEDIATED LABELING AND MORPHOMETRIC ANALYSIS OF ADULT-BORN GRANULE CELLS IN TGBDNF MICE.....	
4.1 Abstract	60
4.2 Introduction.....	61
4.3 Materials and methods	65
4.3.1 Lentiviral injections	65
4.3.2 Image collection.....	66
4.3.3 Reconstruction and criteria	66
4.3.5 Analyses	67

4.4 Results	68
4.4.1 General granule cell morphology.....	68
4.4.2 Adult-born granule cell dendritic lengths and branch points.....	69
4.4.3 Over-expression of BDNF by abGCs increases their dendritic spine number	69
4.4.4 Over-expression of BDNF by abGCs increases their dendritic spine density	72
4.5 Discussion	78
PART V- GENERAL DISCUSSION	84
5.1 Thesis overview	84
5.2 Key findings.....	86
5.2.1 Chapter 2.....	86
5.2.2 Chapter 3.....	87
5.2.3 Chapter 4.....	88
5.3 Study Limitations.....	89
5.3.1- Chapter 2 limitations	89
5.3.1.1 – Existing or adult-born granule cell	89
5.3.1.2- Time constraints	89
Chapter 5.3.2- Chapter 3 limitations.....	90
5.3.2.1- BrdU	90

5.3.3- Chapter 4 limitations	91
5.3.3.1 Granule cell numbers per experimental animals.....	91
5.3.3.2 - Imaging different neurons	92
5.4 Future Directions	92
5.4.1- Periglomerular cells.....	92
5.4.2- Behavior.....	93
5.4.3- Live animal imaging.....	94
5.5 Concluding remarks	94
PART VI- REFERENCES.....	126

LIST OF FIGURES

Figure 1. Olfactory bulb neuronal circuitry organization	96
Figure 2. Histology and laminar organization of the mouse OB.....	97
Figure 3. Reciprocal dendrodendritic synapse.....	98
Figure 4. Migration pattern of abGCs.....	99
Figure 5. The time course and stages of migration and differentiation of abGCs.....	100
Figure 6. TrkB signaling pathways.....	101
Figure 7. Trk-mediated structural remodeling of spines.....	102
Figure 8. BDNF mRNA levels in TgBDNF mice.....	103
Figure 9. Examples of Golgi-Cox impregnated GCs.....	104
Figure 10. ELISA and Western blot BDNF protein analysis.....	105
Figure 11. Reconstructions of Golgi-Cox labeled GCs.....	106
Figure 12. GC length and apical dendritic intersection comparison.....	107
Figure 13. Analyses of GC spine numbers.....	108
Figure 14. Spine type proportions.....	109
Figure 15. Analysis of GC spine density.....	110
Figure 16. BrdU+/NeuN+ confocal imaging and survival analysis.....	111
Figure 17. TUNEL labeling and cell death analysis.....	112
Figure 18. Virally labeled abGC spines.....	113
Figure 19. Examples of virally labeled abGCs.....	114
Figure 20. Reconstructions of virally labeled abGCs.....	115

Figure 21. Dendritic lengths of abGCs.....	116
Figure 22. Dendritic branching of abGCs.....	117
Figure 23. AbGC cell spine development patterns (spine number)	118
Figure 24 AbGC total spine numbers.....	119
Figure 25. AbGC headed spine numbers.....	120
Figure 26. Analysis of total spine density on abGCs.....	121
Figure 27. Analysis of headed spine density on abGCs.....	122
Figure 28. Segment analysis of abGC total dendritic spines.....	123
Figure 29. Segment analysis of abGC headed dendritic spines.....	124
Figure 30. Spine type density proportions in abGCs.....	125

ABBREVIATIONS

abGCs, adult-born granule cells

AKT, protein kinase B

AON, anterior olfactory nucleus

BDNF, brain-derived neurotrophic factor

BrdU, bromodeoxyuridine

BTC, Betecellulin

CaMKII α , calcium/calmodulin-dependent protein kinase II-alpha promoter

CNS, central nervous system

CREB, CRE binding protein

CREs, calcium response elements

CTGF, connective tissue growth factor

dpi, days post infection

EGF, epidermal growth factor

EPL, external plexiform layer

ERK1/ERK2, extracellular signal-regulated kinases 1 and 2

FGF, fibroblast growth factor

GABA, gamma-aminobutyric

GCL, granule cell layer

GCs, granule cells

GFAP, glial fibrillary acidic protein

GFP, green fluorescent protein

GL, glomerular layer

LTP, long-term potentiation

MCL, mitral cell layer

MTCs, mitral and tufted cells

NGF, nerve growth factor

NT3, neurotrophin 3

NT4/5, neurotrophin 4/5

OB, olfactory bulb

OSN, olfactory sensory neurons

PB, phosphate buffer

PBS, phosphate-buffered saline

PG, periglomerular

PLC γ , phospholipase C- γ

PNS, peripheral nervous system

PSA-NCAM, polysialylated form of neuronal cell adhesion molecule

RMS, rostral migratory stream

RT, room temperature

SA, short axon

SEM, standard error of the mean

SVZ, subventricular zone

TBS, Tris-buffered saline

TBST, TBS + 0.1% Tween-20

TC, Tufted cells

TgBDNF, transgenic BDNF

Trk, tropomyosin receptor kinase

TUNEL, terminal deoxynucleotidyl transferase dUTP nick end labeling

UTR, untranslated regions

VEGF, vascular endothelial growth factor

WT, Wild-type

PART I: INTRODUCTION

1.1 Olfactory Bulb Anatomy and Circuitry

Olfaction in rodents starts in the main olfactory epithelium of the nasal cavity, where odor receptors expressed by olfactory sensory neurons (OSN) bind to odorant molecules. OSN axons travel through the cribriform plate towards the olfactory bulb (OB), and axons of OSNs expressing the same odor receptor converge topographically in glomeruli. A glomerulus is a spherical structure composed of the dendrites and axons of OB neurons and sensory neurons. Glomeruli form a layer in the outer portion of the OB, and here the processing of incoming olfactory information begins (Figure 1). Glomeruli are odor-tuned due to their receiving input from OSNs expressing the same odorant receptor gene. Within the glomerulus different neuronal types extend dendrites that are contacted by axons of the OSN's (Adipietro, Mainland and Matsunami, 2012; Lodovichi and Belluscio, 2012; Imai, 2014; Nagayama, Homma and Imamura, 2014).

Glomeruli contain the primary apical dendrites of the major OB glutamatergic projection neurons, the mitral and tufted cells (MTCs). In the glomeruli, MTCs receive sensory input directly from OSN axons (Mori, Nowycky and Shepherd, 1981). Tufted cells (TC) can be divided into at least three subtypes (Nagayama, Homma and Imamura, 2014). One population, the external TCs, is within the glomerular layer (GL). These possess axons that project within the bulb, and do not terminate beyond the OB. Middle and deep TCs sit within the external plexiform layer (EPL) and possess a single primary apical dendrite that branches within a glomerulus, as well as secondary dendrites that extend laterally in the

EPL. MC and deep TCs project axons to higher olfactory forebrain areas including the anterior olfactory nucleus (AON) and the piriform cortex (Mori, Nagao and Yoshihara, 1999; Imai, 2014; Nagayama, Homma and Imamura, 2014). MCs are the OB's chief glutamatergic projection neurons. Their cell bodies form the mitral cell layer (MCL), and each extends a single primary apical dendrite through the EPL and into a single glomerulus where it branches into a dendritic tuft. OSN axons synapse on this portion of the dendrite. Similar to the deeper TCs, MCs have secondary dendrites that extend laterally into the deeper portions of the EPL. Sensory information received by the MCs is relayed to all areas of the olfactory cortex through their axon projections (Mori, Nagao and Yoshihara, 1999; Imai, 2014; Nagayama, Homma and Imamura, 2014). Multiple populations of bulb inhibitory interneurons, as well as centrifugal inputs, control the functional activity of the MTCs. Figure 2 illustrates the laminar organization of the rodent main OB.

Periglomerular (PG) cells are a mixed population of inhibitory interneurons located within the GL of the bulb. PG cell dendrites extend into a single glomerulus and are contacted by OSN axons, centrifugal fibers, dendrites of output neurons, and axons from other interneurons (Nagayama, Homma and Imamura, 2014). Originally thought to have only produced the neurotransmitter gamma-aminobutyric (GABA), subpopulations also express dopamine (M. C. Whitman and Greer, 2007; Kosaka and Kosaka, 2008; Nagayama, Homma and Imamura, 2014). PG cells also can be divided into neurochemical subtypes based on the expression of calbindin, calretinin and parvalbumin, subtypes of calcium binding proteins. Although diverse, almost all PG cells possess an axon that terminates on dendrites of other bulb neurons in the interglomerular space and they rarely extend their dendrites into more than one glomerulus (Nagayama, Homma and Imamura,

2014). PG cells act to mediate lateral inhibition in the GL via their axon projections that inhibit nearby glomerular activity via the primary dendrites of the output neurons they contact. Short axon (SA) cells are another diverse population of OB interneurons and are present throughout all OB layers (Nagayama, Homma and Imamura, 2014). These GABAergic cells regulate the activity of both GCs and the excitatory output neurons and are not yet fully characterized (Burton and Urban, 2015; Burton, 2017). For the purpose of this dissertation, these SA cells will not be further discussed.

Granule cells (GCs) are the largest population of inhibitory interneurons in the main OB. All GCs produce the neurotransmitter GABA and can be divided into subpopulations based on cell body position in the GC layer (GCL), as well as the arborization pattern of their apical dendrite (Nowycky, Mori and Shepherd, 1981; Nagayama, Homma and Imamura, 2014). GCs possess no axons but extend short basal dendrites as well as their apical dendrite. Distal portions of the apical dendrite in the EPL possess spines that form synapses with the lateral dendrites of MTCs. The majority of the GC-MTC synapses located in the EPL are reciprocal dendrodendritic synapses (Shepherd *et al.*, 2007; Nagayama, Homma and Imamura, 2014; Bartel *et al.*, 2015). The dendrodendritic synapse is a unique synapse in which the neurotransmitters glutamate and GABA are released in a reciprocal fashion (Figure 3). OSN activation of MTC primary dendrites causes glutamate release from the lateral dendrite-located presynaptic zone onto spine-located glutamate receptors in the postsynaptic GC. This then triggers activated GCs to release their presynaptic GABA back onto GABA receptors on the postsynaptic side of the lateral dendrite synapse of the MTCs, mediating feedback inhibition. Activated GCs also release GABA at reciprocal synapses located on the secondary dendrites of surrounding projection

neurons, mediating lateral inhibition throughout the EPL (Imai, 2014; Bartel *et al.*, 2015). This inhibition operates to reduce surrounding activity in the mitral cell population in order to heighten the signal being relayed by strongly odor-stimulated MTCs to the olfactory cortex.

Through GC inhibitory interactions with the MTCs, GCs are responsible for modifying the sensory information relayed to the higher olfactory areas. Disruption of GABAergic interneuron function can lead to disturbances in OB network function and in olfactory behaviors (Nusser *et al.*, 2001; Strowbridge, 2010). Reducing GC inhibition of MCs results in weaker odor discrimination ability while increasing GC inhibition can enhance discrimination ability (Abraham *et al.*, 2010; Nunes and Kuner, 2015). Similarly, by using knockout mice to inhibit normal dendritic branching in a select subpopulation of GCs, Takahashi *et al.*, (2016) have demonstrated that both normal odor discrimination and odor detection are disrupted by the resulting changes in their connectivity. Although the OB continues to incorporate new GCs throughout adulthood, the bulk of the GC population is generated during the first few postnatal weeks (Brunjes and Frazier, 1986). Unlike the 50% loss of adult-born granule cells (abGCs), almost all these early generated GCs survive and remain stably incorporated in the outer portion of the GCL (Lemasson *et al.*, 2005). As shown by Imayoshi *et al.*, (2008), most of the adult replacement of pre-existing GCs with new abGCs occurs in the deeper half of the GCL.

1.2 Adult Neurogenesis

The adult mammalian brain was originally thought to be static in terms of neuronal number, with neurogenesis only occurring during development. However, there is now consensus that two regions in the adult rodent brain continue to produce new

neurons throughout adulthood. Adult neurogenesis in the rat was first reported by Altman and Das (1965) in the hippocampal dentate gyrus subgranular zone using injections of tritiated thymidine to label dividing CNS cells. Shortly after Altman's observation of adult hippocampal neurogenesis, he also described ongoing neuron addition in the adult rat OB (Altman and Das, 1965). In 1993-1994, Marla Luskin, Carl Lois and Arturo Alvarez-Buylla tracked the development of cells born in the adult subventricular zone (SVZ) to demonstrate this region as the source of new inhibitory neurons that migrated to the adult bulb and survived (Lois and Alvarez-Buylla, 1993; Luskin, 1993). Scientific interest in adult neurogenesis has escalated since these early studies and a wealth of data has been generated on adult CNS neural stem cells, the process of neurogenesis in both brain regions and factors that regulate this, and the behavioral relevance of adult neurogenesis for both systems (Whitman and Greer, 2009; Ji *et al.*, 2010; Bond, Ming and Song, 2015; Lim and Alvarez-buylla, 2016; Anacker and Hen, 2017; Bedos, Portillo and Paredes, 2018). Neurogenesis was then shown to continue throughout adulthood in the rodent SVZ (Figure 4), which lines the anterior lateral ventricles giving rise to neurons that migrate to the OB and become inhibitory interneurons (Lois and Alvarez-Buylla, 1993; Luskin, 1993; Rousselto, Lois and Alvarez-Buylla, 1995).

1.2.1 Subventricular zone

The adult rodent forebrain SVZ lines the anterior lateral ventricles and continuously gives rise to new inhibitory olfactory interneurons (Figure 4) (Lois and Alvarez-Buylla, 1993; Luskin, 1993). It contains neural stem cells termed type B cells that are thought to derive from neural stem cells (radial glia) present during embryonic forebrain development (Garcia-Verdugo *et al.*, 1998; Anthony *et al.*, 2004; Ihrie and

Alvarez-Buylla, 2008). Type B cells express glial fibrillary acidic protein (GFAP) and were originally thought to be astrocytes due to their glial-like properties. Type B cells slowly divide giving rise to transit-amplifying cells known as type C cells. Type C cells then divide more rapidly and give rise to neuroblasts (Type A cells) that leave the SVZ and undergo long distance migration to the OB (Garcia-Verdugo *et al.*, 1998).

Neuroblasts travel up to ~5mm in the mouse brain through a pathway called the rostral migratory stream (RMS) (Rousselto, Lois and Alvarez-Buylla, 1995; Gritti, Vescovi and Galli, 2002; Ma *et al.*, 2009; Whitman and Greer, 2009). Within the RMS, neuroblasts express proteins characteristic of immature neurons, particularly doublecortin and polysialylated form of neuronal cell adhesion molecule (PSA-NCAM) (Rousselto, Lois and Alvarez-Buylla, 1995). Neuroblasts travel by chain migration within glial tubes or channels formed by RMS astrocytes (Lois and Alvarez-Buylla, 1996; Sun, Kim and Moon, 2010). Although most neuroblasts do not continue to divide once entering the RMS, there are subpopulations of neuroblasts that remain mitotically active and will continue to divide once or twice on the way to the OB (Gritti, Vescovi and Galli, 2002; M. C. Whitman and Greer, 2007; Nissant and Pallotto, 2011). Estimates are that one division of a Type B stem cell ultimately generates about 16 neuroblasts (Ponti *et al.*, 2013). However, there are cells within the progenitor cell populations (Type C) in the SVZ and in the population of migrating neuroblasts in the RMS that undergo apoptosis, so not all newborn cells live to reach the OB (Brunjes and Armstrong, 1996).

1.3 Integration of adult born olfactory granule cells

Most cells born in the SVZ develop into OB GCs or PG cells (~95%), as well as small numbers of astrocytes and oligodendrocytes, with the location of a cell's birth

within the SVZ playing a role determining the type (or neurochemical subtype) of cell that will develop (Young *et al.*, 2007; Lledo, Merkle and Alvarez-Buylla, 2008). Upon exiting the RMS in the OB, neuroblasts migrate radially to their final destination (Carlén *et al.*, 2002; Ma *et al.*, 2009; Whitman and Greer, 2009; Lepousez, Valley and Lledo, 2013). PG cells migrate past the EPL and into the GL. GCs migrate radially into the nearby GCL. In the GCL they differentiate and develop basal dendrites and more complex apical dendrites that extend into the EPL (Figure 5). Innervation of basal dendrites by GABAergic inputs and centrifugal afferents appears to precede synapse formation in the apical dendritic compartment (Carleton *et al.*, 2003; M. C. Whitman and Greer, 2007; Kelsch, Lin and Lois, 2008; Panzanelli *et al.*, 2009; Pallotto *et al.*, 2012).

The integration of new GCs is not complete until sometime between 21-45 days after their birth in the SVZ (+/- ~3 days due to variable cell migration times). During this time (by ~7 weeks) about 40-50% of the adult-born cells will undergo apoptosis (Petreanu and Alvarez-Buylla, 2002; Winner *et al.*, 2002; Lemasson *et al.*, 2005; Mary C. Whitman and Greer, 2007; Imayoshi *et al.*, 2009; Whitman and Greer, 2009). The morphological maturation and integration of new GCs can be divided into 5 stages (Petreanu and Alvarez-Buylla, 2002; Carleton *et al.*, 2003; M. C. Whitman and Greer, 2007; Nissant and Pallotto, 2011). At 2-7 days after cell birth (estimated by expression of green fluorescent protein (GFP) after infection of SVZ cells with retrovirus encoding GFP), neuroblasts appear bipolar with small processes and are migrating through the RMS. At this stage (stages 1-2), some neuroblasts may still be dividing and may not have begun to differentiate. At about 10 days, stage 3 neuroblasts are present in the GCL and extend a spineless, short apical dendrite towards the EPL, and have elaborated many short basal dendritic branches.

By stage 4, several days later, GC morphology is significantly changed. Many apical dendritic branches extend into the EPL, some lacking spines and some with many filopodia. The morphology of neurons aged ~20-56 days is similar, and most have a long apical dendrite with more complex dendritic branching in the EPL and numerous spines (stage 5) (Petreanu and Alvarez-Buylla, 2002; M. C. Whitman and Greer, 2007). Total apical dendritic spine numbers appear to peak by ~21-28 days, and by 56 days, the surviving neurons have undergone spine pruning and have reduced spine numbers (Petreanu and Alvarez-Buylla, 2002; Mary C. Whitman and Greer, 2007; Imayoshi *et al.*, 2009; Whitman and Greer, 2009).

Long-term in vivo imaging of new GCs has shown that during the first month, spines are highly dynamic, with many new spines formed and lost (Sailor *et al.*, 2016). During this time, new GCs gradually become more narrowly responsive to particular odorants, shifting from the broader responses shown shortly after they arrive in the bulb and extend dendrites (Wallace *et al.*, 2017). Beyond one month, numbers of mature spines appear to stabilize, but even when fully mature, a remarkably large proportion the spine population in both adult- and early-born GCs remains dynamic (~40%), with ongoing spine elaboration and elimination, a structural plasticity that may be associated with circuit adaptations to continuing neurogenesis (Sailor *et al.*, 2016). Presumably spine pruning and spine stabilization are experience/activity-dependent processes. All of the mechanisms that contribute to successful integration of a subset of new GCs into adult bulb circuitry are not fully understood. However, neural activity clearly plays an important role in determining the fate of new-born neurons. Increased sensory stimulation increases abGC survival, while reducing activity by blockade of intrinsic activity, or sensory deprivation or by naris

occlusion, reduces their spine density, and their survival rate (Yamaguchi and Mori, 2005; Mandairon *et al.*, 2006; Kelsch *et al.*, 2009; Bastien-Dionne *et al.*, 2010; Lin *et al.*, 2010; Dahlen *et al.*, 2011). There is critical developmental window for GC reliance on sensory activity for survival and synaptic integration, occurring from 2-4 weeks after their birth (Petreanu and Alvarez-Buylla, 2002; Yamaguchi and Mori, 2005; Kelsch *et al.*, 2009). During this period, abGCs are also reliant on development of both glutamatergic and GABAergic inputs which regulate their dendrite and spine development, and consequently their integration (Livneh *et al.*, 2009; Kelsch *et al.*, 2012; Pallotto *et al.*, 2012; Breton-Provencher, Cote and Saghatelian, 2014; Breton-Provencher *et al.*, 2016) For example, knockdown of the GABA receptor scaffolding protein gephyrin in new GCs, or the GluN2 subunit of the NMDA receptor, significantly impairs dendritic development and spine formation, leading to GC death (Kelsch *et al.*, 2012; Deprez *et al.*, 2015).

Adult neurogenesis creates a highly dynamic and unique neural network in the OB. Addition of adult-born neurons is crucial to the ongoing anatomical maintenance and function of OB circuitry, and in the absence of adult neurogenesis, severe depletion of GCs is seen (Imayoshi *et al.*, 2009; Valley *et al.*, 2009). This is due to constant turnover of the GC population through apoptosis of previous incoming GCs, a process that continues even in the absence of neurogenesis (Imayoshi *et al.*, 2008). Conversely, focal elimination of bulb interneurons can lead to their selective replacement through adult neurogenesis, a mechanism that may restore functional circuitry in damaged bulb areas (Liu and Guthrie, 2011; Murata *et al.*, 2011; Lazarini *et al.*, 2014) (Murata *et al.*, 2011; Liu and Guthrie, 2011; Lazarini *et al.*, 2014).

The regular addition of new GCs to bulb circuitry is important to olfactory learning and memory and the appropriate processing of odor information in the bulb (Ming and Song, 2011; Alonso *et al.*, 2012). For example, elimination of neurogenesis in rodents leads to long-term olfactory memory impairments (Lazarini *et al.*, 2009; Sultan *et al.*, 2010). Use of optogenetics to activate adult-born GCs facilitates odor-reward associations in mice, while ablation of abGCs after training degrades odor-reward memories (Lepousez, Valley and Lledo, 2013; Arruda-Carvalho *et al.*, 2014). More recently, other studies have confirmed a role for abGCs in odor-reward associations and their involvement in normal odor discrimination (Breton-Provencher and Saghatelian, 2012; Sakamoto, Kageyama and Imayoshi, 2014; Grelat *et al.*, 2018; Li *et al.*, 2018; Mandairon *et al.*, 2018). Although the function of adult olfactory neurogenesis is still being debated, such studies illustrate how adult neurogenesis may be behaviorally important to an adult animal that relies on changing environmental olfactory cues throughout life to find food, mates, and identify conspecifics and predators.

1.4 Neurotrophic Factors

Olfactory neurogenesis is clearly regulated by activity levels in the OB but a wide variety of other factors also play a role, including a number of growth factors (Patapoutian and Reichardt, 2001; Jin *et al.*, 2002; Yamaguchi and Mori, 2005; Alonso *et al.*, 2006; Reichardt, 2006; Sun *et al.*, 2006; Murata *et al.*, 2011; Gomez-Gaviro *et al.*, 2012; Lindberg *et al.*, 2012; Lazarini *et al.*, 2014). Trophic factors are typically secreted peptides which promote cell proliferation, growth, survival and differentiation. Members of the fibroblast growth factor (FGF) and epidermal growth factor (EGF) families have been shown to regulate SVZ stem cell proliferation (Gritti *et al.*, 1999). Members of the nerve growth

factor (NGF) family of neurotrophins also have been investigated for their effects. There are four members of the mammalian neurotrophin family that include NGF, brain-derived neurotrophic factor (BDNF), neurotrophin 3 (NT3), and neurotrophin 4/5 (NT4/5) (Patapoutian and Reichardt, 2001; Reichardt, 2006; Park and Poo, 2013). These neurotrophins interact with members of the tropomyosin receptor kinase (Trk) family and the p75 neurotrophin receptor, related to the family of tumor necrosis factor receptors (Friedman and Greene, 1999; Huang and Reichardt, 2003). Although not absolute in their specificity, these neurotrophins do exhibit selective Trk binding. NGF preferentially binds the TrkA receptor, NT3 binds TrkC, (but may bind both TrkA and TrkB), and NT4/5 and BDNF bind with high affinity to the full-length TrkB receptor (Huang and Reichardt, 2003). Neurotrophin regulation of peripheral nervous system (PNS) development has been well characterized, but these factors also contribute to the development of central nervous system (CNS) neurons, as well as the function of mature neurons (Barde, 1990). Studies of BDNF effects on olfactory neurogenesis have led to somewhat conflicting results (discussed below). Interestingly, NT3 supplied to SVZ stem cells by the cerebrospinal fluid/vasculature recently has been shown to be required for the life-long maintenance of SVZ neural stem cells (Delgado *et al.*, 2014)

1.4.1 Brain-Derived Neurotrophic Factor in the CNS

In the adult rodent CNS, neuronal BDNF expression is widespread, as is the distribution of neuronal TrkB receptors (Wetmore *et al.*, 1990; Masana *et al.*, 1993). BDNF gene transcription is Ca²⁺-regulated and neural activity-dependent (Shieh and Ghosh, 1999; Matsuda *et al.*, 2009; Kuczewski, Porcher and Gaiarsa, 2010; Zheng *et al.*, 2011, 2012; Park and Poo, 2013). Within the BDNF gene there are nine exons, eight non-coding exons

and one containing the BDNF protein-coding region (exon IV) (Aid *et al.*, 2007). BDNF promoter IV contains several calcium response elements (CREs) that provide binding sites for transcription factors, including the CRE binding protein (CREB). Twenty-two isoforms of BDNF mRNA have been predicted based on splicing regions located in the gene (Aid *et al.*, 2007). Since there is only one coding exon, all of these isoforms are translated into a single species of BDNF protein even though the different mRNA isoforms are preferentially expressed within different neuronal types (Zheng *et al.*, 2012). Translation of BDNF mRNA can take place in both the cell body and in dendritic processes near spines. In hippocampal CA1 neurons there are two different forms of BDNF mRNA with varying 3' untranslated regions (UTR) that determine if BDNF mRNA is translated in the cell body or transported by mRNA binding proteins into the dendrite. The BDNF with the short 3'-UTR is translated in the soma while the transcript with the long 3'-UTR is transported for local translation in the dendrite. This local translation of BDNF regulates spine maturation and pruning, which is impaired when transport of the long transcript is inhibited (An *et al.*, 2008; Kaneko *et al.*, 2012; Orefice *et al.*, 2013). The binding protein translin has been shown to be responsible for dendritic transport of BDNF mRNA in hippocampal neurons in vitro (Chiaruttini *et al.*, 2009; Wu *et al.*, 2011). However translin is likely not the only binding factor, and there may be cell-specific transport methods for trafficking of BDNF mRNA (Wu *et al.*, 2011).

Within the cell body, the larger precursor form of prepro-BDNF and the cleaved, mature BDNF peptide (generated by the enzyme furin or tissue plasminogen activator) are packaged in the trans-Golgi network into secretory vesicles and transported to locations in the cell where BDNF will be released (Lessmann and Brigadski, 2009; Dieni

et al., 2012; Zheng *et al.*, 2012). BDNF release from CNS neurons is well known to be activity-dependent, as well as constitutive (Kuczewski, Porcher and Gaiarsa, 2010). BDNF acts through the full-length tyrosine kinase receptor TrkB. Dimers of mature BDNF bind to TrkB subunits, activating its dimerization and the autophosphorylation of tyrosine residues located in the intracellular kinase domain. Downstream signaling pathways are activated that upregulate expression of pro-survival genes, and stimulate enzyme cascades that promote synaptic plasticity and neuron differentiation (Reichardt, 2006; Cunha, Brambilla and Thomas, 2010). Downstream signaling kinases include protein kinase B (AKT), phospholipase C- γ (PLC γ) and extracellular signal-regulated kinases 1 and 2 (ERK1/ERK2), via the canonical MAP kinase cascade (Figure 6) (Patapoutian and Reichardt, 2001; Reichardt, 2006; Cunha, Brambilla and Thomas, 2010; Cohen *et al.*, 2011). BDNF's binding to the TrkB receptor also promotes glutamate release and increases the opening probability of NMDA receptors (Gottmann, Mittmann and Lessmann, 2009; Zagrebelsky and Korte, 2014). Studies have shown that BDNF acts on the TrkB receptor in both an autocrine and paracrine manner, and neurons that release BDNF may activate TrkB receptor on the same neurons, as well as acting on neighboring neurons. For example, increasing BDNF production in select neurons within rodent cortical slices stimulates the dendritic growth of neighboring neurons up to 4.5 μ m away (English, 2012). More recent work by Yasuda and McNamara has demonstrated in hippocampal neurons that individual spines stimulated with glutamate release fluorophore tagged-BDNF. This was followed by TrkB signaling and enlargement of the same spine, effects that were blocked by removing the released BDNF with TrkB IgG (Harward *et al.*, 2016). *In vivo*, selective expression of BDNF only in adult-born dentate

GCs in conditional forebrain BDNF knock-out mice fully restored the development of their dendrites and spines, providing further evidence of BDNF as an autocrine factor (Wang *et al.*, 2015). Its anterograde and retrograde trophic actions on specific neuronal populations in the CNS are also well known, particularly in the striatum, which lacks endogenous BDNF expression, and relies on cortical axons to supply BDNF for its normal development, and for dendrite and spine maintenance in adult medium spiny neurons (Baquet, 2004; Rauskolb *et al.*, 2010).

1.5 BDNF's role in adult neurogenesis

Although germline BDNF null mice (no BDNF at all during development in embryo and after birth) typically die within the first few weeks after birth, this is due to the death of early-generated PNS neurons and BDNF does not appear to function as necessary survival factor for most developing and adult CNS neurons (Snider, 1994; Rauskolb *et al.*, 2010). However BDNF has been studied recently in terms of its effects on regulating adult neurogenesis in the hippocampus and olfactory system (Chan *et al.*, 2008; Bergami, Berninger and Canossa, 2009; Choi *et al.*, 2009; Bath, Akins and Lee, 2012; Vilar and Mira, 2016). Effects on olfactory neurogenesis have previously focused on its actions in the SVZ in vivo, an area that expresses little if any BDNF (Zigova *et al.*, 1998; Benraiss *et al.*, 2001, 2012; Henry, Hughes and Connor, 2007; Bath *et al.*, 2008). Intraventricular administration of exogenous BDNF (near the SVZ) has been reported to significantly increase survival rates of adult-born GCs in the OB (Zigova *et al.*, 1998). Similarly, increasing BDNF in the rat SVZ by adenovirus-mediated gene transfer has been shown to increase the number of adult-born GCs that accumulate in the RMS and OB (Benraiss *et al.*, 2001, 2012). Survival of adult-born GCs, but not progenitor cell

proliferation, is decreased in BDNF heterozygous mice and in mice expressing a variant form of BDNF (the Val66Met polymorphism), which appears to impair activity-dependent BDNF secretion (Bath, Akins and Lee, 2012). However, BDNF's role in olfactory neurogenesis has been challenged by other investigators that replicated the prior BDNF SVZ delivery methods, or deleted TrkB from newborn GCs, and failed to find any effects on numbers of surviving abGCs in the OB (Galvao, Garcia-Verdugo and Alvarez-Buylla, 2008; Bergami *et al.*, 2013). Moreover these reports failed to find expression of full-length TrkB in the SVZ, where the BDNF treatments were targeted (Galvao, Garcia-Verdugo and Alvarez-Buylla, 2008; Bergami *et al.*, 2013). Although BDNF's involvement in regulating neurogenesis at the level of the SVZ remains debatable, it has been established that abGCs begin to express full-length TrkB as they mature in the OB, which expresses very low levels of endogenous BDNF relative to other olfactory-limbic areas such as piriform cortex and hippocampus (Guthrie and Gall, 1991; Conner *et al.*, 1997; Clevenger *et al.*, 2008; Galvao, Garcia-Verdugo and Alvarez-Buylla, 2008; Bergami *et al.*, 2013). Considering this is where the abGCs integrate and make the decision to survive long term or undergo programmed cell death, increasing BDNF availability in this location could be expected to positively affect their development and survival. In this case, new olfactory GCs may resemble new dentate GCs. BDNF increases within hippocampus (including those triggered by wheel running) promote increased dendritic complexity, spine development, and survival in the abGC dentate population, while TrkB knockout dramatically reduces their dendritic arborization and spine numbers, resulting in GC death at 4-5 weeks after their birth (Sairanen *et al.*, 2005;

Scharfman *et al.*, 2005; Rossi *et al.*, 2006; Chan *et al.*, 2008; Bergami, Berninger and Canossa, 2009; Choi *et al.*, 2009; Gao, Smith and Chen, 2009; Stranahan *et al.*, 2009).

1.7 BDNF's role in dendrite and spine morphology

Dendritic spines are small, micron-sized projections that protrude from the dendritic membrane. These may be found on virtually all CNS neurons, usually indicating the location of an excitatory synapse. The neuronal cytoskeleton contains filamentous actin and changes in actin polymerization within spines can result in spines of different sizes and shapes (Calabrese, Wilson and Halpain, 2006; Tada and Sheng, 2006; Bosch and Hayashi, 2012; Ebrahimi and Okabe, 2014). Dendritic spine numbers and sizes vary greatly throughout different populations of brain neurons. However, presumptive mature-type spines usually contain a bulbous head connected to the dendritic membrane by a thinner stalk, sometimes resembling a mushroom shape, and usually containing mature pre- and postsynaptic specializations (Hering and Sheng, 2001; Calabrese, Wilson and Halpain, 2006; Saneyoshi, Fortin and Soderling, 2010). Immature spines, thought to be the precursors of mature spines, are called filopodia and usually lack a spine head and are highly motile, turning over rapidly with an average life span of about 10 minutes (Calabrese, Wilson and Halpain, 2006). During synaptogenesis, filopodia that are able to form stable contacts with presynaptic inputs may then undergo morphological transformation into mature spines (Yuste and Bonhoeffer, 2004; Yoshihara, De Roo and Muller, 2009). The underlying mechanisms that control the growth of filopodia and their stabilization into mature spines have been extensively studied in cortical and hippocampal pyramidal neurons, particularly those that occur in response to changes in synaptic activity or TrkB signaling (Calabrese, Wilson and

Halpain, 2006; Tada and Sheng, 2006; Tanaka *et al.*, 2008; Panja and Bramham, 2014). The Rho/Rac-family of small GTPases have been implicated as key regulators of the spine actin cytoskeleton in response to glutamate receptor activation, the binding of synapse-located cell adhesion molecules, and BDNF released during synaptic activity (Calabrese, Wilson and Halpain, 2006; Tada and Sheng, 2006; Panja and Bramham, 2014). Activation of Rac1 can promote increased dendritic spine growth, while RhoA signaling tends to decrease spine numbers and limit spine size (Hering and Sheng, 2001; Calabrese, Wilson and Halpain, 2006; Tada and Sheng, 2006; Saneyoshi, Fortin and Soderling, 2010; Ebrahimi and Okabe, 2014). Rac activation stimulates the downstream LIM kinase, which phosphorylates the actin binding protein cofilin, inhibiting its ability to depolymerize filamentous actin (Panja and Bramham, 2014). This leads to increases in the levels of polymerized, filamentous actin within the spine cytoskeleton, promoting spine growth (Calabrese, Wilson and Halpain, 2006; Panja and Bramham, 2014). BDNF activation of TrkB signaling in long-term potentiation (LTP)-stimulated CA1 hippocampal neurons leads to this inhibition of cofilin, and blocking this signal inhibits LTP-induced filamentous actin increases in spines, limiting structural plasticity (Rex *et al.*, 2007, 2009). An example of this is shown in figure 7.

BDNF is well known to regulate spine formation, maturation and stabilization, in part through regulating this actin-based plasticity. Evidence supports BDNF as a regulator of dendritic spine morphology, maturation and maintenance in multiple types of forebrain neurons. For example, in cultured rat hippocampal neurons, acute TrkB activation increases spine elongation and enlargement, while sustained TrkB signaling increases spine neck growth (Ji *et al.*, 2010). Conversely, blocking BDNF signaling in

cultured primary hippocampal neurons causes a reduction in dendritic spine density (Ji *et al.*, 2010; Kellner *et al.*, 2014). In vivo, conditional genetic deletion of postnatal forebrain BDNF expression has significantly negative effects on spines in multiple glutamatergic and GABAergic neuronal populations (Gorski *et al.*, 2003; Rauskolb *et al.*, 2010; Vigers *et al.*, 2012). Medium spiny neurons in the striatum exhibit less complex dendrites and reduced spine densities (Baquet, 2004; Rauskolb *et al.*, 2010; Li *et al.*, 2012), while over-expression of BDNF in the striatum can rescue spine deficits caused by striatal expression of mutant huntingtin protein (Xie, Hayden and Xu, 2010). In layer 2/3 pyramidal neurons in visual cortex, adult mutant mice lacking dendritic BDNF translation exhibit thinner, immature-type spines with smaller heads compared to those in normal mice (Kaneko *et al.*, 2012). Moreover, these mice demonstrate persistently reduced visual responses in deprived eyes after reversal of monocular deprivation, whereas normal mice show no such effects in adulthood (Kaneko *et al.*, 2012). The complexity of BDNF control of neuronal morphology has been shown recently in a series of transgenic mice lacking differently spliced BDNF mRNA transcripts with variable 3' and 5' untranslated regions (UTRs). Selective loss of individual transcript types selectively regulated different features of dendritic complexity (such as apical versus basal effects) and spine morphology in hippocampal neurons (Orefice *et al.*, 2013; Maynard *et al.*, 2017). Recent work by Bergami's group has provided strong evidence that BDNF signaling also regulates spine development and maturation in adult-born olfactory GCs. Knockdown of TrkB receptor expression in abGCs impairs their dendritic arborization and reduces their spine density (Bergami *et al.*, 2013). Our Golgi staining findings in TgBDNF mice indicate that the GC population bears more mature spines than GCs in normal mice and

may therefore also enhance spine maturation in abGCs. Experiments described in the final chapter of this project were designed to test this hypothesis *in vivo*.

1.9 Mouse background

All experiments described in this project used a transgenic mouse line expressing a BDNF transgene (containing the coding exon) under control of the α -calmodulin-dependent protein kinase II (CaMKII α) promoter (Jackson Laboratories, Bar Harbor, ME, strain #006579, Huang *et al.*, 1999). The BDNF transgene is expressed throughout forebrain in α -calmodulin-dependent protein kinase II (CaMKII α)-expressing neurons, in addition to the normal expression pattern of the endogenous mouse BDNF gene. The CaMKII α promoter drives expression in most excitatory forebrain projection neurons, however, OB interneurons, including GCs, express CaMKII α , while excitatory MTCs do not (Zou, Greer and Firestein, 2002). GCs therefore express increased levels of BDNF from the transgene in this mouse strain (hereafter termed TgBDNF), while bulb neurons in wild-type (WT) control mice expressed lower levels of only the endogenous BDNF gene. The mouse strain was maintained at FAU, with male TgBDNF mice bred to female WT mice to obtain litters of both genotypes. All mice were genotyped by PCR amplification of tail DNA samples using primers specific for the transgene.

1.8 Dissertation aims and objectives

The overall aims of this dissertation are to examine how genetically increasing endogenous BDNF in the mouse OB affects the morphology of olfactory GC interneurons, and to determine if this change in neurotrophic factor availability alters adult olfactory neurogenesis, specifically the survival and structural development of GCs generated in the forebrain SVZ.

1.9.1 Chapter 2

Olfactory GCs, the largest population of inhibitory interneurons in the OB, play a vital role in the processing of odor information sent to higher olfactory brain areas through their regulation of the excitatory MTC output neurons. In this chapter we aimed to determine how over-expression of endogenous BDNF in the OB GCL affects dendrite and spine morphology in the established GC population. Following on our previous work confirming increased OB BDNF mRNA levels in mice that carry a transgene encoding BDNF under a *CAMKII α* promotor (hereafter TgBDNF mice), we first quantified and compared OB BDNF protein levels in these animals and WT controls using Enzyme-Linked Immunosorbent Assay (ELISA) and Western blotting methods. To determine if increased BDNF alters normal GC dendritic morphology and/or spine numbers we used the Golgi-Cox staining technique to visualize intact GC neurons in both genotypes. Labeled GCs underwent full 3D reconstruction and morphometric analyses to compare the length and complexity of dendrites, the total number and density of dendritic spines, and the number and density of individual spine types. We reasoned that increases in endogenous BDNF could increase GC spine numbers, particularly mature dendritic spines, based on results of prior studies examining BDNF effects on other populations of CNS neurons in vivo, as well as the effects of TrkB gene knockdown. By determining the effects of excess BDNF on GC morphology, a better understanding of how normal levels of endogenous BDNF, regulated by neural activity, may shape the connectivity of these interneurons within OB circuitry.

1.9.2 Chapter 3

The forebrain SVZ gives rise to olfactory GCs throughout adulthood in rodents. After migrating through the RMS to the OB, only about 50% of these neurons will functionally integrate and survive long term. The factors that determine if any given abGC will integrate or undergo apoptosis are not all known. In this chapter we aim to determine if increasing BDNF in the OB of adult mice promotes increased survival of TrkB-expressing abGCs. In past published literature on this topic there has been debate on BDNF's role in olfactory neurogenesis, particularly its actions on SVZ progenitor cells. Adult-born dentate GCs show improved survival with hippocampal BDNF supplementation in vivo and reduced survival with TrkB knockdown. Like these neurons, increasing BDNF in location where abGCs mature may enhance their survival, however a recent study suggests that TrkB knockdown has little effect on this olfactory population. Using bromodeoxyuridine (BrdU) incorporation in vivo to label dividing progenitor cells in the SVZ, we will monitor the survival rate of BrdU+ GCs at multiple timepoints during their development in the OB of TgBDNF mice. Levels of apoptotic cell death will be assessed using the terminal deoxynucleotidyl transferase dUTP nick end labeling (TUNEL) method to label cells undergoing DNA fragmentation. Since most prior published work has manipulated BDNF levels in the SVZ, this chapter will examine and discuss how increasing BDNF in the OB impacts the survival/death of abGCs, and whether these new olfactory neurons respond differently from adult-born dentate GCs

1.9.3 Chapter 4

The rodent OB successfully incorporates new GCs throughout adulthood. The factors that aid in the development and selective integration of some abGCs while others

are eliminated are not fully understood. Our Golgi study indicates that BDNF can promote increases in numbers of mature spines in established GCs. In this final chapter aim, we will determine if increasing endogenous BDNF promotes the development of dendrites and spines in abGCs, as this would be expected to favor their integration. In this study we will use a lentivirus encoding a tau-mcherry fusion protein to label adult-born GCs in the SVZ before their migration to the bulb. We will then use cell reconstruction and morphological analyses at different time points during their development in the normal and transgenic OB to identify differences in their structural maturation. We expect that both the development and maturation of dendritic spines will be enhanced by higher levels of BDNF. This chapter will compare the morphological development of normal abGCs and those exposed to increased BDNF and discuss how BDNF may regulate circuit plasticity and GC integration

PART II: BDNF OVER-EXPRESSION INCREASES OLFACTORY BULB GRANULE CELL DENDRITIC SPINE IN VIVO

2.1 Abstract

Olfactory GCs are one population of neurons responsible for maintaining normal OB function and circuitry. These axon-less interneurons achieve this through reciprocal dendrodendritic synapses with the OBs glutamatergic projections neurons, the MTCs. The majority of these synapses are located on the GCs middle-distal dendritic spines and contain both presynaptic GABAergic and postsynaptic glutamatergic structures, while the remainder of spines located on the basal and proximal dendrites mainly receive glutamatergic inputs from the olfactory cortices. Proper synaptic connectivity is crucial to the ongoing maintenance and functional circuitry of the OB, which remains highly dynamic into adulthood through activity-dependent spine plasticity and adult neurogenesis. BDNF is one factor known to aid in the regulation of spine development, maintenance and maturation. How or if increasing BDNF in the OB impacts the growth and maturation of GC spines *in vivo* is still not known. In this study we used mice that over-express endogenous BDNF in the OB to determine how sustained increases in BDNF affect the morphology of GCs. Using Golgi-Cox staining and full neuron reconstructions, we have determined that GCs in these mice have higher total spine numbers and increased numbers of mature spines (headed) on their apical dendrites. Increases in the density of spines on the distal and proximal dendrites indicate BDNFs

involvement in the modification of multiple glutamatergic inputs. Our results indicate that BDNF promotes the maturation and/or maintenance of dendritic spines in olfactory GCs, suggesting that it plays a role in regulating OB circuit function via GC connectivity.

2.2 Introduction

Olfactory GCs are a large population of GABA-synthesizing interneurons that maintain normal OB circuit function by regulating the output of odor information to higher olfactory areas in the forebrain (Isaacson and Strowbridge, 1998; Mori, Nagao and Yoshihara, 2007; Shepherd *et al.*, 2007). These axonless interneurons communicate with the OBs excitatory projection neurons, the MTCs, through “headed”, mature spines on their distal apical dendrites that extend into the EPL (Woolf, Shepherd and Greer, 1991; Isaacson and Strowbridge, 1998; Urban, 2002; Balu, Pressler and Strowbridge, 2007; Urban and Arevian, 2009; Nagayama, Homma and Imamura, 2014). The majority of these headed spines contain both presynaptic GABAergic and postsynaptic glutamatergic elements and form reciprocal dendrodendritic synapses with the MTCs (Rall *et al.*, 1966; Egger and Urban, 2006; Balu, Pressler and Strowbridge, 2007; Shepherd *et al.*, 2007; Bartel *et al.*, 2015). Through these headed spines, GCs mediate both feedback and lateral inhibition of output neurons to regulate OB odor processing and refine the olfactory information sent to the forebrain to direct olfactory-mediated behaviors (Urban, 2002; Balu, Pressler and Strowbridge, 2007; Mori, Nagao and Yoshihara, 2007; Shepherd *et al.*, 2007; Urban and Arevian, 2009). Loss of these synapses or modifications in their function can lead to improper odor-processing and disruptions in olfactory-mediated behaviors (Shepherd *et al.*, 2007; Abraham *et al.*, 2010).

During both development and adulthood, dendritic spines on neurons throughout the forebrain are highly plastic (Hering and Sheng, 2001; Knott and Holtmaat, 2008; Yoshihara, De Roo and Muller, 2009; Bosch and Hayashi, 2012; Berry and Nedivi, 2017; Fu and Ip, 2017). This plasticity continuously modifies and refines functional synaptic connections between neurons. Headed spines seen on GC dendrites are considered mature and stable, containing postsynaptic elements that include glutamate receptors and postsynaptic density protein-95, -indicative of excitatory synapses, which are typically located on the spines of CNS neurons (Woolf, Shepherd and Greer, 1991; Matsuzaki *et al.*, 2004; Tada and Sheng, 2006; M. C. Whitman and Greer, 2007; Yoshihara, De Roo and Muller, 2009; Bosch and Hayashi, 2012; Bartel *et al.*, 2015). Spines on mature olfactory GCs are incredibly dynamic with a ~20-25% average spine turnover rate per 24-48 hrs, compared to 1-2% over 3 days in mature neocortical neurons (Mizrahi, 2007; Livneh and Mizrahi, 2012; Sailor *et al.*, 2016). Roughly 40% of the total spine population consists of short-lived, dynamic spines (Sailor *et al.*, 2016). Dendrodendritic synapses do not exhibit LTP and it has been proposed that GCs may instead use structural plasticity in the spine population to adapt circuitry to functional demands, in other words, connectivity changes rather than increasing the strength of individual synapses (Gao and Strowbridge, 2009; Sailor *et al.*, 2016). Many factors, such as neural activity, hormones, and growth factors regulate morphological and physiological changes in dendritic spines (Calabrese, Wilson and Halpain, 2006; Knott and Holtmaat, 2008; Yoshihara, De Roo and Muller, 2009; Bosch and Hayashi, 2012; Wyatt, Tring and Trachtenberg, 2012). Among these, BDNF, a member of the neurotrophin family, has a well-established role in promoting the plasticity, maturation and maintenance of dendritic spines in many

neuronal populations in the adult CNS (Gorski *et al.*, 2003; An *et al.*, 2008; Tanaka *et al.*, 2008; Rauskolb *et al.*, 2010; Dean *et al.*, 2012; Vigers *et al.*, 2012; Hartmann *et al.*, 2012; Kaneko *et al.*, 2012; Orefice *et al.*, 2013; Kellner *et al.*, 2014; Maynard *et al.*, 2017; Guo, Nagappan and Lu, 2018; Kowiański *et al.*, 2018)

Neural activity also regulates spine development and plasticity, and because BDNF transcription and release are activity-dependent and Ca^{2+} regulated, it is thought to be a component in activity-dependent plasticity (Shieh and Ghosh, 1999; Lessmann and Brigadski, 2009; Kuczewski, Porcher and Gaiarsa, 2010; Zheng *et al.*, 2012). The BDNF promotor contains calcium response elements (CRE), which are regulated by transcription factors like CRE binding proteins. Meaning an influx of Ca^{2+} through depolarization, leads to an increase in BDNF transcription (Shieh and Ghosh, 1999; Zheng *et al.*, 2012). BDNF's secretion is also activity-dependent and relies on an influx of intracellular Ca^{2+} after membrane depolarization (Lessmann and Brigadski, 2009; Kuczewski, Porcher and Gaiarsa, 2010). Activity-dependent release of BDNF is one way that activity can have trophic effects on CNS neurons

In hippocampal neurons, BDNF mRNA can be translated into protein in the soma or transported for protein synthesis in the dendrite (An *et al.*, 2008; Orefice *et al.*, 2013). The loss of the dendritically synthesized BDNF greatly prevents spine head enlargement and the pruning of immature spines (An *et al.*, 2008; Orefice *et al.*, 2013). Similarly, in the visual cortex, dendritically synthesized BDNF is required for normal spine maturation and spine pruning (Kaneko *et al.*, 2012). Although studies of BDNF have mainly focused on excitatory neurons, BDNF has shown to promote the differentiation and maturation of new hippocampal GCs through its effects on local GABAergic interneurons and is

necessary for normal development of GABAergic medium spiny neurons in the striatum, and the maintenance of their spines (Rauskolb *et al.*, 2010; Waterhouse *et al.*, 2012a). BDNF's demonstrated ability to regulate connectivity through its actions on spine maturation/maintenance makes it an ideal trophic factor to explore in terms of its impact on the development of adult born olfactory GCs.

BDNFs receptor TrkB is expressed by all neuron populations in the OB, while p75, BDNF's low-affinity receptor, is limited to ensheathing glia and the olfactory nerve layer (Hofer *et al.*, 1990; Guthrie and Gall, 1991; Deckner *et al.*, 1993; Gong *et al.*, 1994; Conner *et al.*, 1997; Nef *et al.*, 2001; Clevenger *et al.*, 2008). BDNF mRNA is localized to subpopulations of neurons in the bulb, but centrifugal afferents from the AON and piriform cortex, where BDNF is highly expressed, may provide the bulb with additional BDNF through anterograde transport (Guthrie and Gall, 1991). BDNF null mice typically die during early postnatal development but BDNF is not required for embryonic bulb development (Maisonpierre *et al.*, 1990; Kolbeck *et al.*, 1999; Nef *et al.*, 2001). In vitro, cultures with SVZ derived interneurons treated with BDNF leads to more complex dendrites through BDNF's TrkB receptor (Gascon *et al.*, 2005). Cultured neonatal OB slices treated with BDNF, show increases in dendritic complexity of olfactory MTCs while inducing spine development on GCs (S. Matsutani and Yamamoto, 2004; Imamura and Greer, 2009). The effects of increased BDNF on olfactory GC dendritic morphology in vivo has not yet been determined. In our current study, we increased endogenous BDNF in the OB of mice and examined the effects on GCs in adult mice. Over-expression of BDNF in the GCL of the OB did not alter the dendritic length or branch number of GCs compared to WT controls. However, increased BDNF altered spine

number and density in the apical dendrites of olfactory GCs. This was accompanied by a significant increase in spine number and density of mature, headed-type spines in TgBDNF animals when compared to WT.

2.3 Materials Methods

2.3.1 Animals

All animal procedures were carried out according to protocols approved by the Florida Atlantic University Institutional Animal Care and Use Committee, in accordance with National Institutes of Health guidelines. TgBDNF mice, maintained on a C57Bl6/J background, were obtained from Jackson Laboratories (strain #006579; Bar Harbor, ME). This strain carries a transgene encoding rat BDNF under control of 8.5 kb of the CAMKII α promoter, in addition to the endogenous BDNF gene (Huang *et al.*, 1999). Postnatal expression of the BDNF transgene follows the developmental pattern of forebrain CAMKII α expression, beginning near the end of first postnatal week and reaching adult levels by 1 month of age (Neve and Beart, 1989; Zou, Greer and Firestein, 2002). TgBDNF males were mated with WT females to obtain litters composed of transgenic and WT offspring. Genotyping was carried out by PCR amplification of genomic DNA isolated from tail samples using the following primers for detection of the transgene: 5'-CAAATGTTG CTTGTCTGGTG-30 and 50 - GTCAGTCGAGTGCACAGT TT-3'. Cycling parameters were as follows: 94°C-30 s, 55°C-30 s, 72°C-45 s (30 cycles). To test for possible progressive effects of cell exposure to increased BDNF over time, brains were collected from young adult mice at 2–3 months of age, and from older mice aged 6– 7.5 months.

2.3.2 BDNF Enzyme-Linked Immunosorbent Assay (ELISA)

Mice at 2–3 months of age (four per genotype; two male, two female) were euthanized as above, decapitated, and the OBs rapidly dissected. Tissue was frozen on dry ice and stored at -80°C . Both OBs were homogenized together on ice in Cell Lysis buffer (#9803, Cell Signaling Technology, Danvers, MA, USA) to which 1 mg/ml complete protease inhibitors and 1 mg/ml complete phosphatase inhibitors (Roche Life Sciences, Indianapolis, IN, USA) were added. Lysates were centrifuged at 14,000 rpm for 20 min at 4°C and supernatants were collected and assayed for protein content by Qubit assay (Invitrogen, Carlsbad, CA, USA). Aliquots were stored at -80°C , prior to performing ELISA assays or Western blotting. ELISA plates were treated overnight with monoclonal antibody to BDNF, according to the manufacturer's instructions for the BDNF Emax immunoassay system (Promega, Madison, WI, USA). Supernatants were thawed and diluted 1:3 in Dulbecco's phosphate-buffered saline (PBS). Samples were acidified by adding 2 μm of 1 N HCl per 100 μm solution and incubated for 20 min at room temperature (RT). The pH was normalized by then adding 2 μm of 1 N NaOH per 100 μm of sample. Duplicate samples (150 μg protein/well) incubated overnight at 4°C , and were assayed for total BDNF protein content (pro- and mature BDNF), according to the Emax kit instructions. A standard curve was generated for each assay using serial dilutions of recombinant BDNF peptide provided in the kit. Following color development, absorbance was measured at 450 nm using a SpectraMax M5 plate reader (Molecular Devices, Sunnyvale, CA, USA), and BDNF concentrations in samples were calculated using SoftMax Pro software. Unpaired, two-tailed t-test comparisons of group

mean values (\pm SEM) were used to determine significance of genotype (defined as $p < 0.05$).

2.3.3 Western blotting

OB lysates prepared from tissue samples (as above) were thawed, diluted in Laemmli buffer and denatured at 95°C for 5 min. Protein was separated by 12% SDS–PAGE (BioRad TGX gels). Control lanes for BDNF blots included 5 ng of human recombinant mature BDNF peptide (PeproTech, Rocky Hill, NJ, USA). Proteins were transferred to PVDF membranes (0.45 μ m) and blocked Odyssey blocking buffer (Li-Cor Biosciences, Lincoln, NE, USA) for 1 hr at RT. Purified polyclonal rabbit IgG antibody to BDNF was from Santa Cruz Biotech (Santa Cruz, CA, USA; Cat# sc-546.) It was generated using mature, human BDNF as antigen (amino acid residues 128–147: RHSDPARRGELSVCDSEW; manufacturer’s data), and does not cross react with other members of the neurotrophin family. It detects mature BDNF at 14 kDa on immunoblots of hippocampal lysates from normal mice, while this band is absent on blots of hippocampal lysates prepared from BDNF knockout mice (Matsumoto et al., 2008). Mouse monoclonal anti-actin antibody was obtained from Cell Signaling Technologies (Danvers, MA, #3700). It was generated against a synthetic peptide corresponding to amino-terminal residues of human β -actin and detects a single band of 42–43 kDa molecular mass in immunoblots of COS and HeLa cells (manufacturer’s data). BDNF antibody (1:200) and actin antibody (1:1000) were diluted together in Odyssey blocker, with 0.2% Tween 20 added. Membrane incubation was carried out at 4°C for two nights. After rinsing in Tris-buffered saline (TBS; 50 mM Tris–HCl, 150 mM NaCl, pH 8.2), containing 0.1% Tween-20 (TBST), membranes incubated in a cocktail of Dylight

infrared dye-labeled IgGs (ThermoFisher Scientific, Waltham, MA, USA) specific for rabbit (dye 680) and mouse (dye 800), both diluted 1:5000 in TBST, for 1 hr. Blot images were examined and digitized using the Li-Cor Odyssey Fc imaging system. For semiquantitative comparisons, band intensities were normalized to actin bands in the same lane, and quantified using Li-Cor Odyssey software. Levels of protein measured from blot samples obtained from transgenic mice (n= 4) are expressed as the mean fold-difference (% of control) in normalized band intensities relative to measures from WT samples (n= 4) on the same blot. Unpaired, two-tailed t-test comparisons of group mean values (\pm SEM) were used to determine significance of genotype (defined as $p < 0.05$).

2.3.4 Golgi–Cox staining

Adult mice of both sexes were euthanized as above at 2–3 months of age, or at 6–7.5 months of age. Mice were then perfused transcardially with ice-cold phosphate-buffered saline (PBS, pH 7.3, 200 ml). Brains were dissected and processed using a modified Golgi staining technique as described (Isgor and Sengelaub, 2003). At 2–3 months of age, brains from two WT mice (one male, one female) and three TgBDNF mice (two male, one female) were processed for impregnation. At 6–7.5 months of age, brains from three WT (one male, two female) and three TgBDNF mice (one male, two female) were processed. Brain tissue was submerged in Golgi–Cox solution containing 5% potassium dichromate, 5% mercuric chloride, and 5% potassium chromate in distilled water, and were stored in the dark for 30 days. The solution was replaced every 2–3 days. Brains were then dehydrated and embedded in celloidin. Coronal microtome sections through both OBs (160 μ m) were cut and processed according to the protocol described by (Glaser and Van der Loos, 1981), without counterstaining. Treatment included

alkalinization in ammonium hydroxide (66%), development in Kodak Dektol and fixation in Kodak photographic fixative. Sections were dehydrated through increasing concentrations of ethanol and cleared in xylene before mounting. To accommodate tissue thickness, sections were mounted on custom-made glass slide compartments using Permount and were air-dried for several weeks before analyses.

2.3.5 Analyses of dendritic morphology

OB GCs were reconstructed at 100x objective magnification using a motorized Axiophot 2-Plus microscope (Carl Zeiss, Jena, Germany) equipped with a Microfire digital camera (Optronics, Goleta, CA, USA). Examples of Golgi-impregnated cells are shown in Figure 9 A, B. For mice at 2–3 months of age, a total of 42 cells from WT mice and 47 cells from TgBDNF mice were reconstructed (minimum of nine cells per animal). To test the effects of longer exposure to increased BDNF with age, GCs from 6 to 7.5 month-old mice were also reconstructed (42 cells for WT, 47 cells for TgBDNF, minimum of 12 cells per animal). Three-dimensional, computer-based neuronal tracing and reconstruction (reconstructions shown in Figure 11), as well as data collection and analyses, were performed using NeuroLucida and NeuroExplorer software (MicroBrightfield, Inc., Williston, VT, USA). Selection criteria for reconstruction and analysis of individual GCs included the following: (1) full impregnation of the cell to ensure visibility of the soma, dendrites and spines, with dendrites remaining intact within the section thickness, (2) no obstruction of the dendrites or soma by other stained cells or artifacts, (3) apical dendrites extending past the MCL and (4) morphology characteristic of mature GCs, including the presence of dendritic spines, and an apical dendrite with at least one branch point (Carleton *et al.*, 2003). Cells with immature features (emerging

from the subependymal layer, dendritic beading, absence of spines, no apical branching) were excluded. Those with few or no visible basal dendrites were included if the apical dendrite and soma were well impregnated and bore spines. While reconstructions were limited to cells with mature features, turnover of the mouse GC population leads to continuous, gradual GC replacement throughout life (Imayoshi *et al.*, 2008). New cells are generated from progenitors in the adult forebrain SVZ, and from here, thousands of immature GCs migrate into the bulb daily (Alvarez-Buylla and García-Verdugo, 2002). About half of these undergo apoptosis during migration and early development, but those that survive undergo maturation and functional integration over a period of 8 weeks, with dendrites achieving adult-like morphology when cells are 1-month old (Carleton *et al.*, 2003; M. C. Whitman and Greer, 2007; Mizrahi, 2007; Kelsch, Lin and Lois, 2008; Pallotto *et al.*, 2012). Therefore populations of reconstructed cells from individual mice are likely included GCs of different cell age. Measurements of dendritic morphology included total, apical and basal dendritic lengths, numbers of dendritic branch points (bifurcations/nodes), and number of terminal branches per cell. Sholl analysis of apical dendrite complexity was performed by counting the number of dendritic segments intersecting concentric spheres (20 μ m intervals) superimposed on reconstructed cells, with the cell soma at the center. Cell soma distance from the MCL/EPL border also was measured. Because a subset of reconstructed cells in all mice lacked visible basal dendrites, data collected for basal measurements at 2–3 months were obtained from 34 cells in WT mice, and 37 cells from TgBDNF mice. At 6–7.5 months, 36 and 32 cells, from WT and TgBDNF mice, respectively, were used. For those cells lacking basal

dendrites, values calculated for total dendritic measurements (total length, total spine number) were the equivalent of values obtained for the apical compartment alone.

2.3.6 Analyses of dendritic spines

Spines were inspected on both apical and basal dendrites of OB GCs, and as illustrated in Figure 9C, were classified into three categories (adapted from Hering and Sheng (2001) and Naritsuka et al., 2009): (1) Headed spines, considered mature or stable (Knott et al., 2006), included all spines with a neck (regardless of neck length) supporting a bulbous spine head that exceeded the width of the neck, (2) elongated, filopodia-like spines, considered immature (Holtmaat et al., 2005), were defined as long spines ($>2.5\ \mu\text{m}$) lacking enlargement of the tip, and (3) other-type spines that did not fall into the either of the above categories (Hering and Sheng, 2001; Holtmaat *et al.*, 2005; Knott *et al.*, 2006; Naritsuka *et al.*, 2009). The latter group consisted primarily of short, headless spines extending $<2.5\ \mu\text{m}$ from the shaft (regardless of thickness, dotted arrow in Figure 9C), and other, stubby spines that appeared as raised bumps on the shaft with no neck. Spines in the other-type category may be spines in morphological transition from other spine types, particularly filopodia, which exhibit rapid formation and retraction on the dendrites of adult-born GCs (Parnass, Tashiro and Yuste, 2000; Breton-Provencher, Cote and Saghatelian, 2014). Spines on the soma were not included in analyses due to the difficulty in resolving them against the dense staining of the cell body. Dendritic spine analyses included the calculation of total number and density per cell, spine number and density in apical and basal dendritic compartments, number and density of individual spine types, and proportions of spines in each category. In order to determine if differences in spine density varied with distance along apical dendrites, NeuroExplorer

software was used to calculate density in three domains along apical dendrites: the most proximal domain (within 50 μm of the soma), the middle domain (the next 50 μm), and the outer apical dendrite (remaining dendrite beyond the first 100 μm). Comparisons of group mean measures obtained from WT and TgBDNF mice at 2–3 months were performed using unpaired, two-tailed t-tests, with significance defined as $p < 0.05$. Group mean values per genotype were also compared by unpaired, two-tailed t-tests for the 6–7.5-month-old animals. Age effects were tested using unpaired t-tests to compare group means obtained from WT mice at 2–3 months and 6–7.5 months, and means obtained from TgBDNF mice at 2–3 months versus 6–7.5 months, with significance defined as $p < 0.05$. Unless otherwise stated, results are reported as group mean values \pm the standard error of the mean (SEM). Additionally, to test for significant interaction, a two-way ANOVA was performed for all measures, with Genotype and Age as between-subject variables.

2.4 Results

2.4.1 BDNF protein levels are increased in the transgenic olfactory bulb

In the OB, CAMKII α is expressed by GABAergic GCs and a subpopulation of glomerular neurons. Due to the expression of BDNF under the CAMKII α promoter, we have previously shown that increased levels of BDNF mRNA were visible by in situ hybridization in the OB GCL and parts of the GL in TgBDNF mice when compared to WT mice (McDole *et al.*, 2015). Increases in BDNF protein were also detectable in the OB. Using ELISA assay, significant increases in BDNF were measured in the OB of transgenic mice when compared to WT controls (Figure 10A, $p < 0.0001$; unpaired *t*-test). Mature BDNF bands at 14 kDa, were detectable in Western blots of bulb lysates.

TgBDNF bulb samples showed a significant increase in BDNF band density when compared to WT control samples (figure 10B, C, $p < 0.05$, unpaired t -test).

2.4.2 GC dendritic lengths and branch complexity

BDNF has known effects on dendrites in several neuron populations around the CNS. In order to determine BDNFs effects on GC dendritic complexity, GCs were reconstructed, and morphometric analysis was carried out. Multiple subtypes of GCs exist in the adult rodent OB making the morphology vary between each GC. Based on previous work, neurons were grouped based on the distribution of their apical dendrites and placement of the GC soma in the GCL. GCs reconstructed most resembled type 1 or 2 GCs described by Greer 1987 or superficial GCs, which appeared similar to type V cells (Greer, 1987; Nagayama, Homma and Imamura, 2014). Two-way ANOVA revealed no interaction of Age and Genotype for any morphometric analysis except for apical dendritic length ($F_{1,10} = 10.79$, $p = 0.013$). TgBDNF mice showed no significant differences in mean apical, basal or total dendritic lengths compared to age matched WT controls (Figure 12A, B, $p > 0.05$, unpaired t -test). However, TgBDNF mice 2-3 months of age had significantly longer dendrites when compared to TgBDNF mice 6-7.5 months of age (Figure 12B, $p < 0.05$, unpaired t -test). Apical, basal and total mean branch number between WT and TgBDNF GCs at both ages was not significantly different, and branch number ranged between 1-7 branches per GC for both genotypes. Sholl analysis was done on the GC apical dendrites and no significant differences were seen in intersections between genotypes at either age (Figure 12C, D).

2.4.3 Over-expression of BDNF by GCs increases their dendritic spine number and density

Next, we focused the analysis on the GCs dendritic spines in both apical and basal compartments of the dendrite. During reconstruction, GC dendritic spines were classified as either headed (mature type), filopodia or “other” type spines and examples of these are shown in figure 9C. Younger WT mice had a mean total spine number of 79.8 ± 5.4 SEM, compared to 130 ± 11.5 in TgBDNF mice ($p < 0.05$, unpaired, two-tailed t-test, $t(3) = 3.31$). In older WT animals, mean total spine number measured 80.9 ± 8.9 compared to 119.0 ± 2.0 in TgBDNF animals. Headed spines were included in the significant changes seen in TgBDNF mice at both ages. At the 2-3 month age, TgBDNF had an mean headed spine number of 69.2 ± 1.9 , which is 25% more than the WT headed spine number average of 49.8 ± 0.9 ($p < 0.01$, unpaired t-test, $t(3) = 7.76$). These significant increases were also seen in the 6-7.5 month old mice where TgBDNF GCs had a mean headed spine number of 67.4 ± 1.9 and WT GCs had a mean headed spine number of 46.8 ± 4.1 ($p < 0.01$, t-test, $t(4) = 4.56$). In addition to total dendrite, apical and basal dendrites were investigated separately. In younger mice, WT GCs had a mean headed spine number of 42.5 ± 1.7 , compared to the Tg GCs 62.6 ± 0.8 ($p < 0.01$, unpaired t-test, $t(3) = 12.14$). Numbers of other-type and filopodia-type spines did not significantly differ between the genotypes at either time point. Relative proportions of the different spine types are seen in figure 14. These did not differ between the 2-3 and the 6-7.5 month old mice for both WT and TgBDNF animals. As shown in figure 15A and B, at 2-3 months, TgBDNF animals had significantly higher mean total spine density at 0.47 ± 0.02 per μm compared to the WT mean total spine density 0.31 ± 0.02 per μm ($p <$

0.05, unpaired t-test, $t(3)=4.47$), a difference that remained stable with age. As illustrated in figure 15C and D, mean headed spine density on the apical dendrites was again significantly increased by 20% in TgBDNF mice (0.237 ± 0.006 per μm), when compared to WT controls (0.185 ± 0.005 per μm ; $p<0.05$, t-test, $t(3)=5.51$). This difference reached 30% in older animals ($p<0.05$, unpaired t-test). No significant effects of age were seen within either genotype for all spine density measurements ($p>0.05$, unpaired t-tests). TgBDNF mice at 2-3 months had a greater spine density in the basal dendrites when compared WT basal dendrites ($p<0.05$), although total numbers did not differ significantly.

2.4.4 BDNF-mediated changes in spine density occur in proximal and distal dendritic domains

To determine if there are specific dendritic regions that show differences between genotypes, apical dendrites were divided into proximal, middle and distal portions for both age groups. Differences were seen in the proximal region for both age groups. In 2-3 month old mice, GCs in TgBDNF mice had significantly greater mean spine densities here (0.47 ± 0.04 per μm) when compared to WT spine densities (0.31 ± 0.01 per μm , $p<0.05$, figure 15E, unpaired t-test, $t(3)=3.35$). In older animals, TgBDNF mice had a mean spine density of 0.48 ± 0.04 per μm , compared to the WT mean spine density of 0.305 ± 0.03 per μm (Figure F, $p<0.05$, unpaired t-test, $t(4)=3.92$). No significant differences were seen in the middle portions of the dendrites between the genotypes for either age group ($p>0.05$, unpaired t-tests). However, significant differences were seen between genotypes in the distal compartments for both age groups (Figure 15E, F, at 2-3 months, TgBDNF = $0.46/\mu\text{m} \pm 0.03$, WT = 0.31 spines/ $\mu\text{m} \pm 0.01$, $p<0.05$, t-test,

$t(3)=3.79$; at 6-7.5 months, $TgBDNF=0.46 \pm 0.01/\mu m$, $WT=0.33 \pm 0.05/\mu m$, $p<0.05$, $t\text{-test}(4)=2.94$)

2.5 Discussion

Olfactory GCs are integral to the functional processing of odor information that ultimately is sent from the OB to higher CNS olfactory areas. Normal bulb circuitry relies on the connectivity of axonless, inhibitory GCs with excitatory bulb output neurons through their dendritic branches and ongoing spine elaboration/plasticity. In this study we used Golgi-Cox impregnation, 3D neuron reconstruction and quantitative morphometric analysis to demonstrate that elevating levels of endogenous BDNF in the OB increases the number and density of GC spines *in vivo*. Significant increases in numbers of mature spines were found in the distal apical dendritic compartment where GCs communicate with MTCs through dendrodendritic synapses. These increases were seen in both the 2-3 month- and 6-7.5-month-old *TgBDNF* mice, indicating that elevations in spine number and density remain stable throughout aging. Our findings demonstrate that endogenous BDNF is capable of shaping GC structure/connectivity to modify OB circuitry. These results compliment recent findings by Bergami et al. (2013) documenting that genetic elimination of *TrkB* receptor expression in abGCs reduces their dendritic spine density *in vivo* (Bergami *et al.*, 2013).

Total apical dendritic spine densities in our control mice ranged from 0.27 to 0.30 spines/ μm , densities similar to measures reported for control mice in experiments that used Golgi staining or lentivirus-mediated gene transfer of green fluorescent protein (GFP) to label established or abGCs, respectively (Greer, 1987; Dahlen *et al.*, 2011; Mandaïron *et al.*, 2018). Mature, or “headed” spine densities on apical dendrites in our

WT mice averaged $\sim 0.18/\mu\text{m}$ which closely resembles densities reported for distal apical dendrites of mature GCs ($\sim 0.20/\mu\text{m}$) measured in acute bulb slices (Breton-Provencher, Cote and Saghatelian, 2014). Filopodia were classified in the present study as long, headless extensions reaching $2.5\mu\text{m}$ or more and our analysis resulted in lower GC filopodia numbers compared to previous studies, which we attribute to their inclusion of shorter headless spines in their criteria (M. C. Whitman and Greer, 2007; Breton-Provencher, Cote and Saghatelian, 2014). Spine types that did not meet our criteria for headed or filopodia-type spines were classified here as "other-type" spines. This category may include immature spines undergoing morphological changes, due to the continuous, rapid turnover and plasticity of GC spines which has been documented in vivo (Mizrahi, 2007; Livneh and Mizrahi, 2011; Sailor *et al.*, 2016). For example, spines on mature GCs can undergo a full cycle of genesis, starting with initial protrusion, extension to filopodia, and then spine retraction/disappearance in as little as 20 min (Mizrahi, 2007; Breton-Provencher, Cote and Saghatelian, 2014; Sailor *et al.*, 2016). An ongoing plasticity seen in other neuron types throughout the forebrain (Parnass, Tashiro and Yuste, 2000; Holtmaat *et al.*, 2005). These other-type spines made up $\sim 35\%$ of all spines in mice of both genotypes at all ages, suggesting that GCs in TgBDNF mice possess an ongoing spine plasticity similar to that seen in WT mice.

GCs in TgBDNF mice exhibited a significant increase in numbers of headed, mature dendritic spines when compared to numbers in WT mice. This contrasts with GCs observed in cultured neonatal OB slices that show increases in filopodia-type spines and more elaborate dendritic branching when treated with BDNF (Shinji Matsutani and Yamamoto, 2004). Differences between these results may be due to the differences in GC

maturity and as well as how the BDNF was presented (over-expression of endogenous BDNF *in vivo* vs. exogenous BDNF administration *in vitro*). Other CNS neurons, also show different responses to BDNF *in vivo* and *in vitro* that vary with cell maturity. *In vitro* treatment with exogenous BDNF on primary hippocampal cultures yields more complex branching in young primary hippocampal neurons (3 days *in vitro*) with little effect on the dendritic complexity of mature primary hippocampal neurons (23 days *in vitro*) (Kellner *et al.*, 2014). However, reducing endogenous BDNF signaling using BDNF blocking antibodies decreases total spine density in the mature primary hippocampal neuron cultures (Kellner *et al.*, 2014). Conditional, *in vivo* ablation of BDNF in adult mice decreased the dendritic complexity of apical dendrites and the frequency of mushroom-type spines without changing overall spine density in CA1 pyramidal neurons (Rauskolb *et al.*, 2010). BDNF-e6 mice lack BDNF mRNA transcript production from their exon 6 splice variant and this results in decreased dendritic complexity in both CA1 and CA3 hippocampal neurons and the loss of large, pedunculated headed spines in CA1 hippocampal neurons (Maynard *et al.*, 2017).

Although the presence of synapses cannot be demonstrated with Golgi-Cox staining, the majority of functional glutamatergic synapses in the CNS are located on spines that exhibit mature morphology, defined by a thin neck and a bulbous head (normally termed “mushroom spine”), though these vary in size in different neuronal populations. (Harris and Stevens, 1989; Schikorski and Stevens, 1999; Hering and Sheng, 2001; Bosch and Hayashi, 2012; Hruska *et al.*, 2018). The increased number of headed spines observed on GC distal apical dendrites in TgBDNF mice suggests that BDNF promotes the maturation and maintenance of glutamatergic synapses on these neurons,

specifically as part of the reciprocal dendrodendritic synapses made with the MTCs (Woolf, Shepherd and Greer, 1991; M. C. Whitman and Greer, 2007). Higher levels of OB BDNF also increased spine density on the proximal and basal dendrites of GCs in these mice. GCs receive multiple excitatory inputs with spatially organized distributions along the dendritic arbor (Price and Powell, 1970; Balu, Pressler and Strowbridge, 2007; Ennis, Hamilton and Hayer, 2007; Laaris, Puche and Ennis, 2007; Matsutani and Yamamoto, 2008; Cauthron and Stripling, 2014). Changes in proximal and basal spine densities suggest increased innervation from populations of neurons in higher forebrain regions that target these dendritic compartments (Balu, Pressler and Strowbridge, 2007; Laaris, Puche and Ennis, 2007; Shepherd *et al.*, 2007; Kelsch, Lin and Lois, 2008). Innervating populations include excitatory centrifugal afferents from the AON and piriform cortex that form axodendritic and axosomatic synapses with the GC population (Shepherd *et al.*, 2007; Matsutani and Yamamoto, 2008; Deshpande *et al.*, 2013). Both of these areas also express increased BDNF under the CamKIIa promoter in TgBDNF mice, suggesting that BDNF from centrifugal neurons may exert anterograde effects on GC spine development as well (McDole *et al.*, 2015; Smail *et al.*, 2016).

GCs also receive GABAergic innervation from local short axon cells, as well as centrifugal afferents from the horizontal limb of the diagonal band (Kunze *et al.*, 1992; Eyre, Antal and Nusser, 2008; Gracia-Llanes *et al.*, 2010; Pallotto *et al.*, 2012). BDNF effects are not limited to excitatory inputs on spines, and its ability to regulate inhibitory circuit development in the CNS have been recently documented (Gottmann, Mittmann and Lessmann, 2009; Jiao *et al.*, 2011). In the visual cortex, increased BDNF expression in TgBDNF mice significantly reduces the duration of the sensory critical period by

accelerating the maturation of inhibitory circuitry (Huang *et al.*, 1999). Cultures of visual cortical neurons exposed to higher BDNF levels develop increased GABA_A receptor expression (Mizoguchi *et al.*, 2003), while neocortical neurons in which BDNF expression is knocked down in vitro develop fewer GABAergic terminals on their somata compared to neurons that express BDNF (Kohara *et al.*, 2007). Early development of GABAergic synapses on the proximal dendrite and soma of adult-born GCs is required for their normal apical dendritic development and functional integration; if this is inhibited, dendritic branching and spine density are significantly reduced (Pallotto *et al.*, 2012). Further research is needed to determine how local BDNF levels/TrkB signaling may alter the inhibitory as well as excitatory connectivity of OB GCs.

Our ELISA results indicate that GCs in TgBDNF mice are likely to be exposed to elevated levels of BDNF in adult mice. During postnatal development, the initial GC population is established during the first three postnatal weeks, but new GCs continue to migrate to the OB from the SVZ throughout adulthood (Frazier-Cierpial and Brunjes, 1989; Whitman and Greer, 2009). Both early-established and adult-born populations of GCs express full-length TrkB and are therefore responsive to BDNF (Frazier-Cierpial and Brunjes, 1989; Nef *et al.*, 2001; Bergami *et al.*, 2013). Under the CAMKII α promoter, significant increases in BDNF mRNA expression occur in all GCs throughout the GCL of TgBDNF mice and is shown in figure 8 (McDole *et al.*, 2015). BDNF may then act as an autocrine or paracrine factor on the GC population, potentially through dendritic spine release (Kolarow, Brigadski and Lessmann, 2007; An *et al.*, 2008; Kuczewski, Porcher and Gaiarsa, 2010; Orefice *et al.*, 2013; Harward *et al.*, 2016). Evidence for CNS autocrine BDNF signaling is mounting. In cultured murine

hippocampal slices BDNF has been shown to act on dendritic spines on CA1 pyramidal neurons through autocrine dendritic release and TrkB signaling (Harward *et al.*, 2016). In neonatal cortical slices, BDNF shows both autocrine and paracrine effects on dendritic branching of neighboring pyramidal neurons up to 4.5µm away, an effect which is blocked with TrkB-IgG treatment to inhibit BDNF/TrkB signaling (Horch and Katz, 2002). Moreover, individual cortical and hippocampal neurons over-expressing BDNF in adult mice exhibit increased spine development compared to their neighboring cells that lack the genetic increase, demonstrating that autocrine BDNF signaling can occur in vivo as well (English, 2012; Wang *et al.*, 2015).

MTCs participate in dendrodendritic synapses with GCs, and because these output neurons express TrkB, excess BDNF expressed by GCs mice may act on the MTCs via this paracrine route (Hinds and Hinds, 1976; Deckner *et al.*, 1993; Panzanelli *et al.*, 2009). There is ample evidence that dense core vesicles transport BDNF in both neuronal axons and dendrites for synaptic release (Gottmann, Mittmann and Lessmann, 2009; Kuczewski, Porcher and Gaiarsa, 2010; Edelmann, Leßmann and Brigadski, 2014). BDNF synaptic release is activity/Ca²⁺-dependent, and BDNF-containing vesicles can be recruited to both activated dendritic and axon synaptic sites (Dean *et al.*, 2012; Hartmann *et al.*, 2012). There are two versions of BDNF mRNA produced in hippocampal and cortical neurons that vary in the length of their 3' UTR, and these sequences determine if the mRNA will be translated in the soma or in dendritic spines. BDNF mRNA transcripts with the short 3' UTR remain and are translated in the cell body, and the protein is packaged into secretory vesicles that are transported for release (Gottmann, Mittmann and Lessmann, 2009; Kuczewski, Porcher and Gaiarsa, 2010; Dean *et al.*, 2012;

Edelmann, Leßmann and Brigadski, 2014). The BDNF mRNA transcripts containing the long 3' UTR are dendritically transported and in this location regulate dendritic spine maturation and pruning in cultured neonatal hippocampal neurons (An *et al.*, 2008; Kaneko *et al.*, 2012; Orefice *et al.*, 2013). TgBDNF mice over-express a BDNF mRNA transcript that lacks the normal endogenous long UTR and is therefore not targeted to the dendritic compartment (An *et al.*, 2008). However, the BDNF protein translated in neuronal somata would undergo normal packaging into secretory vesicles followed by dendritic trafficking of these vesicles (Huang *et al.*, 1999; Gharami *et al.*, 2008).

The OB continues to incorporate new GCs throughout adulthood, and whether BDNF availability affects their integration has yet to be determined. AbGCs initially over-produce dendritic spines before eliminating some of these they mature through a pruning process (M. C. Whitman and Greer, 2007; Nissant and Pallotto, 2011; Pallotto *et al.*, 2012). The signals that control selective spine elimination are not well understood, although sensory activity is proposed to play a role. Conditional BDNF knockout in adult mice has demonstrated that BDNF is required for long-term spine maintenance/stability in both excitatory and inhibitory CNS neuronal populations (Rauskolb *et al.*, 2010; Kaneko *et al.*, 2012; Vigers *et al.*, 2012). Determining if BDNF promotes the maturation and maintenance of spines as abGCs integrate into the OB may give us valuable insight into BDNF's role in regulating adult OB circuitry in conjunction with ongoing adult neurogenesis. Additional studies are needed to determine if increased OB BDNF availability impacts the process of adult olfactory neurogenesis, and studies examining this are described in following chapters.

PART III: OVER-EXPRESSION OF BDNF IN THE OLFACTORY BULB DOES NOT INCREASE ADULT-BORN GRANULE CELL SURVIVAL

3.1 Abstract

Throughout adulthood in rodents, new neurons are continuously generated and incorporated into the OB and hippocampal dentate gyrus. The majority of neurons incorporated into the adult OB are GCs, the bulb's largest population of inhibitory interneurons which regulate the output of the excitatory projection neurons, the MTCs. Many internal and environmental factors are known to promote the successful integration and survival of new GCs. The neurotrophin BDNF regulates the survival and differentiation of developing neurons in the PNS, and the growth and maintenance of spines in multiple neuronal populations in the adult brain. Moreover, evidence shows that BDNF also regulates adult hippocampal neurogenesis, promoting enhanced survival of adult-born dentate GCs. Prior studies have shown that increasing BDNF in the adult rodent SVZ stimulates neurogenesis to increase the numbers of new OB GCs. However, other investigators performing similar studies using intraventricular infusions of BDNF or viral-mediated BDNF gene transfer in the VZ/SVZ failed to find any effects on the generation or survival of adult-born OB GCs. The enhanced survival of hippocampal GCs appears to be due to the local effects of increasing BDNF in the dentate gyrus, where new GCs are born and mature. The aim of this study is to determine if increasing endogenous BDNF in the GCL of the OB, where new olfactory GCs mature and

integrate, also promotes the survival of this population. In order to determine this, we used transgenic mice that over-express BDNF under the CamKII α promoter (TgBDNF mice). This transgene drives increased BDNF expression throughout OB GC population. Adult TgBDNF mice and control WT littermates were treated with BrdU, which incorporates into dividing SVZ stem cells and the GCs these ultimately give rise to. Sections through the OBs were co-labeled using antibodies to BrdU and the neuronal nuclear protein (NeuN), to quantify numbers of surviving abGCs at 2, 4, and 9 weeks after BrdU treatment. Changes in programmed cell death in the GCL were determined using the TUNEL labeling technique, which detects DNA fragmentation associated with apoptosis. My findings indicate that increasing BDNF in the OB GCL does not impact the survival of new GCs at any of the time points examined. TgBDNF mice and WT mice showed no differences in the numbers of BrdU+ cells or TUNEL + cells in the GCL. These findings show that although increasing local levels of BDNF in hippocampus may enhance survival of dentate GCs, it does not enhance the survival of abGCs in the OB.

3.2 Introduction

The rodent OB continuously incorporates new neurons throughout adulthood. About 95% of the neurons generated are olfactory GCs, the main population of inhibitory interneurons responsible for the modulation of out-going sensory information to higher olfactory brain areas (Urban, 2002; Lledo, Saghatelian and Lemasson, 2004; Saghatelian *et al.*, 2005; Mori, Nagao and Yoshihara, 2007; Shepherd *et al.*, 2007; Abraham *et al.*, 2010; Livneh, Adam and Mizrahi, 2014) . These adult-born neurons are generated from neural stem cells in the SVZ and migrate as neuroblasts through the RMS to the OB. Once in the OB, neuroblasts migrate radially into the GCL and develop into functioning,

mature neurons (Petreanu and Alvarez-Buylla, 2002; Carleton *et al.*, 2003; Whitman and Greer, 2009). Normally, about 50% of these new neurons undergo programmed-cell death and fail to fully integrate functionally (Petreanu and Alvarez-Buylla, 2002; Lemasson *et al.*, 2005). A wide variety of extrinsic and intrinsic signals regulate adult olfactory neurogenesis, with neural activity playing a major role.

Among the intrinsic factors identified, the growth factors FGF-2, epidermal growth factors (EGF), vascular endothelial growth factor (VEGF), connective tissue growth factor (CTGF), and Betecellulin (BTC) have all been shown to play a role in the regulation of SVZ stem cells proliferation and/or net neurogenesis (Jin *et al.*, 2002; Sun *et al.*, 2006; Gomez-Gaviro *et al.*, 2012; Lindberg *et al.*, 2012; Khodosevich *et al.*, 2013). The neurotrophins are a family of secreted peptides that aid in the growth, differentiation and survival of developing neurons (Patapoutian and Reichardt, 2001; Reichardt, 2006). BDNF is one member of this family that has been implicated in olfactory neurogenesis (Zigova *et al.*, 1998; Benraiss *et al.*, 2001; Xie, Hayden and Xu, 2010). BDNF gene expression and secretion is Ca²⁺ regulated and activity dependent, and it acts through binding the receptor tyrosine kinase TrkB (Patapoutian and Reichardt, 2001; Kolarow, Brigadski and Lessmann, 2007; Dean *et al.*, 2012; Hartmann *et al.*, 2012; Kellner *et al.*, 2014). In the OB, all neuronal populations express TrkB and abGC's begin to express full-length TrkB receptors shortly after they arrive in the OB, making BDNF an attractive candidate factor to investigate in the development and survival of these interneurons (Masana *et al.*, 1993; Imamura and Greer, 2009; Bergami *et al.*, 2013).

BDNF-null animals typically die at early postnatal ages (2-3 weeks of age), so determining BDNFs full role in OB development and adulthood cannot be assessed in

null mouse strains, however the OB in BDNF null mice shows normal, gross anatomical organization (Maisonpierre *et al.*, 1990; Kolbeck *et al.*, 1999; Nef *et al.*, 2001; Berghuis *et al.*, 2006). Conditional knock-out mice have shown that BDNF is required for postnatal growth of some brain areas, particularly the striatum, while the rest of the brain appears largely normal and shows no evidence of significant neuronal death (Rauskolb *et al.*, 2010). Instead, the effects of conditional BDNF depletion in postnatal or adult mice are evident as reductions in spine numbers and density in multiple neuronal populations (Gorski *et al.*, 2003; Rauskolb *et al.*, 2010; Vigers *et al.*, 2012).

In terms of adult neurogenesis, manipulations of hippocampal BDNF levels or TrkB signaling have been shown to alter survival of new dentate GCs in rodents. Wheel running increases hippocampal BDNF levels, and stimulates neurogenesis (Kobilo *et al.*, 2011; Marlatt *et al.*, 2012; Vivar, Potter and van Praag, 2012; Toda and Gage, 2017). Forebrain BDNF knockout and impaired activity-dependent release of BDNF in adults reduces dentate GC survival and prevents running induced increases in numbers of new dentate GCs, while TrkB knockout in these neurons reduced long term survival (Bergami *et al.*, 2008; Bergami, Berninger and Canossa, 2009; Gao, Smith and Chen, 2009; Taliaz *et al.*, 2010; Ieraci *et al.*, 2016). Manipulations to test BDNF effects on olfactory neurogenesis have focused on the SVZ and its progenitor cells, rather than the OB, where new GCs incorporate. Increasing BDNF in the VZ/SVZ by intraventricular injections of BDNF or BDNF-encoding viruses was shown to increase the numbers of new GCs accumulating in the OB (Zigova *et al.*, 1998; Benraiss *et al.*, 2001). Conversely, mice heterozygous for BDNF (BDNF^{+/-}) and mice expressing a variant form of BDNF have smaller numbers of abGCs in the OB (Bath *et al.*, 2008). Although these studies are in

agreement with BDNF being a survival factor, other research has indicated otherwise. Replications of earlier SVZ BDNF injection studies, as well as genetic deletion of TrkB in new GCs, have shown that BDNF applied to the SVZ has no effect on numbers of surviving abGCs (Galvao, Garcia-Verdugo and Alvarez-Buylla, 2008; Bergami *et al.*, 2013). Since BDNF's receptor TrkB is not expressed until after GCs arrive in the OB, it is here that increasing levels of BDNF may impact their development and long term survival (Bergami *et al.*, 2013). This factor is normally expressed at low levels in the rodent OB, but is highly expressed in external sources that include centrifugal afferents from the piriform cortex and the AON (Hofer *et al.*, 1990; Phillips *et al.*, 1990; Guthrie and Gall, 1991; Conner *et al.*, 1997; Clevenger *et al.*, 2008; McDole *et al.*, 2015). In this study we employ a transgenic mouse strain to genetically increase levels of BDNF expression in the OB GCL, as well as in the olfactory cortices (Huang *et al.*, 1999). Using BrdU cell birth-dating, immunofluorescent cell markers, TUNEL staining and confocal microscopy, we demonstrate that increasing BDNF in the GCL does not increase survival of abGCs or reduce cell death in the GC population.

3.3 Materials and methods

3.3.1 Animals

Animal procedures were carried out in accordance with the National Institutes of Health Guidelines for the Care and Use of Laboratory Animals under protocols approved by the Florida Atlantic University Animal Care and Use Committee. The TgBDNF mice are maintained on a C57Bl6/J background (Jackson Laboratories strain #006579; Bar Harbor, ME), and in addition to the native BDNF gene, carry a transgene that encodes rat BDNF under the control of the CAMKII α promoter (Huang *et al.*, 1999). CAMKII α is

expressed in the OB by a subpopulation of glomerular neurons and by GABAergic GCs, resulting in significantly increased bulbar BDNF levels (Zou, Greer and Firestein, 2002; McDole *et al.*, 2015). Although the transgene is not expressed by mitral cells, which lack CAMKII α expression, it is highly expressed by other glutamatergic, CAMKII α -expressing neurons throughout forebrain, including those that project to the bulb from the AON and piriform cortex (Huang *et al.*, 1999). TgBDNF males were bred with WT females to obtain litters containing both TgBDNF and WT offspring. To verify the presence of the transgene, genomic DNA was isolated from tail samples for PCR amplification using the following primers: 5'-GTGAAGGAACCTTACTTCTGTGGTG-3' AND 5'-GTCCTTGGGGAAGCTGAGGA-3. Cycling parameters were: 94°C-30s, 54°C-30s, 72°C-45s (32 cycles).

3.3.2 BrdU injections

WT and TgBDNF mice at 7.5-8 weeks of age were treated once daily with 5-bromo-2'-deoxyuridine (BrdU: i.p., Roche Life Sciences, #10-280-879) at a dose of 50 mg/kg for four consecutive days. Mice survived for 2, 4 or 9 weeks after the first BrdU injection (n=4, 2 males and 2 females per genotype and time point). Animals were euthanized with sodium pentobarbital (150 mg/kg in Euthasol, i.p.) and transcardially perfused with PBS (pH 7.3), followed by 4% paraformaldehyde in 0.1 M PB (pH 7.35, 4°C). Brains were dissected and postfixed overnight at 4°C and cryoprotected in 30% sucrose in PB for 3-4 days (4°C). Forebrains were embedded in 10% gelatin, postfixed for 4-5 hours and returned to 30% sucrose (4°C). Tissue was snap frozen in isopentane (-45°C) and stored at -80°C. Brains were sectioned in a cryostat (-21°C; 30 μ m) and serial,

free-floating coronal sections were collected through the bulbs (1 in 5) for immunostaining and TUNEL labeling.

3.3.3 Immunofluorescence

Combined labeling for BrdU and NeuN was used to identify adult-born GCs. Serial sections incubated in 0.6% H₂O₂ for 8 min, followed by 50% formamide in 1x saline-sodium citrate buffer for 30 min at 65°C. Sections were transferred to 2N HCl for 30 min at 37°C, then 0.1 M sodium borate (pH 8.5) for 10 min. After blocking in 5% normal goat serum, sections incubated for 3 nights at 4°C in rat antibody to BrdU (1:400; #OBT0030; Accurate Chemicals, Westbury, NY; Antibody registry: AB_2313756) combined with mouse antibody to NeuN (1:500; #MAB377, EMD Sciences/Millipore, Temecula, CA; Antibody registry: AB_2298772). Secondary cocktail contained mouse-adsorbed AlexaFluor (AF)-488-conjugated goat anti-rat IgG (#A-11006) and AF594-labeled goat anti-mouse IgG (#A-11032, Life Technologies, Grand Island, NY), each diluted 1:1000.

3.3.4 Imaging

Serial bulb sections from age- and sex-matched WT and TgBDNF littermates were processed together for immunolabeling. Confocal image collection was performed with a Zeiss 710 LSM at 20x objective magnification (zoom factor 1.3; 1 airy unit = 4 µm). Collection started in the anterior bulb where the GCL measured ~1 mm from dorsal to ventral. A sample box (150 µm x 250 µm; 0.16 µm/pixel) was placed in each of four regions of the GCL (ventral, medial, dorsal, lateral) with one outer edge positioned superficially along the internal plexiform layer, and the remaining box extending down over the GCL as shown in figure 16 and previously described in (Smail *et al.*, 2016).

Images of immunolabeling for each marker were collected for each sample region (BrdU only, NeuN only, and combined labeling). These were used for cell counts using NIH ImageJ software and the Cell Counter plugin (Rasband *et al*, 2010; de Vos *et al*, 2010). Six serial sections (both bulbs) were imaged per subject, giving a total of 48 sample regions per animal. In each section 0.15 mm² of the GCL was sampled for a total GCL sample area of 1.8 mm² per subject. Numbers of Brdu+ and BrdU+/NeuN+ cells were counted for each subject and used to calculate the mean density of labeled cells, and the proportion of presumptive glia (BrdU+ only). Orthogonal projections of z-stacks (0.7 µm steps) were used to verify nuclear co-localization of BrdU and NeuN in random labeled cells in the GCL of each subject. Group mean values were calculated from mean cell counts and densities measured in each subject (+/- SEM). Unpaired, two-tailed *t*-test comparisons were performed to test for significant differences between genotypes ($p < 0.05$).

3.3.5 Terminal deoxynucleotidyl transferase dUTP nick end labeling (TUNEL)

Slide-mounted serial sections were processed for TUNEL labeling of apoptotic cells as described (Smail *et al.*, 2016). Treatment included incubation with 40 mg/ml (~1.5 units/ml) proteinase K for 20 min at 37°C, followed by 2.5 hrs of incubation in TUNEL reaction solution at 37°C [25mM Tris-HCl, 200mM Na cacodylate, 0.25mg/ml BSA, 1mM cobalt chloride, 13mM biotin-14-dATP (Life Technologies, #19524-016), 200U/ml terminal transferase (New England Biolabs, Ipswich, MA, #M0315)]. Following overnight incubation in avidin-biotin-HRP complex (1:100; Vector Laboratories), chromagen was developed with Vector's Impact-DAB kit as above. Controls included pre-treatment of some sections with DNase (5 units/µl, Sigma-

Aldrich, St. Louis, MO), as well omission of terminal transferase. Numbers of TUNEL+ cells per bulb (left and right) were counted microscopically in the GCL (40x objective magnification) from 6 serial sections (150 μ m spacing), starting with the most caudal section anterior to the appearance of the AOB GCL, and moving rostrally. Counts included labeled cells in the subpendymal layer. Cell counts were made in 5 WT and 5 TgBDNF mice. Group mean values were calculated from total cell counts obtained for bulbs in individual subjects for each genotype (+/-SEM). Unpaired, two-tailed *t*-test comparisons with Welch's correction were performed to test for significant differences between genotypes ($p < 0.05$).

3.4 Results

In previous studies, BDNF was increased in the SVZ/ventricles in order to determine its effects of olfactory neurogenesis via the stem cell niche. However, full length TrkB is only expressed on abGCs after they reach the OB, and increasing BDNF here could potentially impact their development and survival. In order to determine how increased BDNF affects abGC survival, TgBDNF and WT mice received BrdU treatment and new bulb GCs were quantified over three time points. As shown in figure 16, large numbers of new cells were present at 2 weeks post-injection in both WT and TgBDNF mice. Mean density of BrdU+/NeuN+ cells in the WT GCL was 505.4/mm² +/- 38 SEM, and in TgBDNF mice measured 560.4 cells/mm² +/- 39 SEM ($p > 0.05$, unpaired *t*-test, $t(6) = 0.345$). By 4 weeks, gradual elimination of some new cells by apoptosis reduced mean numbers of BrdU+/NeuN+ cells in WT mice to 433.6/mm² +/- 42 SEM, while the mean density in TgBDNF mice dropped to 460.6/mm² +/- 45 SEM ($p > 0.05$, unpaired *t*-test, $t(6) = 0.674$). By 9 weeks, mean density of BrdU+/NeuN+ cells in the WT GCL fell

to 359.4 cells/mm² +/- 55 SEM and to 352.0 cells/mm² +/- 34 SEM in the TgBDNF GCL (p>0.05, unpaired t-test, t(6) = 0.913). Between 2 and 9 weeks, the density of BrdU+/NeuN+ cells in the GCL dropped ~31% for WT mice, and ~36% for TgBDNF mice. BDNF over-expression therefore did not increase survival of abGCs. This was also reflected in the numbers of TUNEL+ cells in the GCL, which did not differ in TgBDNF and WT mice (Figure 17, p>0.05, t-test with Welch's correction, t(6)=0.961).

3.5 Discussion

From the birth of abGCs to their complete integration into OB circuitry, a wide variety of factors-influence their development and survival. Here, we injected transgenic mice that over-express BDNF in the GCL of the OB with BrdU to test BDNF's ability to promote long-term abGC survival. TUNEL staining was used to assess BDNF's impact on levels of programmed cell death. Using these approaches, we have shown that increasing endogenous BDNF availability in the OB does not promote the survival of abGCs beyond normal levels, or reduce their apoptotic death in vivo.

Previous work has implicated BDNF as a regulatory factor in adult olfactory neurogenesis, primarily by altering BDNF levels in the SVZ to impact resident stem cells. Low levels of BDNF are detectable in the rodent SVZ, however BDNF is mainly detected in the RMS and OB (Maisonpierre *et al.*, 1990; Galvao, Garcia-Verdugo and Alvarez-Buylla, 2008; Snapyan *et al.*, 2009; Bagley and Belluscio, 2010), Truncated TrkB, which lacks the intracellular kinase domain, is expressed by both ependymal cells and slowly dividing type B cells in the SVZ and on migrating neuroblasts in the RMS (Chiaramello *et al.*, 2007; Bath *et al.*, 2008; Galvao, Garcia-Verdugo and Alvarez-Buylla, 2008). Although full-length TrkB expression remains absent in SVZ stem cells, migrating

neuroblasts express full-length TrkB upon entering the OB (Galvao, Garcia-Verdugo and Alvarez-Buylla, 2008; Bath, Akins and Lee, 2012; Bergami *et al.*, 2013). The presence of full-length TrkB shows that neurons generated in the SVZ can eventually respond to BDNF. This response has been explored through *in vitro* studies using SVZ stem cells. Cultures of SVZ stem cells treated with BDNF show significant increases in cell survival in new neurons by 25% at 42 days compared to untreated cultures (Kirschenbaum and Goldman, 1995). In addition to promoting cell survival, BDNF has shown to play a role in the regulation of normal neuroblast migration *in vitro*. In cultured SVZ tissue, BDNF promoted neuroblast migration through activation of the PI3-K and MAP-K signaling pathways (Chiaramello *et al.*, 2007). Similarly, in acute brain slices, increasing BDNF increased the motility of migrating neuroblasts while decreasing BDNF in slices reduced motility and even altered the direction of neuroblast migration (Bagley and Belluscio, 2010). BDNF also regulated morphology of SVZ cultured neurons by inducing late-phase dendritic development via increased TrkB activation (Gascon *et al.*, 2005).

In vivo, increasing BDNF in the VZ/SVZ by intraventricular BDNF infusions or adenovirus-mediated gene transfer has been used to test for neurogenesis effects on progenitor cell populations. Increasing BDNF via intraventricular administration increased the number of BrdU labeled cells in the OB by 100%, 90% double labeled for a neuron-specific antibody (Zigova *et al.*, 1998). Similar results were obtained when BDNF expression in the SVZ was increased using infection with BDNF-encoding adeno-associated virus (Benraiss *et al.*, 2001). It is important to note that these studies focused mainly on the proliferation and not survival of new born neurons. In the second study, mice were injected with BrdU daily for 2-3 weeks, so cells present in the OB could have

been anywhere from 5 days through 2-4 weeks old depending on the time point. This may mean that increased BDNF stimulated the production of new cells but does not tell us how increased BDNF in the SVZ affected GC survival. In contrast to the evidence pointing to SVZ BDNF treatments stimulating OB neurogenesis, work from the Alvarez-Buylla laboratory replicated several of the studies above using SVZ/intra-ventricular infusions of BDNF and Brdu treatments (Galvao, Garcia-Verdugo and Alvarez-Buylla, 2008). They found no evidence of full-length TrkB in either the SVZ or RMS, and intraventricular infusions of BDNF had no effect on the number of BrdU labeled neurons in the OB in mice, contradicting earlier claims that BDNF regulates SVZ proliferation (Galvao, Garcia-Verdugo and Alvarez-Buylla, 2008). Additionally, this study, as well as a recent study by Bergami et al. deleted full-length TrkB gene expression in SVZ progenitor cells and showed that normal numbers of new GCs migrated to the bulb and matured, challenging some of the earlier findings (Galvao, Garcia-Verdugo and Alvarez-Buylla, 2008; Bergami *et al.*, 2013).

The results of our strategy to up-regulate BDNF expression in the OB, where only about 50% of abGCs normally survive within the first few weeks of their birth, makes it clear that, regardless of BDNF effects on SVZ progenitors, increasing endogenous BDNF in the environment where new GCs mature and integrate does not alter their survival rate. We found no significant differences between WT and TgBDNF mice in terms of the numbers of BrdU+ GCs present at 2, 4 or 9 weeks after BrdU treatment. We also found that numbers of new cells reaching the OB at 2 weeks post-BrdU were not altered by increased OB or striatal BDNF levels in transgenic mice, indicating no significant effects on SVZ cell proliferation (as seen with Ki-67), or on neuroblast migration. These results

are complimented by TUNEL staining results, in which TgBDNF and WT mice showed no significant difference in the prevalence of apoptotic cells in the GCLs. By 9 weeks, the majority of the remaining abGCs would be expected to live long-term, having survived the peak period of normal apoptotic elimination (Kelsch *et al.*, 2009). Although our results indicate that BDNF does not appear to act as a survival factor for new GCs within the OB of TgBDNF mice, where BDNF is increased both locally and in populations of olfactory cortical neurons that project to bulb GCs. Our Golgi staining work demonstrates that over-expression of OB BDNF increases the numbers and densities of dendritic spines in the GC population, including the numbers of mature spines (McDole *et al.*, 2015). This is consistent with numerous studies that have documented BDNF's involvement in the development, maturation and maintenance of spines in many populations of forebrain neurons (Waterhouse and Xu, 2009; Bath, Akins and Lee, 2012; Zagrebelsky and Korte, 2014; Kowiański *et al.*, 2018; Liu and Nusslock, 2018; von Bohlen Und Halbach and von Bohlen Und Halbach, 2018). Such effects could be expected to enhance the synaptic integration of adult-born olfactory GCs, and therefore their survival, but this does not appear to be the case.

Our findings contrast with recent results reported for adult-born dentate gyrus GCs. In the absence of BDNF using knockout mice, BrdU labeled neurons in the hippocampus were reduced by 28.5% after one month (Gao, Smith and Chen, 2009). Similarly, dentate GCs had a reduction in their long-term survival when BDNFs receptor, TrkB, was absent (Bergami *et al.*, 2008). Wheel running increases BDNF levels in the hippocampus and promotes adult neurogenesis (Kobilo *et al.*, 2011; Marlatt *et al.*, 2012; Vivar, Potter and van Praag, 2012; Toda and Gage, 2017). Through TrkB knockout mice,

they showed that BDNF/TrkB signaling was necessary for exercise induced neurogenesis (Li *et al.*, 2008). Meaning in the absence of TrkB, neurogenesis stimulated by wheel running does not take place, this and other studies lead scientists to believe BDNF is one factor responsible for regulating adult hippocampal neurogenesis. Differences between areas of adult neurogenesis may be the result of differences between the populations of new neurons. Unlike adult-born dentate GCs, olfactory GCs lack an axon, are GABAergic and migrate a great deal farther to their destination. These differences may result in olfactory abGCs to not necessarily need BDNF for proliferation and cell survival.

Although over-expression of endogenous BDNF does not increase abGC survival, this does not rule out that reducing or eliminating BDNF in the OB would not have effects. However, this is unlikely the case based on evidence provided in which absence of TrkB on new neurons does not affect the proliferation or survival of abGCs, but hinders survival of the new born PG population (Galvao, Garcia-Verdugo and Alvarez-Buylla, 2008; Bergami *et al.*, 2013). Increasing BDNF does not affect abGC survival, but its role in the maintenance and maturation of GC dendritic spines remains promising and more research is needed to determine how increasing BDNF will affect abGCs *in vivo*.

PART IV- VIRAL-MEDIATED LABELING AND MORPHOMETRIC ANALYSIS OF ADULT-BORN GRANULE CELLS IN TGBDNF MICE

4.1 Abstract

Olfactory GCs are one population of neurons that continue to be born and functionally integrate throughout adulthood in rodents. GCs, both early- and adult-born, are crucial to normal olfactory circuit function and behaviors, and the study of abGCs may be useful for determining the factors that aid in the integration of new neurons into existing circuitries. BDNF is known to regulate dendritic spine growth and maintenance of many CNS neuronal populations. We have previously shown that elevated levels of OB BDNF increase total spine density and the prevalence of mature spines on existing populations of GCs. Similarly, knocking out genetic deletion of TrkB alters normal spine development in abGCs implicates BDNF/TrkB signaling in the development and integration of these interneurons. How changes in local BDNF availability alter the growth and integration of abGCs has not been previously determined. In this study we placed bilateral injections of a lentivirus encoding a tau-mCherry fusion protein into the SVZs of adult TgBDNF and WT mice to compare the structural development of abGCs. OB tissue was collected at 12, 22, 35, and 60 days post-infection, and using confocal microscopy, z-stacks images of labeled cells were collected, and intact GCs were fully reconstructed using Neurolucida/NeuroExplorer software (MicroBrightfield Inc.). Our analyses demonstrate that beginning early in their maturation, increased BDNF significantly enhanced total spine

numbers, as well as numbers of mature spines, in abGCs, and that these effects were maintained into their maturity. Our results indicate BDNF can regulate the density and maturation of spines in abGCs and may therefore promote their structural and functional integration into existing OB circuitry.

4.2 Introduction

The rodent olfactory system continues to generate and incorporate new interneurons throughout adulthood, making this a valuable experimental model in which to identify factors that aid the integration of new neurons into established CNS circuitries, in order to develop potential cell-based therapies for neurological diseases causing neuron loss. Olfactory GCs are an inhibitory population that continues to undergo neuronal turnover throughout life, with newborn GCs replacing established GC that gradually die by apoptosis. These GABA-synthesizing neurons comprise the bulb's largest population of interneurons and are vital for the normal processing of odor information prior to its relay from the OB to higher olfactory areas, including the piriform cortex. These axonless interneurons achieve this through pedunculated, headed spines located on their apical dendrites which form reciprocal dendrodendritic synapses on the lateral dendrites of MTC output neurons, as well as spines located on their basal dendrites and proximal apical dendrite, where inputs from excitatory centrifugal afferents modulate their activity (Yokoi, Mori and Nakanishi, 1995; Mori, Nagao and Yoshihara, 1999; Shepherd *et al.*, 2007; Imai, 2014; Nagayama, Homma and Imamura, 2014; Bartel *et al.*, 2015). Elimination of GCs or alterations in their physiological functions can cause irregularities in odor processing and in olfactory-mediated behaviors (Shepherd *et al.*, 2007; Abraham *et al.*, 2010; Gheusi and Lledo, 2014).

New GCs are continuously being added to the adult OB as preexisting GCs are slowly eliminated. These abGCs originate in the SVZ and migrate rostrally through the RMS towards the OB as neuroblasts where they then migrate radially into the surrounding GCL and mature structurally and physiologically (Alvarez-Buylla and García-Verdugo, 2002; Lledo and Saghatelian, 2005; Lledo, Alonso and Grubb, 2006; Whitman and Greer, 2009). Normal GC turnover leads to significant remodeling of OB circuitry as entire GCs are removed and new GCs are functionally integrated, a process that is thought to adapt the system to changes in the animal's odor/sensory environment (Malvaut and Saghatelian, 2016). In rodents, this adult-born interneuron population contributes to OB network synchrony and to specific types of olfactory learning and memory (Lledo, Alonso and Grubb, 2006; Sultan *et al.*, 2010; Alonso *et al.*, 2012; Breton-Provencher and Saghatelian, 2012; Gheusi and Lledo, 2014; Moreno *et al.*, 2014; Sakamoto *et al.*, 2014; Malvaut and Saghatelian, 2016).

The normal GC integration process in rodents has been observed over an ~8 week period following their birth in the SVZ, divided into stages based on their morphology and age (Petreanu and Alvarez-Buylla, 2002; M. C. Whitman and Greer, 2007; Sailor *et al.*, 2016). During the first 2-7 days (post retroviral injection), neuroblasts with bipolar morphology extend a large leading process and smaller following process while migrating towards the OB in the RMS (Petreanu and Alvarez-Buylla, 2002). At days 10-14, GCs have left the anterior RMS and moved radially into the GCL, where they begin to extend a single apical dendrite that rapidly develop branches in the MCL and EPL. By days ~18-20 visible spines (about half immature-type spines) become visible and at day 21, spines are denser along the dendrites and there is an increase in the prevalence of the mature spine

phenotype. During days 28-42, spine density increases from that seen at 21 days, but remains fairly stable during this time frame. Finally, by day 56, spine density decreases due in part to reductions in the proportion of filopodia-type spines, and to spine pruning (cite the new microglia paper showing pruning (Petreanu and Alvarez-Buylla, 2002; M. C. Whitman and Greer, 2007; Sailor *et al.*, 2016). New GCs cells that survive to 2-3 months will usually survive for a year and beyond under normal conditions (Winner *et al.*, 2002). The mechanisms that control the successful incorporation of about half of these new neurons within existing circuitry, while others are eliminated by apoptosis during their first 2-8 weeks, have not yet been fully determined, although neural activity is known to play a dominant role in survival, as well as normal spine and synapse development (Petreanu and Alvarez-Buylla, 2002; Yamaguchi and Mori, 2005; Kelsch *et al.*, 2009; Dahlen *et al.*, 2011).

GC dendritic spines are highly dynamic even in mature cells, turning over at about 20% per day (Mizrahi, 2007; Livneh and Mizrahi, 2011; Sailor *et al.*, 2016). Successful spine maturation and maintenance is required for integration of these axonless neurons as they form functional connections with MTCs and excitatory centrifugal axons. Synaptic activity leading to glutamate release onto spine-located glutamate receptors activates postsynaptic signaling that promotes spine stabilization and growth, as described for hippocampal CA1 neurons following LTP (Tanaka *et al.*, 2008; Panja and Bramham, 2014). However a large body of evidence has shown that BDNF, which is widely expressed in the CNS, aids in the development and maintenance of spines in many different neuron populations in the young and mature brain (Horch and Katz, 2002; S. Matsutani and Yamamoto, 2004; Kohara *et al.*, 2007; An *et al.*, 2008; Waterhouse *et al.*, 2012b;

Orefice *et al.*, 2013; Kellner *et al.*, 2014). Its conditional knockout in developing and adult forebrain reduces spine density in both glutamatergic and GABAergic neurons (Gorski *et al.*, 2003; Rauskolb *et al.*, 2010; Vigers *et al.*, 2012). Synthesized BDNF is released in an activity-dependent manner from axons, however BDNF mRNA can be transported into the dendritic compartment, where it can be locally translated and released at dendritic synapses as well, acting on TrkB receptors on innervating terminals, nearby cells and in an autocrine fashion on spines (Kuczewski *et al.*, 2009; Lessmann and Brigadski, 2009; Harward *et al.*, 2016).

Like the OB, the rodent hippocampus also exhibits adult neurogenesis, and BDNF has demonstrated actions on the morphological development of adult-born dentate GCs. Increases in hippocampal BDNF, including those triggered by wheel running, enhance spine maturation and cell survival in this population (Scharfman *et al.*, 2005; Rossi *et al.*, 2006; Vivar, Potter and van Praag, 2012). In vivo knockdown of either BDNF or TrkB expression in abGCs impairs their dendritic maturation and reduces spine density (Sairanen *et al.*, 2005; Chan *et al.*, 2008; Choi *et al.*, 2009; Gao and Strowbridge, 2009). Prolonged loss of TrkB causes death of new hippocampal abGCs, while conditional over-expression of BDNF only in abGCs in mice lacking forebrain BDNF restores their normal dendritic development (Wang *et al.*, 2015).

BDNF is normally expressed at low levels in the rodent OB, and we have previously shown with Golgi staining that increasing local BDNF levels here leads to increases in spine density throughout the GC population (Guthrie and Gall, 1991; Conner *et al.*, 1997; Clevenger *et al.*, 2008; McDole *et al.*, 2015). Like abGCs in hippocampus, new olfactory GCs begin to express full-length TrkB as they mature (Galvao *et al.*, 2008; Bergami *et al.*,

2013). To determine if increasing BDNF in vivo has morphological effects on the maturation of adult-born olfactory GCs similar to those seen in new dentate GCs, in the present study we use a transgenic mouse line overexpressing a BDNF transgene under control of the α CaMKII α (Huang *et al.*, 1999). We have previously confirmed and quantified genetically increased levels of BDNF expression in the GCL of these mice. Using SVZ lentivirus infection to drive expression of tau-mCherry in new GCs, followed by cell imaging, 3D reconstruction, and quantitative analyses of their morphology, the project described in this chapter aims to test the hypothesis that increasing endogenous OB BDNF levels can enhance dendrite and spine development in integrating abGCs.

4.3 Materials and methods

4.3.1 Lentiviral injections

Two ~0.5 μ l injections of virus encoding tau-mCherry were injected bilaterally into the SVZ of eight week old WT and TgBDNF male mice at the following coordinates relative to bregma: anterior +1.0 mm; lateral +/- 1.2 mm; depth 1.9 mm below the tissue surface. The coding sequence of mouse tau (1100 bases) was PCR-cloned in our laboratory from IMAGE clone 4504850 (MGC 25379) obtained from the American Type Culture Collection. This was then cloned into Clontech's pLVX-mCherry-N1 lentiviral plasmid vector, and the resulting construct was sequenced by Davis Sequencing (UC Davis, CA) to confirm sequence identity by NIH BLAST alignment. The Vector Core facility at the University of North Carolina (Chapel Hill, NC) generated high titer ($>10^{10}$ pfu/ml), purified lentivirus from this construct.

Following infection, mice survived 12, 22, 35, or 60 days. Mice were euthanized with sodium pentobarbital (150 mg/kg; i.p.) and were perfused transcardially with

phosphate-buffered saline (pH 7.3), followed by ~150 mL of chilled 4% paraformaldehyde in 0.1 M phosphate buffer (PB; pH 7.35). Brains were then dissected and postfixed overnight at 4°C, followed by cryoprotection for 2-3 days in 30% sucrose in PB (4°C). Forebrains were embedded in 10% gelatin and were then fixed ~4 hrs in 4% paraformaldehyde and then cryoprotected in 30% sucrose for at least 2 days. Brains were snap frozen in isopentane (-45°C) and stored at -80°C. Coronal sections of 60 microns were cut through the OBs in a cryostat (-21°C) and stored in PB at 4°C for short term storage, and then in cryoprotectant solution (30% sucrose, 30% ethylene glycol, and 1% polyvinylpyrrolidone in PB) at -20°C for long term storage. Tissue sections were slide mounted using Vectashield mounting media (Vector Laboratories, Burlingame, CA).

4.3.2 Image collection

Z-stack images were collected at 63X objective magnification from well-labeled, intact GCs using a Zeiss 710 confocal microscope and Zeiss Zen software (Zeiss Inc, Oberkochen Germany). All z-stacks for reconstruction were collected with a pinhole setting of 1.00 Airy Unit, a zoom of 1.3X and step size in the z axis of 0.5 microns. For reconstruction purposes, individual z-stacks were collected using a frame size of 512 x 512 pixels, pixel size=0.15µm, with ~20% overlap along adjacent portions of the cell and dendrites to facilitate image stitching. A total of 282 GCs were imaged, and remained unaltered before tracing.

4.3.3 Reconstruction and criteria

Z-stacks were stitched to generate images of entire neurons using Montage software, and were imported into Neurolucida (MicroBrightfield Inc., Williston, VT) In order to determine the effects of BDNF on the morphology of adult born GCs as they

matured, images of labeled GCs at 12 days (WT=32, TG=30), 22 days (WT=38, TG=35), 35 days (WT=38, TG=32), and 60 days post-infection (dpi, WT=39, TG=38) were traced manually in their entirety using Neurolucida software. Morphometric analyses of each reconstruction were carried out using NeuroExplorer (MicroBrightfield Inc.). Criteria for the selection and reconstruction each GC neuron was as follows: (1) the cell soma, dendrites, and spines were clearly and brightly labeled, (2) no part of the neuron was obstructed by other neurons or artifacts, and (3) the apical dendrite extended past the OB MCL into the EPL. In order to prevent bias, all visible neurons in each animal that fell within the criteria were collected and used for analysis and reconstructions were done using only each animal's coded surgical number.

4.3.5 Analyses

Analysis of dendritic morphology included counts of numbers of apical, basal, and total (apical and basal combined) dendritic branch points (bifurcations/nodes) and measures of apical, basal and total dendrite length. Cells lacking basal dendrites were excluded from basal dendrite analysis. Total numbers of analyzed GCs with basal dendrites we as follows: at 12 days (WT=28, TG=27), 22 days (WT=35, TG=30), 35 days (WT=32, TG=23) and 60 days (WT=34, TG=30).

During reconstruction, apical and basal dendritic spines were inspected and categorized as one of three spine types. These types were termed headed, filopodia, or other-type spines as described previously in chapter 2, seen in figure 18. Spines on the cell body were not easily visualized due to the soma's bright labeling intensity and were not included in any analysis. Dendritic spine quantifications included numbers of total, apical, and basal spines, and numbers of spines within individual categories of spine type. Apical, basal, and total

spine densities were calculated using all spine types per cell, as well as the density of each spine type. Sholl analysis was performed to assess dendritic complexity/branching and to evaluate the distribution of all spines, and of spine types, along apical dendritic segments. For this purpose, the apical dendrite was divided into three segments defined as proximal (within the first 50um from the soma), middle (the second 50um) and distal (100um and more from the soma). At a given survival interval (dpi), unpaired, two-tailed t-tests were used compare dendrite and spine measurements from age-matched TgBDNF and WT mice. Data is presented as group mean values \pm SEM). Any time-point comparisons were performed using one-way ANOVA, followed by Tukey's post hoc comparison. Two-way ANOVA was performed with Genotype (WT, TgBDNF) and Time point (12, 22, 35, or 60 days dpi) as between-subjects variables.

4.4 Results

4.4.1 General granule cell morphology

Lentivirus encoding tau-mCherry was injected bilaterally into the SVZ of WT and TgBDNF adult mice to visualize the maturation of abGCs. To account for varying neuroblast migration times, analysis focused on the most mature-appearing GCs at each post-injection time point as described in previous work (Whitman and Greer 2007; Petreanu and Alvarez-Buylla 2002). As shown in figure 19 and 20, at low magnification at 12 days post-injection (dpi), GCs were seen in the GCL, with many extending basal dendrites and an apical dendrite projecting upward toward or into the MCL-in both WT and TgBDNF animals. Most, but not all, GCs at this age already possessed at least one branch point along the apical dendrite. Spine protrusions were also visible on both the apical and basal dendrites and no obvious differences between WT and TgBDNF animals

could be determined. These neurons closely resembled 14 dpi GCs in normal mice as described by Whitman and Greer (2007), using lentivirus encoding GFP. At 22 dpi, GCs showed more structural variations across the labeled population than at other time points, in both genotypes. GC's extended more apical dendritic branches and exhibited an apparent increase in spine numbers in both WT and TgBDNF animals (Figure 19). Again, no obvious genotype-related differences in new GCs were visualized at this time point. At 35 and 60 dpi, GC's appeared grossly similar, but with far more structural complexity compared to cells at 12 dpi in both WT and TgBDNF animals (figure 19, 20). As shown in figure 19, 20, at these survival intervals, GC's possessed many secondary and tertiary dendritic branches with visible increases in spine numbers along their apical dendrites located in the external plexiform layer (EPL), compared to the earlier time points.

4.4.2 Adult-born granule cell dendritic lengths and branch points

Two-way ANOVA comparisons of apical dendritic spine lengths showed a main effect of time point [$F=20.48$, $p < 0001$], but no effect of genotype or interaction between genotype and time point. Seen in figure 22, no significant effects of genotype or timepoint for apical or basal dendritic branch points were detected with two-way ANOVA analysis. This is not surprising considering abGCs at this age are immature and are rapidly developing into the OB at this time.

4.4.3 Over-expression of BDNF by abGCs increases their dendritic spine number

Two-way ANOVA analysis of total spine number, which included all types, showed significant main effects of genotype [$F=19.63$, $p<0.0001$], and time point [$F=77.25$, $p<0.0001$], but no significant interaction between these variables. Comparisons of only mature, headed spine number also had main effects of genotype [$F=28.15$,

$p < 0.0001$], and time point [$F = 94.37$, $p < 0.0001$], and again no interaction. Tukey's post hoc showed that mean headed-type spines significantly increase in both WT and TgBDNF mice from 12 dpi to 22 dpi ($p < 0.0001$) and increases from 35 dpi to 60 dpi in TgBDNF mice (Figure 23, $P = 0.031$). Between genotype comparisons were performed using unpaired, t -tests and are reported below. Mean apical other-type spine number showed a main effect of time point [$F = 18.6$, $p < 0.0001$], but no effects of genotype or interaction between genotype and time point. Mean filopodia-type spine number also had main effects of time point [$F = 14.2$, $p < 0.0001$], but no effect of genotype or interaction between genotype and time point. Seen in figure 23, Tukey's post hoc comparison revealed that mean apical filopodia number increased from 12 dpi (WT = 7.7 ± 0.77 SEM, Tg = 6.94 ± 0.91 SEM) to 35 dpi (WT = 18.55 ± 2.5 SEM, Tg = 20.3 ± 4.1 SEM) in both WT and TgBDNF mice (WT, $p = 0.006$; Tg, $p = 0.007$), followed by a decrease between 35 dpi and 60 dpi (Mean number = WT = 9.31 ± 1.5 SEM, Tg = 7.77 ± 1.4 SEM) in both genotypes (WT, $p = 0.013$; Tg, $p = 0.008$). Young abGCs develop quite rapidly and may account for the significant increases in spine numbers seen between 12 dpi and later time points. Decreases in other-type and filopodia-type spines from 35 dpi to 60 dpi may be explained by the abGCs pruning of immature spines typically seen between those cell ages.

At 12 dpi time, abGCs had the lowest mean total spine numbers in both WT and TgBDNF animals (Figure 23, 68.9 ± 7.0 SEM, Tg = 76 ± 3.98 SEM) and mean headed spine numbers in both WT and TgBDNF mice (Figure 23, 3.32 ± 4.1 SEM, Tg = 38.6 ± 2.61 SEM). However, no significant differences were seen in total spine and headed-type spine number between WT and TgBDNF mice at this time point (Figure 24, $p > 0.05$). Hereafter, total spine number will refer to counts that include headed, filopodia, and other-

type spines. Between 12 dpi and 22 dpi, mean total and headed spine numbers increased in both genotypes (Figure 23). However, illustrated in figure 25, TgBDNF mice had 29% more headed-type spines when compared to WT mice (Mean number = WT = 107.27 \pm 6.0 SEM, Tg = 139.2 \pm 8.95 SEM, $p=0.025$, unpaired, t-test, $t(6)=2.96$). In the apical dendrite alone, mean headed-type spine number in TgBDNF mice measured 124.5 \pm 7.85 SEM, a 31% increase compared to 95.2 \pm 5.7 SEM measured in WT mice (Figure 25, $p<0.023$, unpaired, t-test, $t(6)=3.03$). At 35 dpi, spine numbers increased again and total spine number in TgBDNF mice measured 269.16 \pm 15.12 SEM, 26% more total spines when compared to 208.29 \pm 9.39 SEM measured in WT mice and illustrated in figure 23, 24 ($p=0.014$, unpaired, t-test, $t(6)=3.4$). When assessing the apical dendrite alone, TgBDNF mice had 30% more total apical spines (Mean number=247.91 \pm 14.35 SEM), compared to WT mice that measured 190.14 \pm 9.78 SEM ($p=0.016$, unpaired, two-tailed, t-test, $t(6)=3.3$). Mean apical headed-type spine number at this time point was also significantly higher in TgBDNF mice (152.15 \pm 9.06 SEM) when compared to WT mice that measured 110.9 \pm 7.78 SEM (Figure 25, $p=0.014$, unpaired, t-test, $t(6)=3.5$). Shown in figure 23, mean total spine number for both genotypes decreased between 35 dpi and 60 dpi, however, TgBDNF maintained a significantly higher mean total spine number measuring 246.1 \pm 16.21, ~29% more compared 190.22 \pm 8.03 measured in WT mice (figure 25, $p=0.015$, unpaired, t-test, $t(8)=3.08$). This significance is again seen in the apical compartment, where mean apical total spine number in WT mice measured 169.61 \pm 6.32 SEM, compared to 220.83 \pm 12.13 SEM in TgBDNF mice ($p=0.0057$, unpaired, t-test, $t(8)=3.8$). As shown in figure 25 significant increases in mature, headed type spine number is also seen at 60 days. TgBDNF mice at this age measured 203.07 \pm 11.07 SEM, 38% more

headed spines compared to WT mice (Mean number=146.94 +/- 8.21 SEM, $p=0.0036$, unpaired, t-test, $t(8)=4.073$). This significance is seen in the apical dendrite where mean headed spine number in TgBDNF mice measured 182.39 +/- 7.46 SEM compared to WT mice that measured 131.04 +/- 7.011 SEM ($p=0.001$, unpaired, t-test, $t(8)=5.02$). No differences were seen between genotypes for basal spine numbers (Figure 24, 25, $p > 0.05$).

The data above demonstrates that TgBDNF mice have significantly more total spines in the apical dendrite at 35 dpi and 60 dpi, and more mature type headed-type spine numbers in the apical dendrites of abGCs at 22 dpi, 35 dpi, and 60dpi. GCs extend their apical dendrites into the MCL of the OB, leading us to speculate that increases in endogenous BDNF may increase the abGCs dendrodendritic synapses with the MTCs at the above cell ages.

4.4.4 Over-expression of BDNF by abGCs increases their dendritic spine density

Two-way ANOVA comparisons of total spine density, which included all types, showed significant main effects of genotype [$F=71.595$, $p<0.0001$], and time point [$F=141.5$, $p<0.0001$], and significant interaction between these variables [$F=6.213$, $p=0.03$]. Between genotype analysis were performed using unpaired, t-tests and are reported below. Comparisons of only mature, headed spine density also showed main effects of genotype [$F=101.9$, $p<0.0001$], and time point [$F=186.1$, $p<0.0001$], as well as interaction [$F=5.99$, $p=0.003$]. Tukey's post hoc revealed that headed-type spine density significantly increases from 12 dpi to 35 dpi ($p<0.0001$) and continues to increase in TgBDNF mice from 35 dpi to 60 dpi (Figure 26, $p=0.037$). Other-type spines showed a main effect of time point [$F=18.45$, $p < 0.0001$], but no effect of genotype or interaction

between genotype and time point. Tukey's post hoc comparison demonstrated that other-type apical spine density significantly increases from 12 dpi (WT = 0.075 spine/ μ m +/- 0.005 SEM, Tg = 0.083 spine/ μ m +/- 0.003 SEM) to 35 dpi (WT = 0.124 spine/ μ m +/- 0.01 SEM, Tg = 0.15 spine/ μ m +/- 0.02 SEM) in both WT and TgBDNF mice (WT, $p=0.007$, Tg, $p=0.016$), but significantly decreases in the apical dendrite from 35 dpi to 60 dpi (WT=0.06 spine/ μ m +/- 0.006 SEM , Tg= 0.06 spine/ μ m +/- 0.01 SEM) in both WT and TgBDNF mice (Figure 26, WT, $p<0.0001$, Tg, $p=0.001$). Filopodia-type spines showed main effect of time point [$F=18.45$, $p < 0.0001$], but no effect of genotype or interaction between genotype and time point. Tukey's post hoc revealed that filopodia-type spine density decreases from 35 dpi (WT=0.039 spine/ μ m +/- 0.006 SEM , Tg= 0.04 spine/ μ m +/- 0.009 SEM) to 60 dpi (WT=0.02 spine/ μ m +/- 0.004 SEM , Tg= 0.015 spine/ μ m +/- 0.002 SEM) in both WT and TgBDNF mice (Figure 26, WT, $p=0.014$, Tg, $p=0.012$).

Analysis of spine density showed that in WT animals, GCs at 12 dpi had the lowest total mean spine density at 0.168 spine/ μ m +/- 0.009 SEM (Figure 26). Hereafter, total spine density will refer to counts that include headed, filopodia, and other-type spines. About 45% of this total was comprised of headed-type spines, at a density of 0.075 spine/ μ m +/- 0.006 SEM (Figure 31). Figure 27 illustrates that in contrast, GCs at 12 dpi in TgBDNF mice had significantly more spines than WT mice, at a total density of 0.208 spine/ μ m +/- 0.007 SEM ($p=0.013$, unpaired, two-tailed t-test, $t(6)=3.47$), with significantly higher density of headed spines as well (mean=0.107 spine/ μ m +/- 0.006 SEM), which made up ~51% of the total (Figure 28,31, $p= 0.007$, unpaired, t-test, $t(6)=4.07$). Further analysis revealed that in the apical dendrite significant increases in total spine density occurred in TgBDNF mice, when compared to WT mice (Figure 27,

(TgBDNF mean=0.212 spine/ μ m +/- 0.006 SEM; WT mean=0.175 spine/ μ m +/- 0.009 SEM, $p=0.014$, unpaired, two-tailed, t-test, $t(6)=3.41$). However, for headed spines, density in TgBDNF mice was higher in both apical (mean=0.109 spine/ μ m +/- 0.005 SEM) and basal dendrites (mean=0.09 spine/ μ m +/- 0.013 SEM) compared to densities in WT mice (Figure 28, apical = 0.078 spine/ μ m +/- 0.006 SEM; basal = 0.049 spine/ μ m +/- 0.008 SEM; $p=0.01$ and 0.047 , unpaired, t-tests, $t(6)=3.78$ and 2.67 , apical and basal, respectively). Segment analysis revealed significant increases in total spine density in the middle portion, but not proximal and distal portions, of apical dendrites on GCs at this stage in TgBDNF animals compared to WT controls (Figure 29, TgBDNF = 0.194 spine/ μ m +/- 0.013 SEM, WT = 0.152 spine/ μ m +/- 0.006 SEM, $p = 0.042$, t-test, $t(4.155)=2.91$). BDNF-related increases in mature, headed spine density were also seen in the middle portion of the apical dendrite (Figure 30, TgBDNF = 0.093 spine/ μ m +/- 0.006 SEM, WT = 0.063 spine/ μ m +/- 0.006 SEM, $p = 0.013$, t-test, $t(6)= 3.46$). The distal apical dendrite of GCs in TgBDNF mice also exhibited a higher density of mature spines relative to density in WT mice (Figure 30, TgBDNF = 0.126 spine/ μ m +/- 0.01 SEM, WT = 0.088 spine/ μ m +/- 0.01 SEM, $p = 0.034$, t-test, $t(6) = 2.743$). These data clearly indicate that as early as 12 dpi, developing abGCs exposed to higher levels of endogenous BDNF have elaborated more spines, including significantly more mature spines, than abGCs in control mice. New GCs arrive in the OB at ~6-9 days dpi, demonstrating that BDNF effects emerge early in their structural maturation.

At 22 dpi, mean total spine density in GCs in WT mice increased to 0.31 spine/ μ m +/- 0.012 SEM, with ~61% of these classified as headed spines (Figure 27, 31, density=0.189 spine/ μ m +/- 0.012 SEM). Figure 27 shows that TgBDNF GCs had a higher

total spine density of 0.345 spine/ μm \pm 0.006 SEM ($p=0.041$, unpaired, t-test, $t(6)=2.6$), compare 0.31 spine/ μm to 0.345 spine/ μm , with headed spines comprising $\sim 70\%$ (mean density headed spines = 0.241 spine/ μm \pm 0.018 SEM). Headed spine density was higher in the apical dendrite of GCs in transgenic mice (mean = 0.243 spine/ μm \pm 0.013 SEM) when compared to WT densities (mean = 0.193 spine/ μm \pm 0.011 SEM (Figure 28, $p=0.026$, unpaired, t-test, $t(6)=2.59$). Segment analysis revealed slightly greater mean headed spine density in the distal apical dendrite when measures were compared across genotypes, but this did not reach statistical significance (Figure 30, TgBDNF = 0.255 spine/ μm \pm 0.18 SEM, WT = 0.20 spine/ μm \pm 0.014, $p=0.051$, t-test, $t(6)=2.43$).

For both WT and TgBDNF animals, total GC spine density at 35 dpi exceeded measures at 22 dpi (Figure 26, 27). Total spine density was 0.383 spine/ μm \pm 0.003 SEM. For WT mice, with headed spines making up $\sim 59\%$ of this total (mean density = 0.225 spine/ μm \pm 0.01 SEM). Again, cells in TgBDNF mice had significantly greater total spine density (0.505 spine/ μm \pm 0.029 SEM) in comparison to WT values (Figure 27 $p=0.024$, unpaired, t-test, $t(3)=4.69$). This included significantly more headed spines (mean density = 0.310 spine/ μm \pm 0.018 SEM), comprising $\sim 61\%$ of the total (figure 28, 31, $p=0.007$, unpaired, t-test, $t(6)=4.03$). When considering only the apical dendrite mean spine density measured 0.501 spine/ μm \pm 0.023 SEM in TgBDNF mice compared to a mean value of 0.391 spine/ μm \pm 0.004 SEM in WT controls (Figure 27, $p=0.003$, unpaired, two-tailed, t-test, $t(6)=4.77$). Headed spine density was also increased in the apical dendrite of GCs exposed to increased BDNF (mean = 0.312 spine/ μm \pm 0.018 SEM compared to 0.228 spine/ μm \pm 0.009 SEM in controls; $p=0.005$, unpaired, t-test, $t(6)=4.27$). Within the apical dendrite, the distal domain showed significant increases in total and headed spine

density transgenic mice (Figure 30, TgBDNF total = 0.498 spine/ μ m \pm 0.007 SEM, WT total = 0.393 spine/ μ m \pm 0.01 SEM, $p < 0.0001$, t-test, $t(6) = 8.67$); TgBDNF distal = 0.311 spine/ μ m \pm 0.017 SEM, WT distal = 0.23 spine/ μ m \pm 0.012 SEM, $p = 0.008$, t-test, $t(6) = 3.86$).

As noted in several prior studies, between 35 and 60 dpi, when GCs become fully mature, those in WT mice showed a decrease in mean total spine density to 0.323 spine/ μ m \pm 0.004 SEM. As shown in figure 26, 27, TgBDNF mice also exhibited a decrease in GC mean spine density to 0.429 spine/ μ m \pm 0.013 SEM, providing evidence that abGCs exposed to higher levels of BDNF also undergo spine pruning before reaching full maturity. In spite of this decrease, spine density in TgBDNF mice remained significantly higher than that measured in WT mice ($p < 0.0001$, unpaired, t-test, $t(8) = 7.6$). Although total spine density decreased between 35 and 60 dpi, the density of headed spines continued to increase during this time in GCs from both WT (mean = 0.249 spine/ μ m \pm 0.007 SEM) and TgBDNF (mean = 0.353 spine/ μ m \pm 0.004 SEM) animals, making up roughly 77% and 82% of total spines, respectively (figure 28, 31), with the difference between TgBDNF and WT mice remaining significant ($p < 0.0001$, unpaired, t-test, $t(8) = 12.8$). As at earlier stages, GC total apical dendritic spine density in transgenics exceeded values from WT mice (Figure 27, TgBDNF mean = 0.43 spine/ μ m \pm 0.014 SEM, WT mean = 0.323 spine/ μ m \pm 0.003 SEM, $p < 0.0001$, unpaired, t-test, $t(8) = 7.68$). With BDNF over expression, the density of mature, headed spines was higher in both apical (mean = 0.354 spine/ μ m \pm 0.005 SEM) and basal dendrites (mean = 0.326 spine/ μ m \pm 0.025 SEM) when compared to control measures (WT apical = 0.248 spine/ μ m \pm 0.008 SEM and basal = 0.249 spine/ μ m \pm 0.007 SEM; apical, $p < 0.0001$, unpaired, t-test, $t(8) = 11.6$; basal,

$p=0.024$, unpaired, t-test, $t(8)=2.8$). The distal apical dendrite showed BDNF-related increases in total mean spine density when compared to WT control values (Figure 29, TgBDNF = $0.426 \text{ spine}/\mu\text{m} \pm 0.021 \text{ SEM}$, WT = $0.325 \text{ spine}/\mu\text{m} \pm 0.008 \text{ SEM}$, $p=0.002$, t-test, $t(8)=4.55$). Similarly, the mean density of headed spines was significantly higher in this domain with BDNF over-expression (Figure 30, TgBDNF = $0.353 \text{ spine}/\mu\text{m} \pm 0.013 \text{ SEM}$, WT = $0.254 \text{ spine}/\mu\text{m} \pm 0.013 \text{ SEM}$, $p=0.001$, t-test, $t(6)=5.4$). Notably, increased BDNF also increased mean headed spine density in the proximal apical dendritic domain, although the difference did not reach significance (Figure 30, TgBDNF = $0.404 \text{ spine}/\mu\text{m} \pm 0.04 \text{ SEM}$, WT = $0.286 \text{ spine}/\mu\text{m} \pm 0.032 \text{ SEM}$, $p=0.051$, t-test, $t(8)=2.3$).

The above data show that increasing endogenous BDNF in the mouse OB significantly increases spine density, specifically mature, headed type spines throughout abGC development and that TgBDNF abGCs have a similar morphological development pattern when compared with the WT GCs. Mean headed-type spine number is increased in the apical dendrites of all time points in both genotypes and is specifically increased in the distal apical dendrites of GCs at 12, 22, and 60 dpi. GCs extend their apical dendrites in the MCL, where they make dendrodendritic synapses with the MTCs. The significant increases seen in the distal dendrites of TgBDNF mice could mean increases in synapses with the OBs excitatory projection neurons. Significant increases in headed spine density is also seen in the basal dendrites at 12 dpi and 60 dpi. Centrifugal axons terminate on the basal and proximal apical dendrites of the GCs and may aid in development. Increases in headed-type spines in the basal dendrites at 12 dpi could mean an increase in these synaptic connections facilitating abGC growth. In both WT and TgBDNF mice, total spine density and headed spine density increased from 12 dpi to 35 dpi, however from 35 dpi to 60 dpi,

GC total spine density decreased. Typically, between 35 dpi to 60 dpi, abGCs become mature and prune immature spines, this can be further demonstrated in the data showing significant decreases in other-type and filopodia-type spine density while headed-type spine density continued to increase between 35 dpi and 60 dpi.

4.5 Discussion

Maintenance of the GC population, OB network function and specific types of olfactory learning and memory, depend on the continuous integration of abGCs. Here we used lentiviral infection of progenitor cells in the SVZ to permanently label abGCs with a fluorescent cytoskeletal protein in order to monitor their morphological development in vivo. Morphometric analysis of fully reconstructed cells was performed to show that elevations in endogenous OB BDNF levels alters the structural maturation of abGCs in vivo. Although TrkB knockout experiments previously have shown impairments in spine maturation and maintenance in adult-born dentate and olfactory GCs, this is the first demonstration that increasing endogenous BDNF availability robustly stimulates the morphological development of TrkB-expressing abGCs in vivo (Bergami, Berninger and Canossa, 2009; Bergami *et al.*, 2013). Our most significant findings were the notable increases in both total and mature spine density that occurred with OB BDNF over-expression, indicating that abGCs are highly responsive to local BDNF availability.

In this study, the development of abGCs in normal WT mice was consistent with what has been reported in some previous studies. At 12 dpi, GCs had a mean total spine density of 0.168 spines/ μm , which nearly doubled as the cells reached 22 dpi (0.320 spines/ μm), and then continued to increase up to 35 dpi (0.383 spines/ μm). When fully mature at 60 dpi a decrease in spine density was observed (0.323 spines/ μm), a decline of

~16%, similar to results reported in previous studies, presumably reflecting the process of spine pruning, which was recently shown to involve resident microglial cells (Mary C. Whitman and Greer, 2007; Reshef *et al.*, 2017). A similar pattern of developmental increases occurred in the mature spine population, starting with a density of 0.075 spines/ μm at 12 dpi, however density continued to increase out to 60 days reaching 0.249 spines/ μm (about a three-fold change), similar to the report of Breton-Provencher *et al.* (2014) that demonstrated increases in mature spine density throughout abGC maturation. We found that this increase was accompanied by a decrease in filopodia and other-type spines from 35 days to 60 days. Similar increases in “stable” spines and declines in the proportion of “new or lost” spines have been observed in elegant work by Pierre Marie Lledo’s laboratory using long term, in vivo imaging of mouse abGCs through cranial windows (Sailor *et al.*, 2016). The persistence of many filopodia and “other” type spines can be explained by the ongoing, rapid spine turnover/plasticity that has been documented in abGCs in vivo (Mizrahi, 2007; Livneh and Mizrahi, 2011; Sailor, Schinder and Lledo, 2017). The other types may be spines in structural transition that are just emerging or are filopodia that have retracted.

Our previous studies have documented that TgBDNF mice have increased BDNF mRNA and protein levels in the adult OB (McDole *et al.*, 2015). New, infected GCs maturing in this strain showed overall patterns of structural development similar to that in WT controls. Total spine density was lowest at 12 dpi (0.208 spines/ μm) but continued to increase through 22 to 35 dpi (0.505 spines/ μm) and then declined ~16% by 60 days (0.429 spines/ μm). As in WT mice mature spine density increased over time, with a density at 12

dpi of 0.107 spines/ μm , 0.241 spines/ μm at 22 dpi, and reaching a maximum of 0.353 spines/ μm by 60 days (again an approximate three-fold change).

At all survival intervals examined, abGCs over-expressing BDNF had increased total and mature dendritic spine density when compared to normal GCs in WT littermates. By 12 dpi, total spine density was already 24% higher than control measures, with 43% higher density of mature spines. This shows that increases in BDNF can act to promote GC structural integration by increasing the production and maturation of spines shortly after GCs reach the OB and elaborate dendrites. The effects on spine maturation are consistent with effects of BDNF treatment in vitro, or BDNF knockout in vivo, reported for other TrkB-expressing CNS neuronal populations (Bergami, Berninger and Canossa, 2009; Rauskolb *et al.*, 2010; Chapleau and Pozzo-Miller, 2012; Vigers *et al.*, 2012; Kellner *et al.*, 2014). BDNF effects were not restricted to the apical dendrite where dendrodendritic contacts are established, as basal dendrites also showed increased density of mature spines by 12 dpi. Basal dendrites and the proximal apical dendrite are innervated by glutamatergic and GABAergic centrifugal afferents early in GC maturation, both of which are necessary for full morphological and functional development of new GCs (Mary C. Whitman and Greer, 2007; Panzanelli *et al.*, 2009), Genetic knockout of GABA_A receptor $\alpha 2$ subunit expression in abGCs stunts their dendritic growth, while NMDA GluN2B receptor subunit knockout leads to failed maturation of functional glutamateric inputs in the proximal domain, followed by GC death (Kelsch *et al.*, 2012; Pallotto *et al.*, 2012). Our evidence suggests that endogenous BDNF, made by the centrifugal populations (anterograde) or the GCs themselves (autocrine or retrograde to afferents), may help regulate the initial stabilization or maturation of basal and proximal dendritic spines.

Notably, at 22 days, although GCs over-expressing BDNF show an 11% increase in total spine density above normal GCs, they exhibit 28% higher mature spine density and at this point have already matched the density of mature spines in 60 day-old GCs in WT mice (TgBDNF 22 dpi = 0.241 spines/ μ m compared to WT 60 dpi = 0.249 spines/ μ m). Although one may infer that increases in endogenous BDNF may have accelerated full dendritic maturation, spine density did not reach a plateau and continued to increase beyond this point, leading us to conclude that these cells are still establishing connections. Although total spine density decreased between 35 and 60 dpi within both genotypes, the difference between genotypes continued to widen at 60 days when spine density in mature GCs over-expressing BDNF exceeded of normal GCs by 33%. At this time, the prolonged effects of increased BDNF resulted in a striking 42% increase in mature spine density.

Although most prior studies have focused on BDNF effects in glutamatergic neurons, GABAergic populations are also BDNF responsive, and olfactory GCs fall into this group. BDNF enhances the dendritic growth and complexity of interneurons in cultured cortical slices (Jin *et al.*, 2003). Genetically increasing BDNF in the mouse forebrain results in accelerated development of GABAergic circuitry in visual cortex, while knockout of activity-dependent BDNF expression retards development of circuit inhibition in somatosensory cortex (Huang *et al.*, 1999; Jiao *et al.*, 2011). Conditional BDNF forebrain knockout significantly reduces dendritic complexity and spine density in GABAergic medium spiny neurons (Rauskolb *et al.*, 2010). Whether functional synapses are present on the abundant spines we observe in TgBDNF mice cannot be determined in this study, though it is likely that the increases in mature spines in the distal apical dendrites indicate

more dendrodendritic synapses. Additional studies are needed to determine if synapses have developed on most or all of the mature-appearing GC spines in TgBDNF mice.

There are multiple sources of increased BDNF that may act on abGCs in TgBDNF mice. MTCs cells do not express CAMKII α and do not over-express BDNF in this strain, however the AON and piriform cortex, which normally express high levels of BDNF, express even higher levels in these mice (Smail *et al.*, 2016). Therefore, an increase in anterograde supplies of BDNF to GCs targeted by these higher olfactory regions is a possibility. Within the bulb, the GCs express high levels of BDNF under the transgene, and may release this via dendrites to MTCs, or as an autocrine factor that activates their own TrkB receptors. Dendritic release of BDNF has been documented in vitro, and more recently the autocrine activation of TrkB via BDNF release from glutamate-stimulated spines (Lessmann and Brigadski, 2009; Kuczewski, Porcher and Gaiarsa, 2010; Harward *et al.*, 2016). This is of interest since it has been recently shown that abGCs in hippocampus express and use BDNF as an autocrine factor (Wang *et al.*, 2015). Mice with forebrain knockout of BDNF show impaired dendritic development and few spines in abGCs, and similar effects occur if BDNF is knocked out only in the abGCs themselves. If BDNF expression is restored in *only* the abGCs of the knockouts, dendritic development is rescued (Wang *et al.*, 2015). In the normal OB, BDNF expression by GCs is extremely low compared to brain areas like hippocampus. Over-expressing BDNF in new olfactory GCs may have autocrine effects on their morphology similar to the rescue effects seen in new dentate GCs. Based on our current findings we conclude that increasing OB BDNF levels enhances spine development and maturation in abGCs throughout the course of their development. Since BDNF expression and release is controlled by activity, sensory-

dependent changes in local levels of BDNF within normal OB circuitry may help shape the connectivity of abGCs as they mature and integrate.

PART V- GENERAL DISCUSSION

5.1 Thesis overview

BDNF has been proposed as a key regulatory factor in adult olfactory neurogenesis and is well established as a regulator of dendrite and spine development/maturation in multiple CNS neuron populations. This dissertation work took advantage of a transgenic mouse line that over-expresses endogenous BDNF in OB GCs to determine the *in vivo* effects of increased BDNF on established and adult-born GC interneurons. We tested the hypotheses that local elevations BDNF would stimulate morphological changes in abGCs, as well as enhance their survival, to provide insight into how changes in normal BDNF levels, in response to sensory drive/activity, may shape the network connectivity of new GCs as they integrate. The results highlight how increased OB BDNF alters dendritic morphology in GCs in both young and old mice, its ability to promote abGC dendritic spine development and maturation, and how despite this, it does not enhance the survival rate of these new cells. This finding contrasts with previous reports of increased GC generation and survival with BDNF administration in the SVZ stem cell niche. In chapter 2 work, I used ELISA and Western blotting techniques to confirm that mature BDNF protein is significantly elevated in the OBs of TgBDNF animals, consistent with prior work in the laboratory that measured and localized OB BDNF mRNA expression. To reconstruct GCs in this strain, Golgi-Cox staining was first used to impregnate olfactory GCs in both young and old transgenic and WT mice. Morphometric analysis after reconstruction showed that over-expression of BDNF had no effect on GC

dendritic complexity, but increased total spine number and density, and significantly increased prevalence of mature, headed spines in the proximal and distal domains of apical dendrites in both young and old mice. This suggested that BDNF regulates the maturation/maintenance of dendritic spines in the existing GC population throughout the life span of the animals. If abGCs are similarly affected, it may impact their integration and potentially improve their survival, since manipulations that reduce spine development in these neurons increase their apoptotic death, including sensory deprivation. Chapter 3 experiments focused on BDNF's role in the survival of abGCs using BrdU cell labeling to visualize and quantify OB GCs generated from resident stem cells in the SVZ. Measurements taken at three different time points after BrDU treatment revealed that, against our expectations, there were no differences in abGC numbers in TgBDNF and WT mice. From this we concluded that BDNF does not play a major role in regulating survival of this TrkB-expressing population, in contrast to some of the BDNF survival effects reported previously for new dentate GCs. The finding that increased BDNF did not rescue GCs from apoptosis, as seen with TUNEL labeling, also favors this conclusion. The results described in chapter 3 demonstrate that increasing BDNF in the OB does not change the survival rate of abGCs from that measured in normal mice. This study used a novel approach to test for BDNF effects within the OB in vivo and will add to the ongoing debate of BDNF's role in adult olfactory neurogenesis. Chapter 4 experiments directly examined BDNF's role in the structural development of abGCs, using lentiviral injections to transfer a gene sequence encoding a tau-mCherry fusion protein into progenitor cells in the SVZ of mice of both genotypes. New GCs expressing this red fluorescent cytoskeletal protein were imaged and reconstructed over the course of their maturation in order to compare their

structural development. The results demonstrate that abGCs over-expressing BDNF have a similar pattern of development as far as early elaboration of dendrites and spines, followed by apparent spine pruning/reductions between 35 and 60 days of approximate cell age. However, starting as early as 12 days, while dendritic branches are still developing, abGCs in TgBDNF mice exhibited significantly higher total and mature spine densities compared to those in WT mice, and maintained these increases to full maturity, even after the pruning phase. This analysis suggests that one of BDNF's roles within OB circuitry is the regulation of dendritic spine development, maturation and maintenance in GC interneurons as the population turns over during the process of adult neurogenesis. The increase in BDNF did not enhance the survival of abGCs, possibly because established GCs maintained their higher spine density as well. BDNF expression was elevated throughout the GCL, rather than selectively within the abGC population. It would be interesting to determine if over-expressing BDNF in only abGCs would provide a competitive, autocrine benefit that could lead to improved survival.

5.2 Key findings

5.2.1 Chapter 2

Quantitative analysis of Golgi-impregnated GCs revealed that BDNF protein levels were significantly increased in the OB of TgBDNF mice when compared to WT mice. This was in line with initial predictions and increases seen in OB BDNF mRNA in previous work from our laboratory in this mouse strain, with the entire GCL showing dramatically increased BDNF mRNA expression (McDole *et al.*, 2015). The over-expression of endogenous BDNF in the mouse GCL resulted in significant increases in spine numbers on the apical dendrites of GCs in both young and old mice. In particular, I found that these

GCs had more mature, headed-type spines in apical dendrites compared to GCs from WT mice. Similarly, GC total apical dendritic spine density in both young and old transgenic mice was increased, as was the density of mature spines. Segment analysis of the extended apical dendrite revealed that increases in headed spines were located in the proximal dendritic domain where they are more likely to receive centrifugal inputs from the higher olfactory cortices, and on the distal portions where dendrodendritic synapses are made with the MTCs. No genotype-associated differences were seen in dendritic branching or total dendritic length expectations based on previous research literature demonstrating BDNFs role in spine development/maturation in multiple types of CNS neurons as discussed in chapter 2. They are also consistent with a recent study in which deletion of BDNF's receptor TrkB in GCs, causes deficits only in spine numbers and density, and not in their dendritic complexity (Bergami 2013), and further confirms that endogenous BDNF can regulate spine maturation and maintenance in these interneurons.

5.2.2 Chapter 3

Using quantitative comparisons of Brdu+ GC numbers in both mouse genotypes I found there were no differences in the density or numbers of abGCs that arrived in the OB, matured, and survived out to nine weeks of cell age. Numbers of dividing Ki67+ SVZ progenitor cells were similar as well, as was the rate of GC loss by apoptosis over time, indicating that increases in BDNF had no significant effects on stem cell proliferation or GC survival. These results were not in line with predictions that new, TrkB expressing GC would show improved survival in the OB. BDNFs role in GC generation and survival been tested previously through manipulation of BDNF levels in the SVZ and my approach differed because BDNF levels were elevated in the OB, where new GCs express TrkB as

they mature. However, these results are in consensus a recent study that showed TrkB deletion in abGCs impaired spine development, but had no significant effect on cell survival (Bergami *et al.*, 2013). As demonstrated by sensory deprivation studies, neural activity is likely to be the dominant factor. GCs exposed to high BDNF have more mature spines, but undergo apoptosis at normal rates, and abGCs lacking functional TrkB have significantly reduced spine density and also die at normal rates. CGs that failed to receive sufficient stimulation, or lack NMDA GluR2B receptor subunits, die even after spines have formed (Dahlen *et al.*, 2011; Kelsch *et al.*, 2012).

5.2.3 Chapter 4

My morphometric analysis of virus-labeled abGCs revealed that abGCs developing under the influence of increased BDNF show similar developmental progression when compared to GCs developing in normal conditions. GCs in both TgBDNF and WT mice elaborate dendrites with normal complexity and show an increase in spine density out to 35 days, followed by spine loss that likely indicates pruning. However, by 12 dpi, GCs in TgBDNF mice already possessed 24% higher total spine density 43% higher mature spine density than GCs in WT mice. GC speak spine density in TgBDNF mice occurred at 35 days with a nearly 40% increase in mature spine density compared to WT GCs. Even after pruning reduced the total spine density, mature GCs in exposed to high BDNF possessed 42% more headed spines than normal. The results of this study compliment previous work describing the stages of structural maturation and synapse development in normal GCs (Petreanu and Alvarez-Buylla, 2002; M. C. Whitman and Greer, 2007). The findings on increased BDNFs role in abGC development patterns are novel, however, the analysis is in line with previous work of BDNFs influence in both the development and maturation of

spines in various non-adult born CNS neurons (Horch and Katz, 2002; Gorski *et al.*, 2003; Shinji Matsutani and Yamamoto, 2004; Kohara *et al.*, 2007; An *et al.*, 2008; Waterhouse *et al.*, 2012a; Orefice *et al.*, 2013; Kellner *et al.*, 2014; McDole *et al.*, 2015). BDNF/TrkB morphological effects are not necessarily linked to abGC survival, but may instead help regulate how those that live establish adaptive, functional connectivity.

5.3 Study Limitations

5.3.1- Chapter 2 limitations

5.3.1.1 – Existing or adult-born granule cell

This study used a modified Golgi-Cox staining method that randomly labels spares numbers of neurons throughout the brain. Due to the nature of this method, we were unable determine if the stained, reconstructed GCs were recently adult-born or part of the established population generated during early development, or during earlier adult stages. As a result, GCs used in the analysis may be part of any of these populations of olfactory GCs. To limit the contribution of recently born GCs in the analysis, criteria were set in place that favored the inclusion of GCs with mature-looking dendritic features according to those described in previous studies of GC morphology (Greer, 1987; Petreanu and Alvarez-Buylla, 2002; M. C. Whitman and Greer, 2007). Although we cannot exclude the possibility that abGCs were included, these neurons were examined in detail in the later study that used lentivirus infection, allowing estimations of cell birth date/age.

5.3.1.2- Time constraints

Due to occasional periods when mouse breeding success rate dropped, and high rates of litter cannibalism occurred, the sex and genotypes of mice needed for experiments were limited. Because of the time needed for breeding, for gestation and for mice to reach

the appropriate age, tissue generated for the older group (6-7.5 months) took almost a year to generate and several brains were eliminated from the study due to either inadequate fixation, or the poor quality of Golgi staining. Every GC cell that fell within criteria was reconstructed within the samples that remained to combat lower animal numbers in this group. Expanding the breeding colony to over produce litters in order to obtain sufficient numbers of each sex and genotype at older ages would greatly reduce this limitation in further studies.

Chapter 5.3.2- Chapter 3 limitations

5.3.2.1- BrdU

Animals in the chapter 3 project were treated with bromodeoxyuridine (BrdU), a thymidine analog that gets incorporated into the DNA of dividing cells during the S-phase of the cell cycle. Although this is one of the most reliable and used methods to birthdate new neurons to date, this does not come without some limitations and pitfalls. BrdU can be both toxic and mutagenic when administered repeatedly at high doses, triggering cell death and altering DNA stability. This can make cells prone to unpredictable DNA replication errors when affected. In addition, BrdU may also be incorporated into DNA of cells during DNA repair, labeling cells that have been injured rather in addition to those that are dividing. Previous studies have used relatively high doses of BrdU for extended lengths of time (for example: 100mg/kg, 18 consecutive days), which may have greatly increased the probability of toxicity and of new cells experiencing mutagenic effects (Benraiss *et al.*, 2001). To combat this, I injected animals daily at a low dose of 50mg/kg over only 4 days to reduce the possibility of cell damage and to limit the amount of time BrdU could be incorporated through other forms of DNA alteration.

5.3.3- Chapter 4 limitations

5.3.3.1 Granule cell numbers per experimental animals

One limitation of this study was the number of labeled abGCs available for reconstruction and analysis in each animal. These numbers depended on the virus titer, the volume injected, the placement of the SVZ injections, and the survival interval. Some injections resulted in only a few labeled cells per OB, and due to the normal loss of ~50% of new GCs by ~6 weeks, animals that survived beyond this point had limited numbers of labeled cells that met the criteria for analysis. This included the need for the cells to be fully intact within a 60-micron section, and many cells encountered had portions of dendrites or entire cell somas lacking due to sectioning.

Coordinates chosen for injection may have also created some limitations in this experiment. Although more difficult to hit, injections into the RMS where abGCs are already migrating may have ensured greater numbers of infected cells in the OB. A limitation to injecting virus into the SVZ is that the virus can infect both TypeB stems cells, and type C transit amplifying cells, which undergo divisions over several days to produce postmitotic neuroblasts. Neuroblasts also undergo variable migration rates in the RMS. Convention has been to date abGCs based on virus injection date, or define cell age using "+/- 3 days". This may create a slight age differences in cells imaged at the same survival intervals, although this is well recognized in the field of olfactory neurogenesis. Injecting into the RMS in the future can reduce some of the cell age variance that occurs when injecting into the SVZ.

5.3.3.2 - Imaging different neurons

In this study, mice survived for different intervals after lentiviral infections. This means that different neurons were imaged at a single time point/age, which did not allow for the same GC to be imaged and analyzed throughout its development. Newer technologies and imaging techniques that allow for multiphoton confocal imaging in vivo would allow the same new neuron to be monitored over the course of development to full maturation. This would allow more accurate morphological analyses, reducing the variability associated with imaging different neurons at different time points.

5.4 Future Directions

5.4.1- Periglomerular cells

PG cells are another population of inhibitory interneurons born in the SVZ that continue to integrate into the OB throughout adulthood. The numbers of arriving PG cells are far smaller than abGC numbers (~5% of all new cells) but they are necessary for processing information from incoming OSNs within the OB glomeruli. Although we have found that over-expression of local BDNF does not affect abGC survival, recent literature has reported that TrkB receptor deletion in SVZ progenitor cells reduces the survival of new dopaminergic/GABAergic PG cells (Bergami *et al.*, 2013). Adult neurogenesis can preferentially restore dopaminergic PG neurons lost to 6-hydroxydopamine treatment in the OB (Lazarini *et al.*, 2014). Knowing that this process shows some plasticity, and that unlike GCs, dopaminergic PG require full length TrkB expression for normal survival, we can test whether increases in endogenous BDNF enhances PG survival as a future direction in exploring BDNF's role in olfactory circuitry.

The coordinates used in chapter 4 experiments would not have provide enough viral-labeled PG cells for workable analysis. However, the location of PG neuron origin within particular domains within the SVZ (based on transcription factor expression) has been mapped (Lledo, Merkle and Alvarez-Buylla, 2008). Focusing on SVZ coordinates where PG cells originate would provide us with an increased number of PG cells to test for BDNF effects on their development, combined with antibodies to tyrosine hydroxylase to verify their dopaminergic phenotype. This could give us valuable insight into how BDNF may shape the connectivity of the glomerular layer as new inhibitory neurons are incorporated here.

5.4.2- Behavior

The majority and location of distal apical dendritic spines on GCs contact the OB's major excitatory projection neurons, the MTCs, and ultimately modify olfactory information sent to the higher olfactory cortices. Adult neurogenesis is important for some types of long-term olfactory memory, odor-reward associations, and odor discrimination (Sultan *et al.*, 2010; Lepousez, Valley and Lledo, 2013; Arruda-Carvalho *et al.*, 2014; Grelat *et al.*, 2018; Li *et al.*, 2018; Mandairon *et al.*, 2018). Future work would be aimed at determining how increased spines and synaptic connections in GCs impacts olfactory behaviors in TgBDNF mice. Simple olfactory behavioral tasks can be done to test for the ability to normally detect and discriminate odors. Simple "cookie bury" tasks, as well as nose-poke tasks in response to rewarded or non-rewarded odors can assess odor detection and odor learning and memory. Olfactory detection threshold could be tested, as well as discrimination of similar odorants. This would allow assessments of how the increases in GC dendritic spines affect odor processing and behavioral outputs in TgBDNF mice.

Additionally, c-fos expression mapping in the OB in response to odor exposure could be used test for change in functional bulb circuitry.

5.4.3- Live animal imaging

As noted above in study limitations, there are available technologies to image labeled neurons in situ in live animals at different time-points during their development. With access to a two-photon microscope, we would be able monitor individual GCs or PG cells as they integrate into the OB of TgBDNF animals. The mouse bulb is relatively small and is positioned just under the skull. It is accessible to live imaging through a cranial window and with a two-photon microscope, the same neurons could be examined at different time points in their development. The use of this technology in previous studies has already shown this method to be effective in capturing GCs (Sailor *et al.*, 2016). This would aid in characterizing BDNF effects during defined intervals of GC development with more accuracy in order to better understand BDNFs role in regulating their structural maturation.

5.5 Concluding remarks

The outcomes of this dissertation work elucidate some of the roles BDNF plays in the regulation of adult olfactory neurogenesis. Here we employed a non-invasive, genetic method to significantly increase the normally low levels of BDNF expressed in the GCL of the mouse OB. This allowed analyses of BDNF effects within the GC integration environment, rather than in region of their birth. The results of this work document that augmenting BDNF promotes the maturation of dendritic spines during abGC development, as well as the maintenance of mature spines in the overall GC population. This includes the spines where their dendrodendritic synapses on MTCs are located, synapses that

regulate the activity of these principal output neurons. Somewhat surprisingly, and in contrast to BDNF effects reported for abGC in the dentate gyrus, the enhancement in spine density, an indirect indication of integration, did not significantly alter abGC survival rate in the OB (at the expense of preexisting GCs), as assessed with Brdu cell birth-dating. While somewhat counter-intuitive this result compliments recent work by the Bergami laboratory, that has demonstrated abGCs lacking TrkB also show normal survival rates. However, they do exhibit reduced dendritic spine density. Taken together, these findings demonstrate that BDNF/TrkB signaling is not required for survival of abGCs, but clearly is required for normal spine development and maturation. BDNF expressed under the endogenous, normal promoter is activity-dependent, as is BDNF secretion, which can occur in both axons and dendrites, and we and others have shown that OB BDNF expression fluctuates with changes in sensory drive (McLean, Darby-King and Bonnell, 2001; Degano *et al.*, 2014). Our results suggest that in the normal OB, activity-dependent changes in local BDNF availability may selectively regulate GC spine maturation, maintenance and plasticity to adapt their network connectivity to the meet the environmental/sensory demands of the olfactory system.

Figure 1. ONL, Olfactory nerve layer; GL, Glomerular layer; EPL, External plexiform layer; MCL, Mitral cell layer; IPL, Internal plexiform layer; GCL, Granule cell layer. Adapted from: Nagayama et al., 2014.

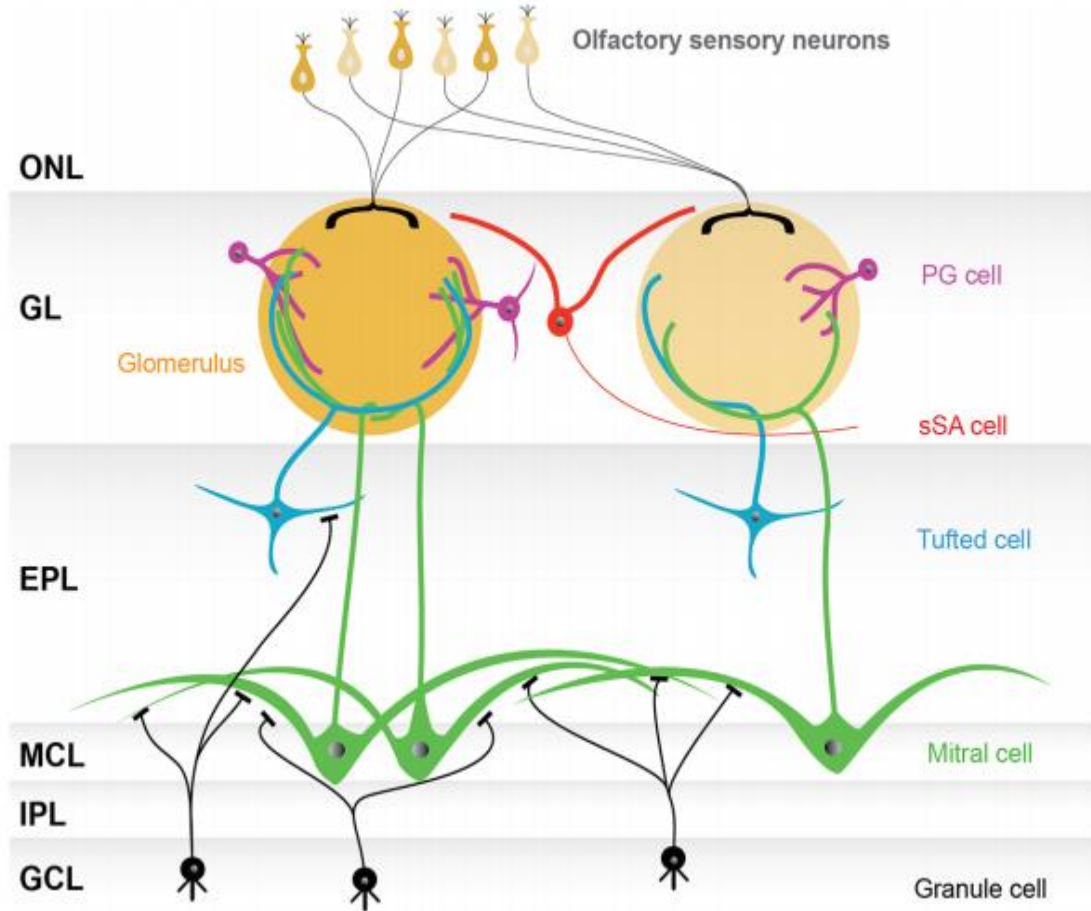


Figure 1. Olfactory bulb neuronal circuitry organization

Figure 2. GL, Glomerular layer; EPL, External plexiform layer; MCL, Mitral cell layer; IPL, Internal plexiform layer; GCL, Granule cell layer; SEL Subependymal layer.



Figure 2. Histology and laminar organization of the mouse olfactory bulb.

Figure 3. Electron micrograph of a reciprocal dendrodendritic synapse formed between a granule and mitral cell. The image contains curved arrows pointing in the direction of the vesicle release. The **f** is pointing to the post-synaptic density seen normally on the postsynaptic membranes of glutamatergic synapses. g, granule cell; m, mitral cell. Adapted from: Shepherd, et al., 2007.

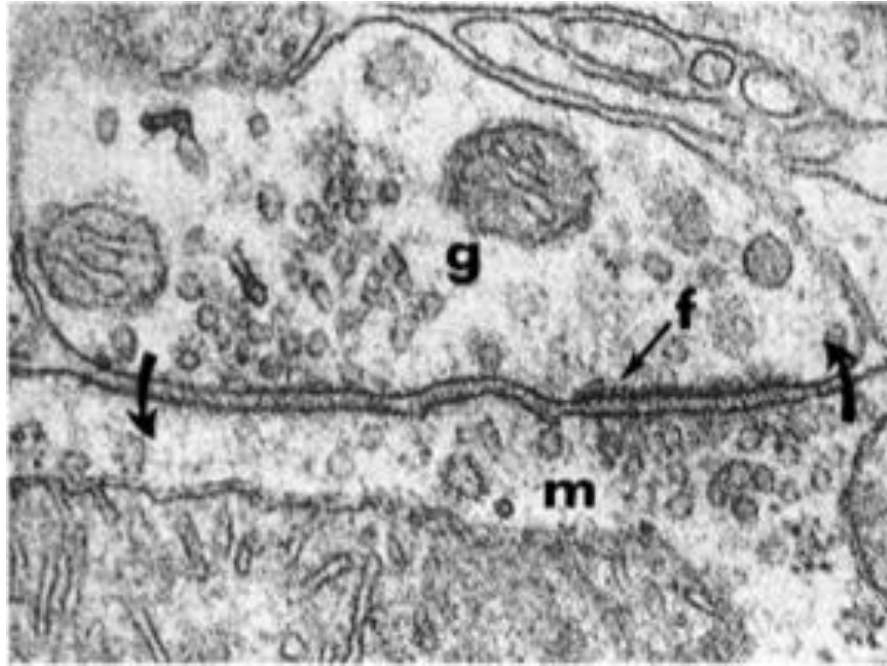


Figure 3. Reciprocal dendrodendritic synapse

Figure 4. The birth (1 & 2), migration (3) and incorporation of abGCs (4) and PG cells (5) in the adult mouse brain. GL, glomerular layer; GCL, granule cell layer; RMS, rostral migratory stream; SVZ, subventricular zone. Adapted from Sui et al., 2012.

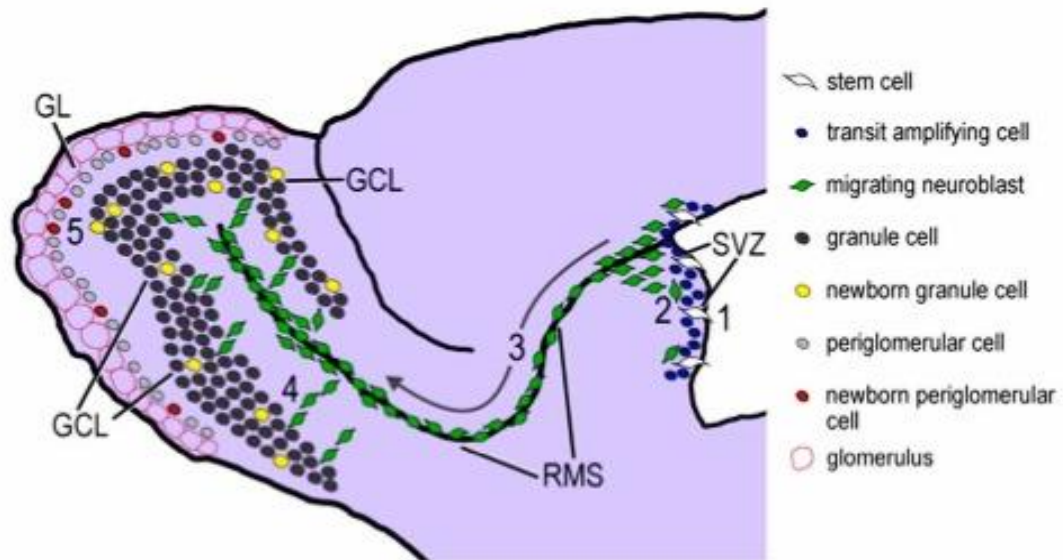


Figure 4. Migration pattern of abG

Figure 5. DG, dentate gyrus; CC, corpus callosum; Ctx, cortex; SVZ, subventricular zone; RMS, rostral migratory stream; OB, olfactory bulb. Adapted from: Whitman & Greer, 2009.

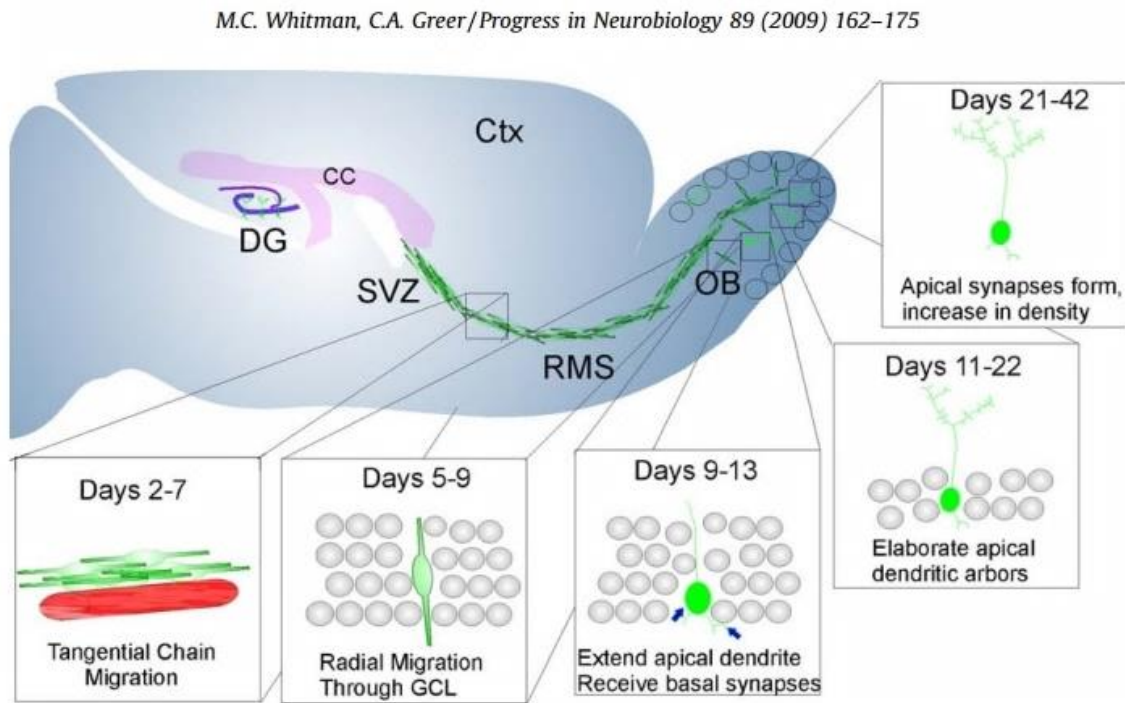


Figure 5. The time course and stages of migration and differentiation of abGCs.

Figure 6. TrkB signaling pathways activated by BDNF receptor binding

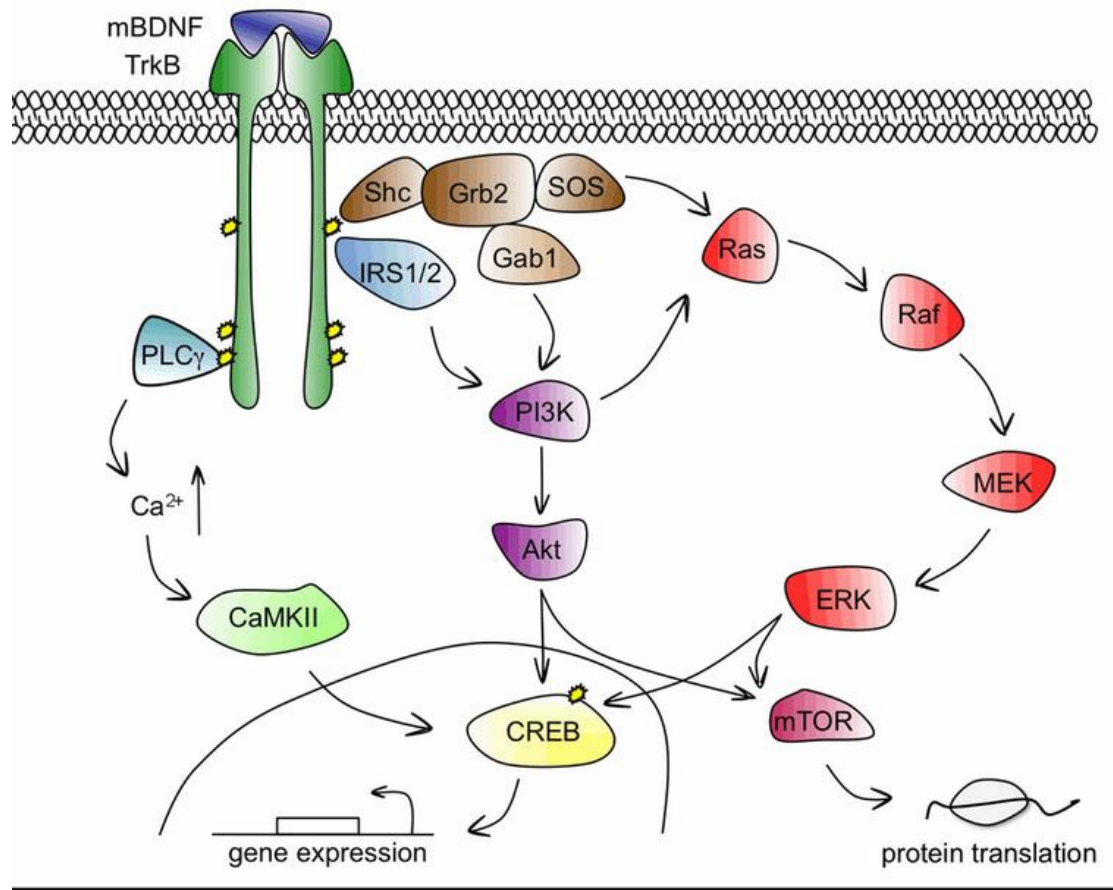


Figure 6. TrkB signaling pathway

Figure 7. Signaling events in Trk-mediated structural remodeling of spines

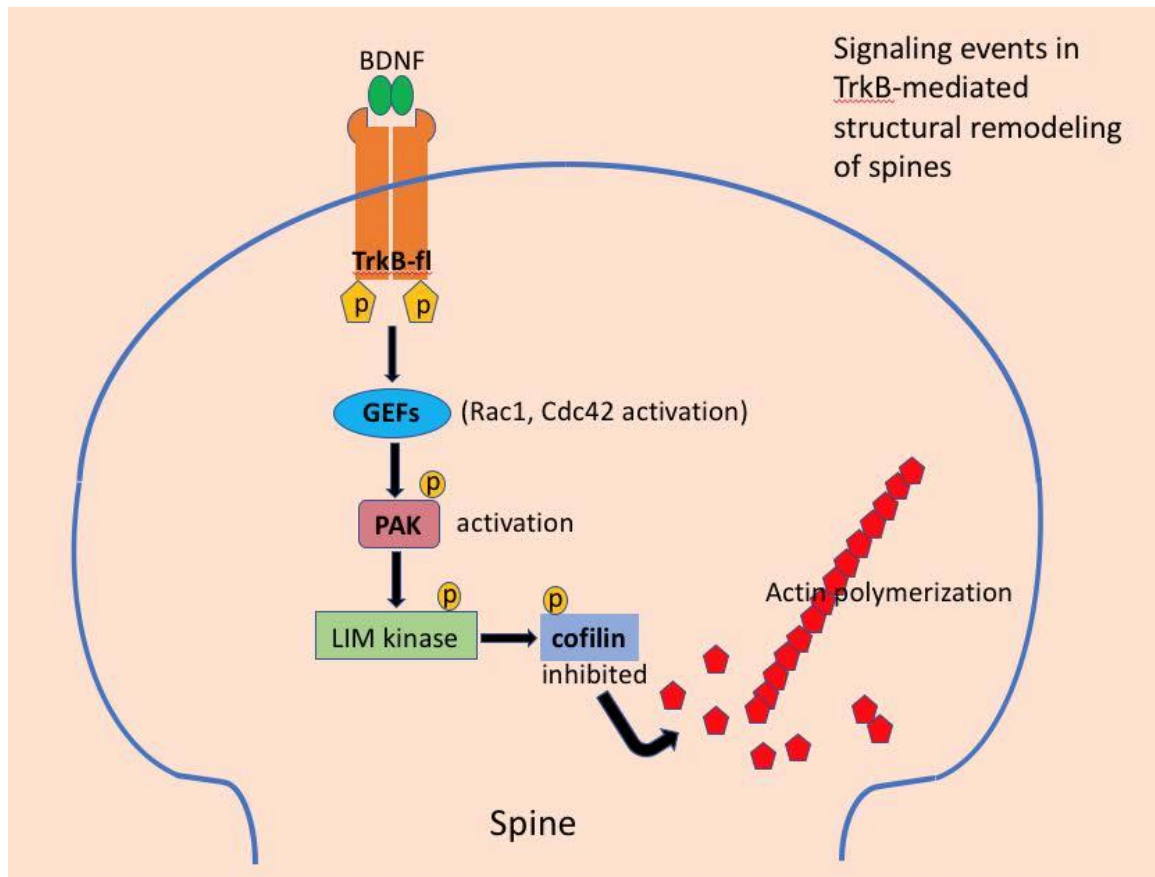


Figure 7. Trk-mediated structural remodeling of spines

Figure 8. Levels of OB BDNF mRNA were quantified by in situ cRNA hybridization and densitometry. (A) Pseudocolor images of film autoradiograms. The top shows BDNF expression in WT OB, the bottom section is from a TgBDNF mouse. (B) Quantitative comparison of hybridization density in the OB GCL. Bars indicate group mean value \pm SEM (* $p < 0.01$ unpaired t-test). Adapted from McDole *et al* 2015.

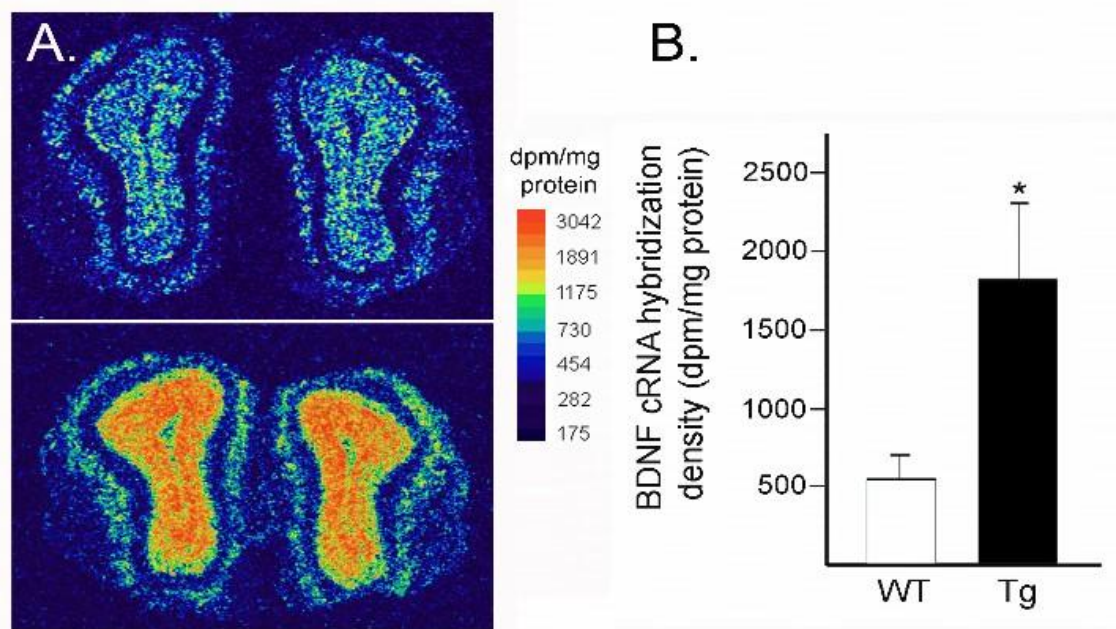


Figure 8. BDNF mRNA levels in TgBDNF mice

Figure 9. Photomicrographs showing examples of Golgi–Cox impregnated GCs bearing dendritic spines (A, B). (C) Proximal apical dendritic segment from a GC in a mouse over-expressing BDNF. Arrows indicate the different morphologies of GC spines. The solid black arrow indicates an example of a headed spine, the open arrows indicate filopodia, and the dotted arrow indicates a spine classified as other-type. Bar = 10 μm in A, B, and 5 μm in C.

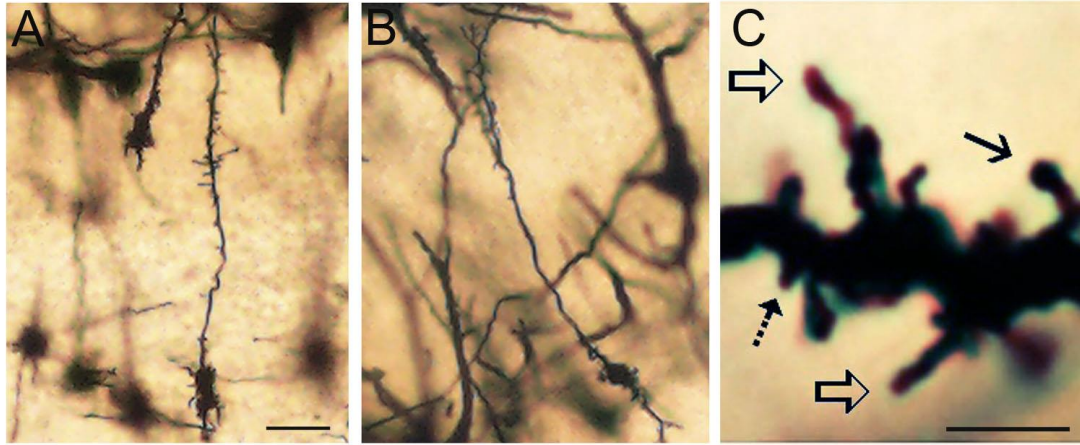


Figure 9. Examples of Golgi-Cox impregnated GC

Figure 10. Olfactory bulbs from adult mice over-expressing BDNF contain higher levels of BDNF protein. (A) ELISA quantification of total bulb BDNF content show significantly higher levels of BDNF in bulbs from adult transgenic (Tg) mice (* $p < 0.0001$; unpaired t-test, $n = 4$ per genotype). (B) Mature BDNF (?14 kDa) was visualized in Western blots of bulb lysates from wild-type (WT) and transgenic mice, with recombinant BDNF peptide (5 ng) as control. This antibody also detects non-specific bands of higher molecular mass. (C) Semi- quantitative measures of mature BDNF (14 kDa bands) from Western blots of olfactory bulb lysates. Bar graph shows group mean relative levels \pm SEM (* $p < 0.05$, $n = 4$ per genotype).

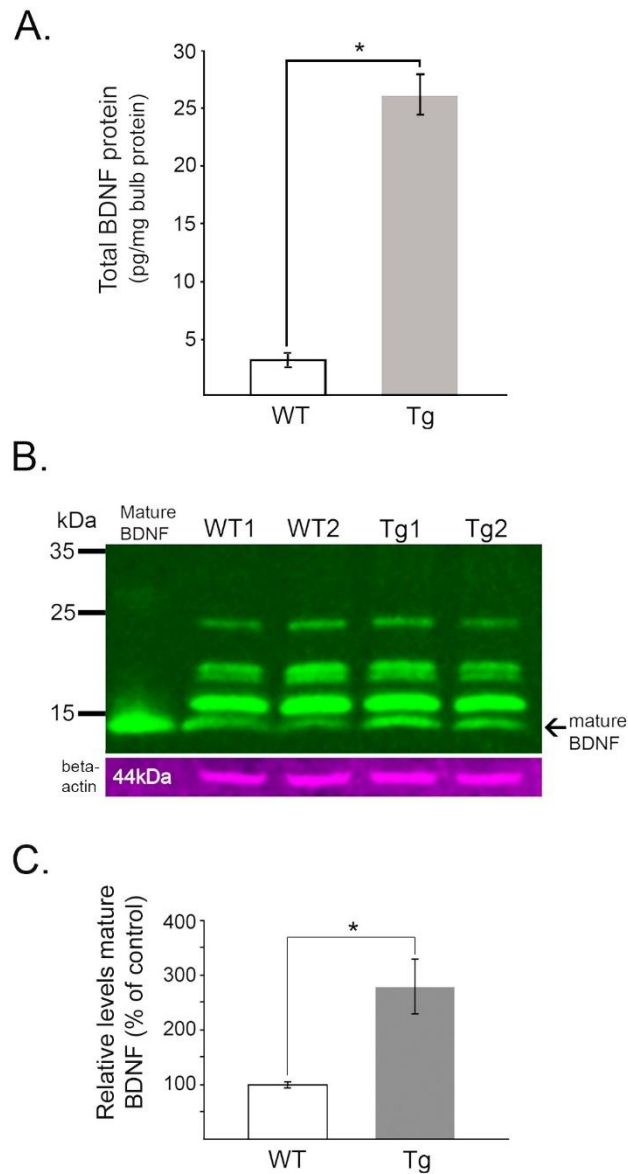


Figure 10. ELISA and Western blot BDNF protein analysis

Figure 11. Representative Neurolucida reconstructions of GCs from mice of each genotype and age. A total of 178 GCs were reconstructed. Labels to the left indicate cell location relative to bulb laminae. EPL, external plexiform layer; GL, glomerular layer; GCL, granule cell layer; Tg, transgenic mouse; WT, wild-type control.

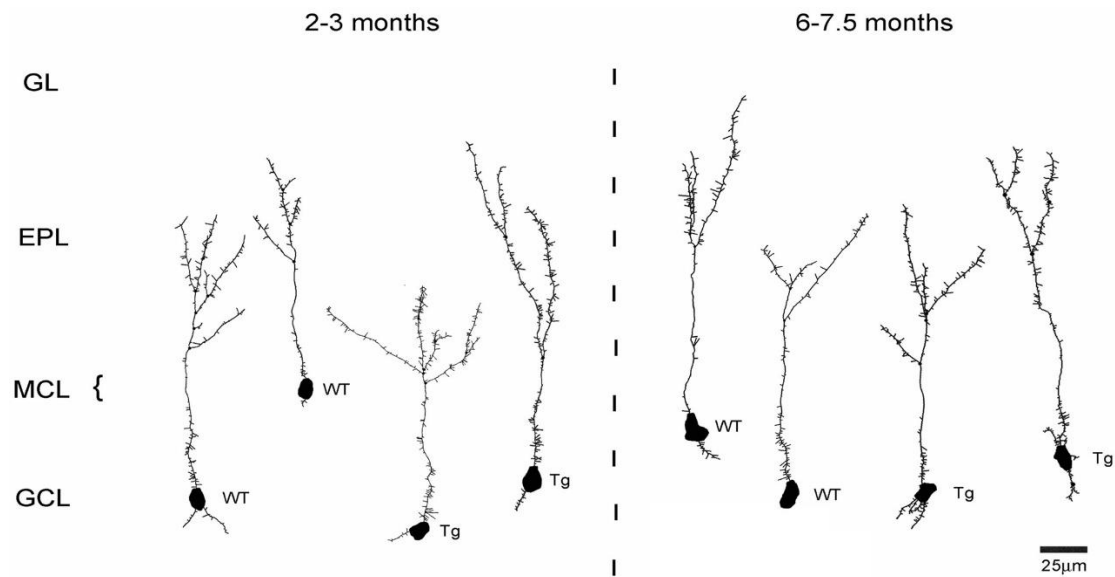


Figure 11. Reconstructions of Golgi-Cox labeled GCs

Figure 12. (A, B) Comparison of GC dendritic length in normal and transgenic mice (TgBDNF) at 2–3 months of age (A) and 6–7.5 months of age (B). Total, apical, and basal dendritic lengths show no significant differences between TgBDNF mice and their age-matched, wild-type (WT) controls ($p > 0.50$, unpaired t-tests). However, an age difference in apical dendritic length was measured in TgBDNF mice (compare bar in A vs bar in B; $p < 0.05$, unpaired t-test). (C, D) Sholl analysis of mean numbers of GC apical dendritic intersections at 20- μm intervals from the cell soma obtained for 2–3-month-old mice (C) and 6–7.5-month-old mice (D). No significant genotype-related differences were evident at any distance from the soma ($p > 0.05$ for all, unpaired t-tests)

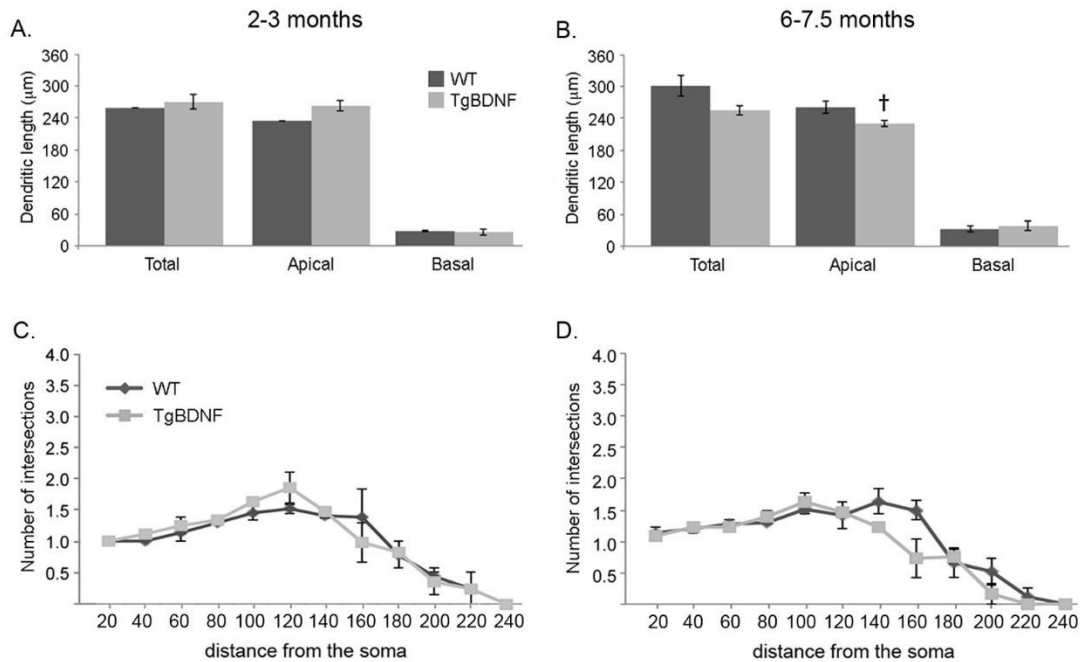


Figure 12. GC length and apical dendritic intersection comparison

Figure 13. Bars indicate group mean values \pm SEM (unpaired t-tests). (A, B) TgBDNF mice show a significant increase in total spine number in the apical compartment when compared to age-matched WT mice ($*p < 0.05$, unpaired t-test). (C, D) Headed spine number in the apical compartment is also increased in transgenic mice versus controls at both ages ($**p < 0.01$, unpaired t-test).

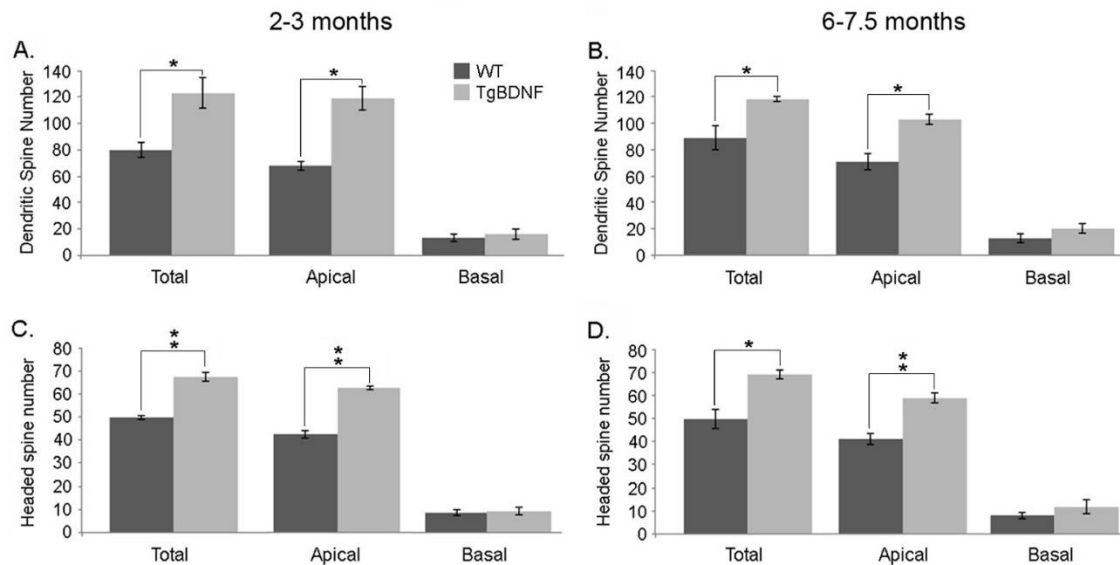


Figure 13. Analyses of GC spine number

Figure 14. Bar graphs representing the proportions of different spine types comprising the total numbers for each age and genotype. Group mean values were used.

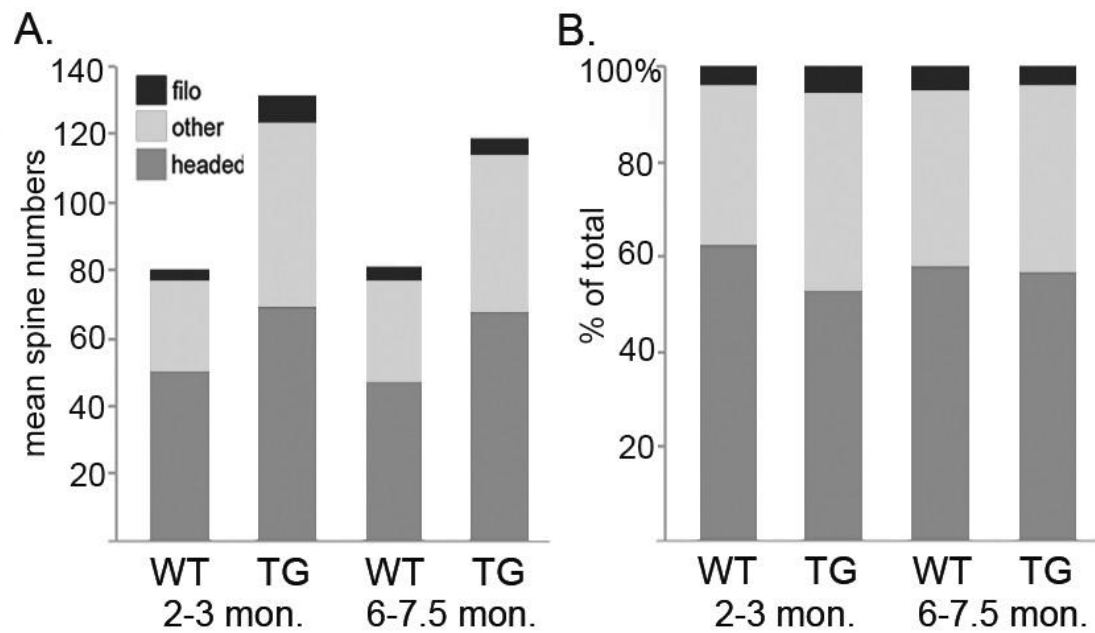


Figure 14. Spine type proportions

Figure 15. Bars indicate group mean values \pm SEM. (A, B) TgBDNF mice show increased spine density in apical and basal dendrites at 2–3 months. In older mice, differences in basal spine density did not reach significance, while apical measures remained significantly higher in transgenic mice. (C, D) Densities of headed spines in TgBDNF mice exceeded measures from WT mice at both ages. (E, F) Measures of apical spine density in the proximal (first 50 μ m), middle (second 50 μ m) and distal (dendrite beyond the first 100 μ m). Proximal and distal spine densities were significantly increased in TgBDNF mice compared to WT controls (* $p < 0.05$, ** $p < 0.01$, t-tests).

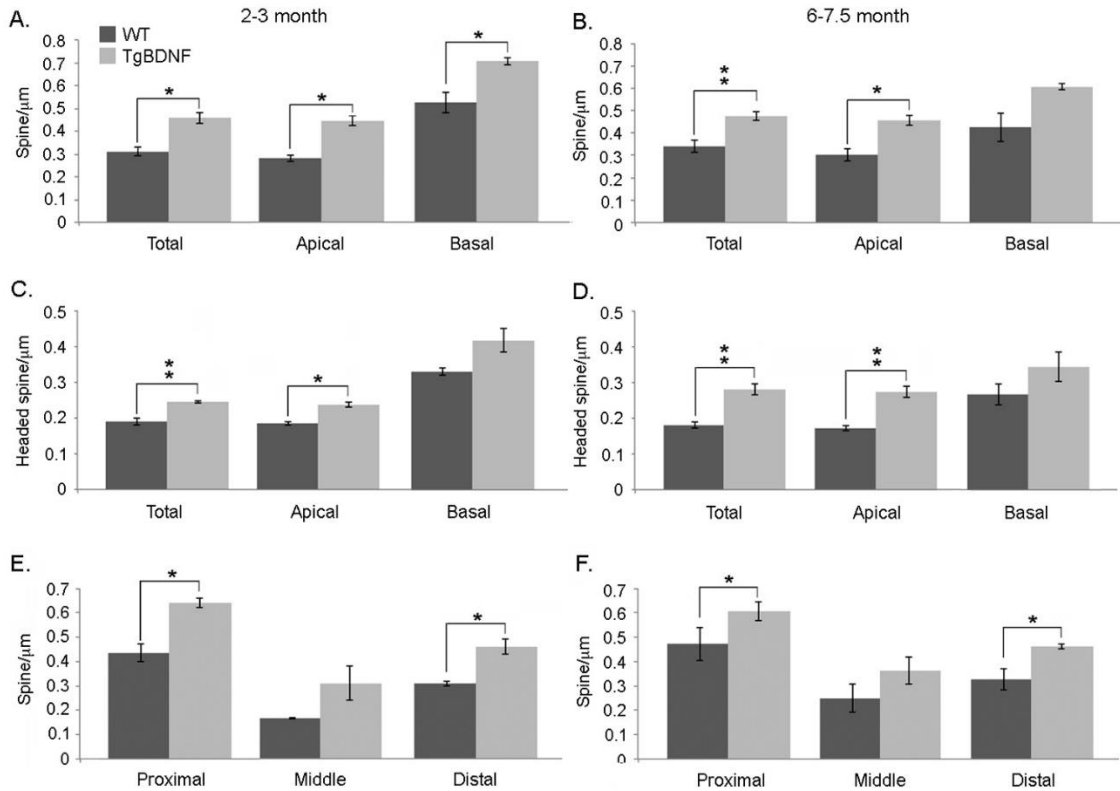


Figure 15. Analysis of granule cell spine density.

Figure 16. Survival of adult-born granule cells is not altered by increasing BDNF. (A) Representation of areas selected for counts in the GCL. (B-D) Confocal images BrdU/NeuN co-labeling in the GCL of a TgBDNF mouse. Arrows indicate double-labeled cells. (E) Orthogonal projection of a BrdU+/NeuN+ granule cell. (F) No differences are found in BrdU+/NeuN+ cell density between WT and TgBDNF mice at any survival interval ($p \geq 0.05$, unpaired, two tailed t-tests). Bars in A-B= 20 μ m

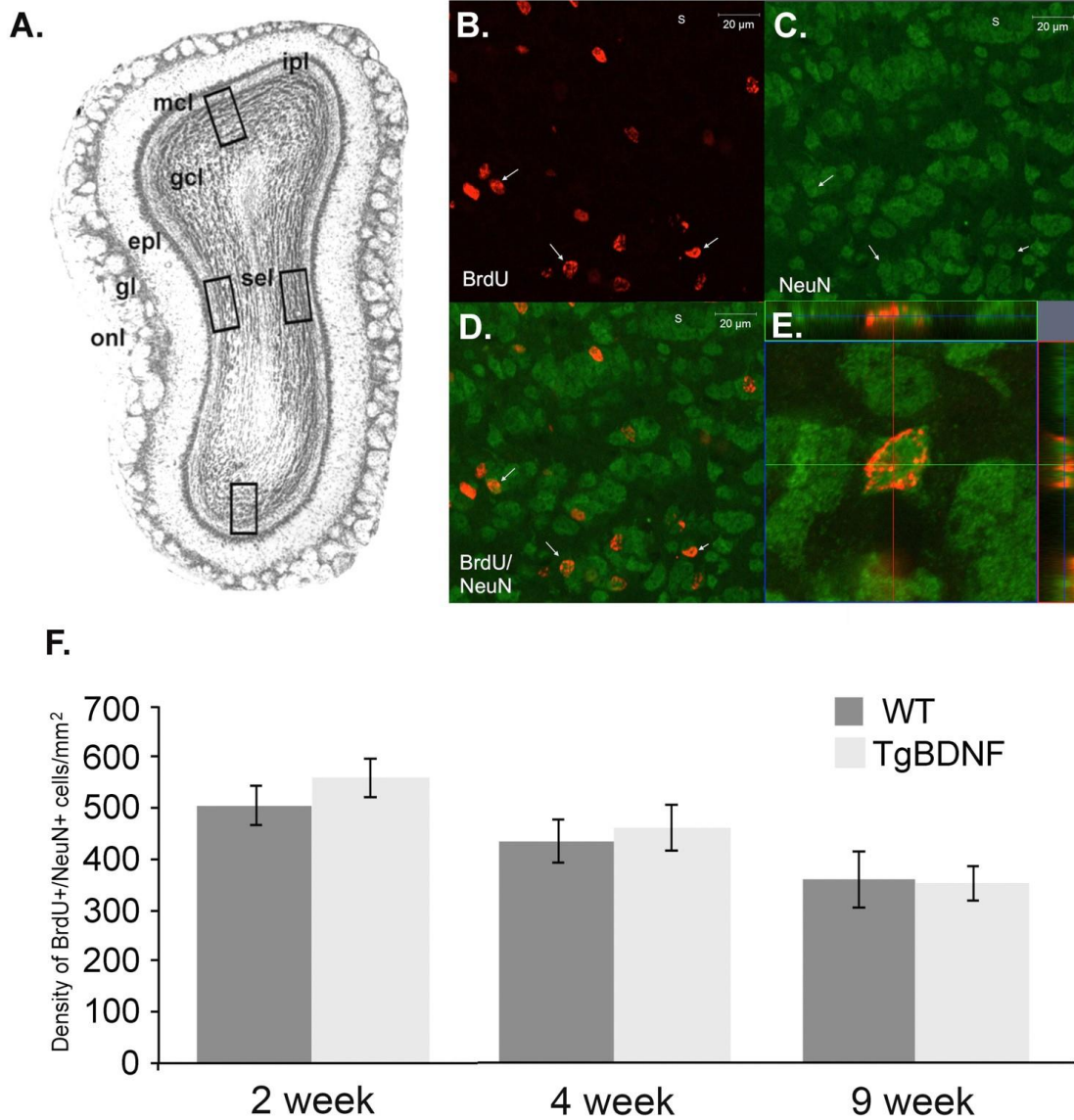


Figure 16. BrdU+/NeuN+ confocal imaging and survival analysis

Figure 17. Levels of programmed cell death in OB are not altered by BDNF over-expression. (A-B) Examples of TUNEL-labeled nuclei (arrows) in the deep granule cell layer in a WT (A), and TgBDNF mouse (B). (C) No differences in numbers of TUNEL+ cells were observed between genotypes. Bars indicate group mean value \pm SEM ($p \geq 0.05$, unpaired t-test with Welch's correction, $n=5$ per genotype). sel, subependymal layer. Bar in B= 50 μ m.

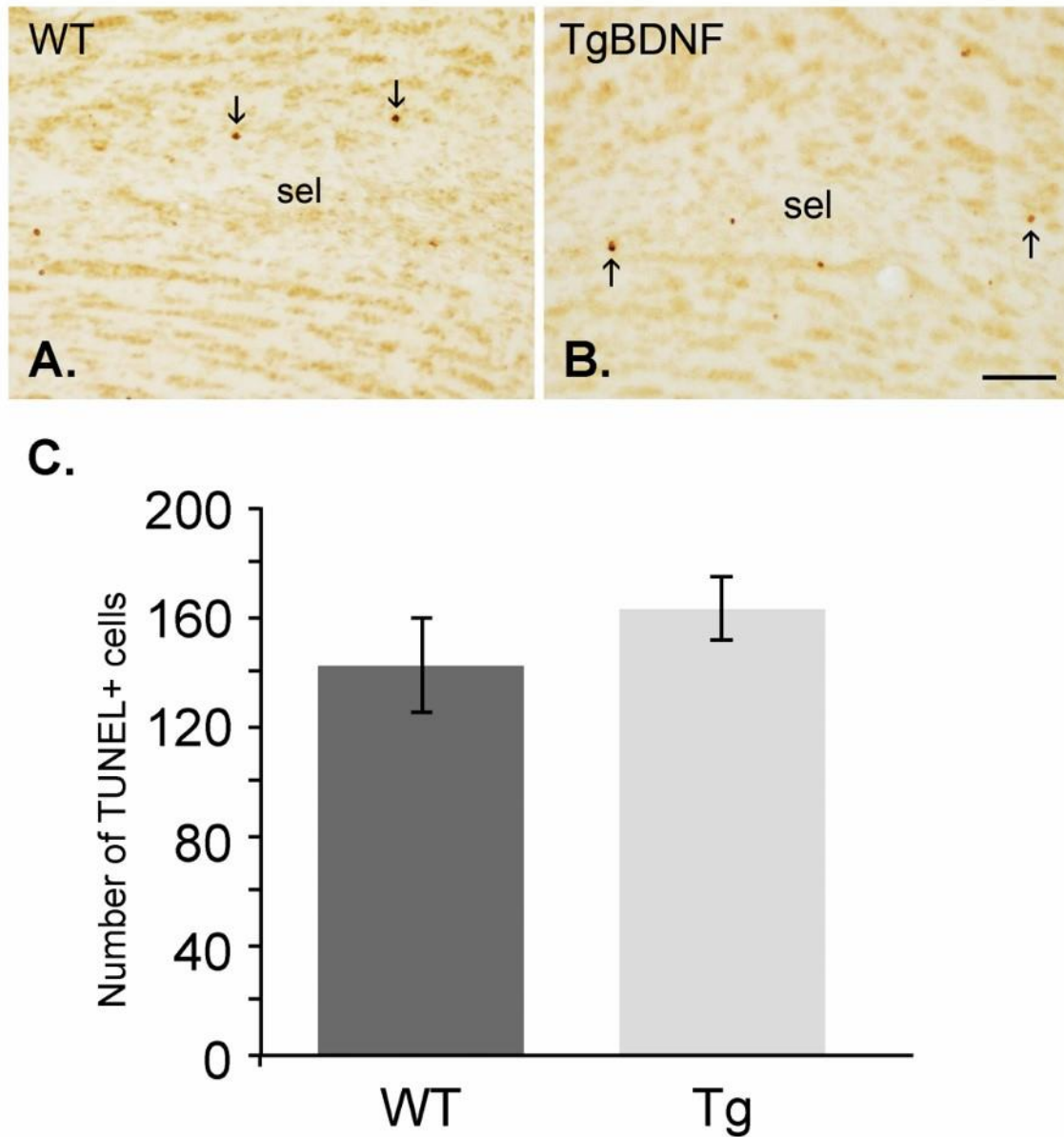


Figure 17. TUNEL labeling and cell death analysis

Figure 18. Proximal apical dendritic segment from a GC expressing tau-mCherry at 60 days PI in a mouse over-expressing BDNF. Arrows indicate the different morphologies of GC spines. The solid white arrow indicates an example of a headed spine, the dotted arrows indicate filopodia, and the open arrow indicates a spine classified as other-type. Bar = 5 μ m.

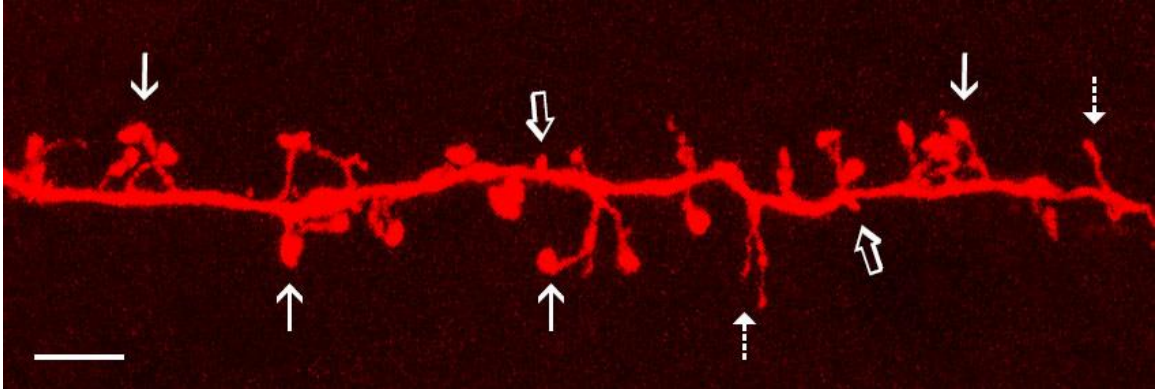


Figure 18. Virally labeled abGC spines

Figure 19. Representative GCs infected with Tau-mCherry from mice of each age and genotype. (For reconstructed versions see figure 20)

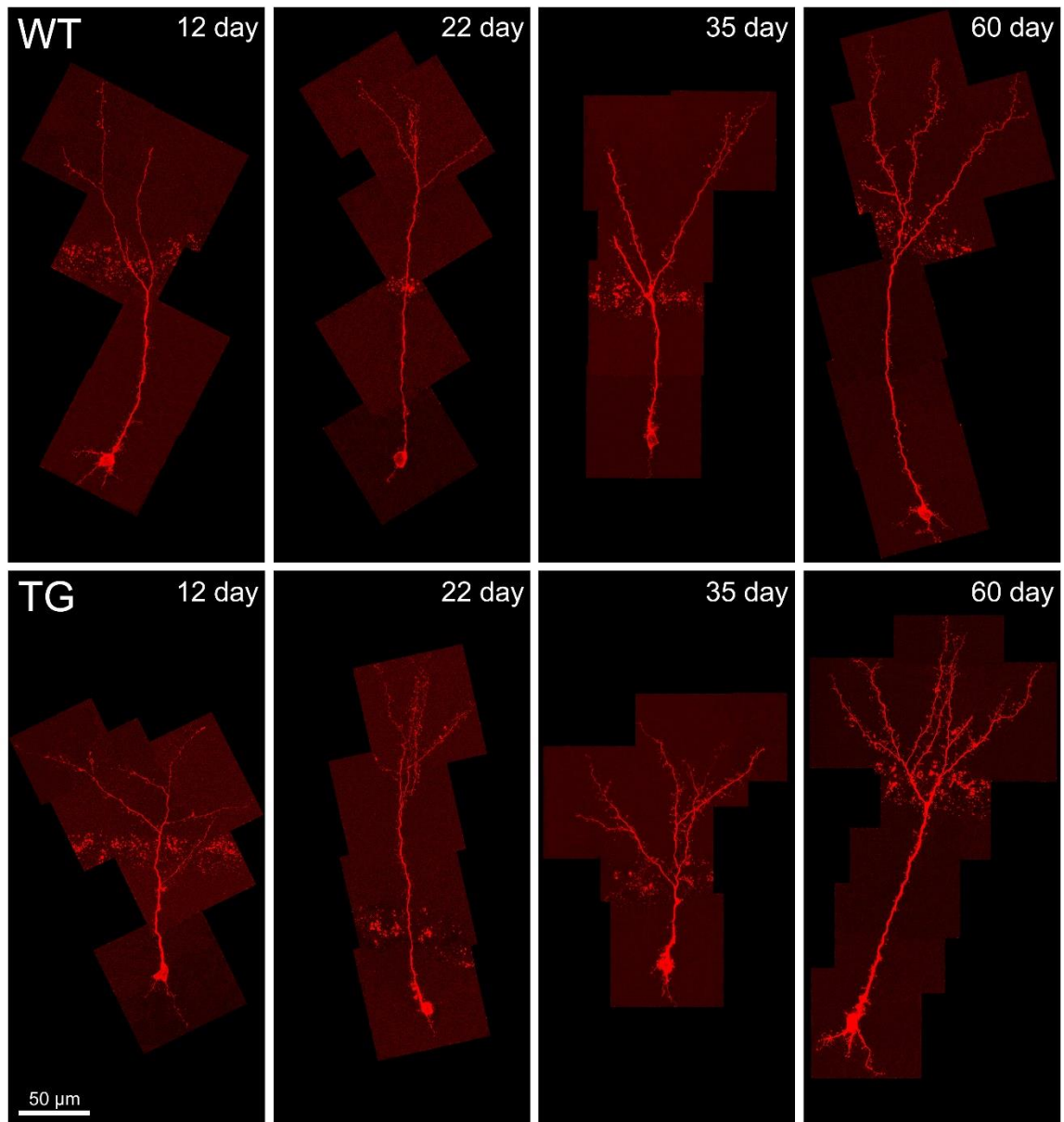


Figure 19. Examples of virally labeled abGCs

Figure 20. Representative Neurolucida reconstructions of GCs from mice of each genotype and age. GCs shown below are reconstructed versions of the neurons in figure 21. A total of 282 GCs were reconstructed and used for analysis.

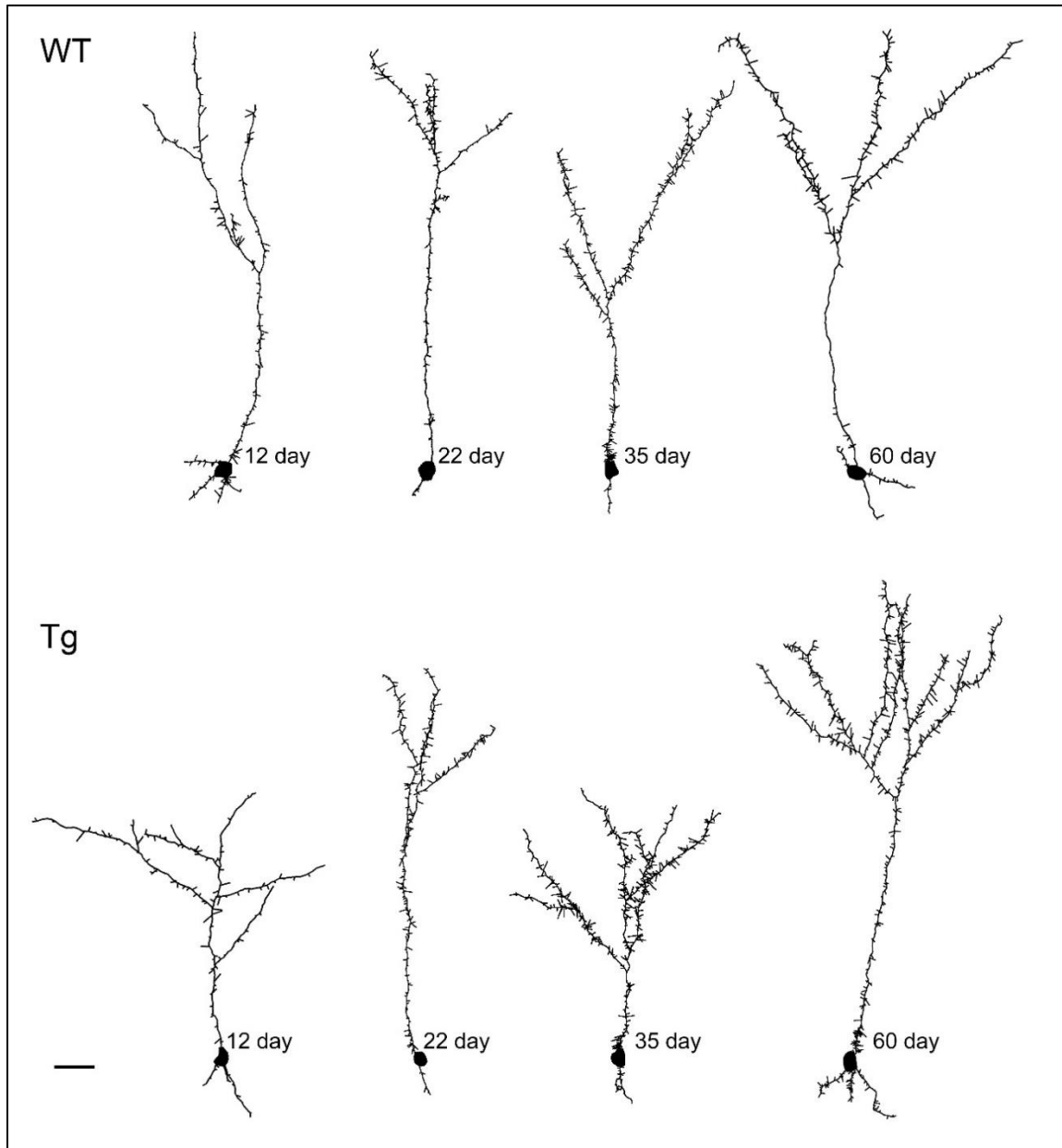


Figure 20. Reconstructions of virally labeled abGCs

Figure 21. Bars indicate group mean value \pm SEM (A-D) Comparison of GC dendritic length in normal and TgBDNF mice at 12 dpi (A) 22 dpi (B), 35 dpi (C), and 60 dpi (D). Total, apical, and basal dendritic lengths show no significant differences between TgBDNF mice and their age-matched, wild-type (WT) controls ($p > 0.50$, unpaired t-tests). However, an age difference between 12 dpi and subsequent cell ages was present (Tukey's post hoc comparison, $p < 0.05$).

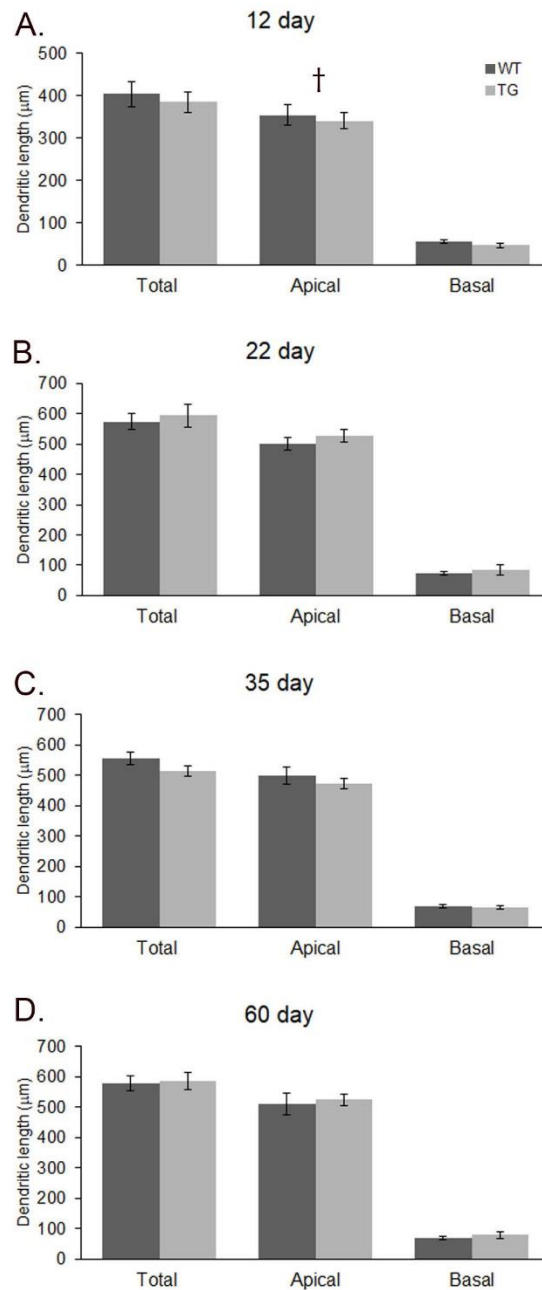


Figure 21. Dendritic lengths of abGCs

Figure 22. (A-D) Comparison of GC dendritic branch points in normal and TgBDNF mice at 12 dpi (A) 22 dpi (B), 35 dpi (C), and 60 dpi (D). Total, apical, and basal dendritic branch points show no significant differences between TgBDNF mice and their age-matched, WT controls ($p > 0.50$, unpaired, t-tests).

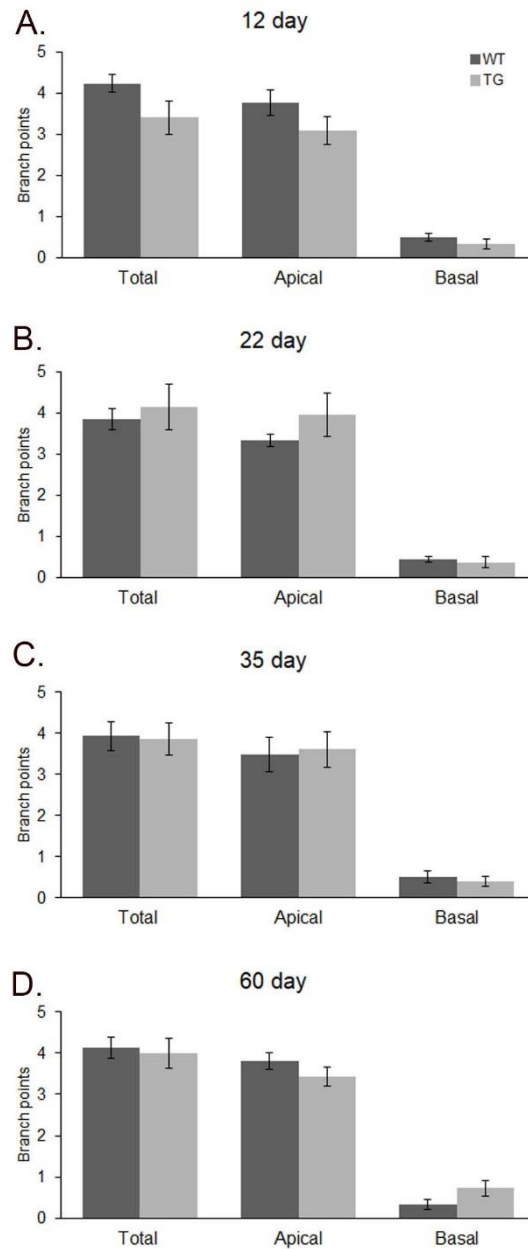


Figure 22. Dendritic branching of abGCs

Figure 23. A representative figure showing GC spine development of mean apical total spine number (A), apical headed-type spine number (B), apical other-type spine number (C), and apical filopodia-type spine number (D) at different cell ages. TgBDNF GC spine development/pruning stages show a similar pattern to WT GC spine development/pruning stages.

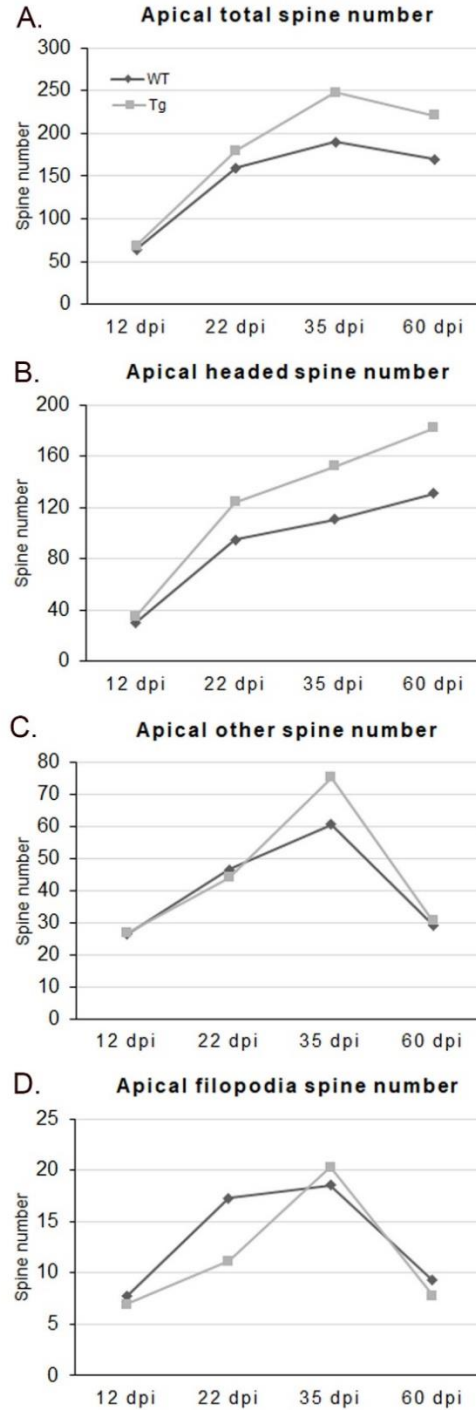


Figure 23. Spine developmental patterns of abGCs (spine densities)

Figure 24. Bars indicate group mean values \pm SEM (unpaired t-tests). (A, B) No significant difference were seen in total spine number at 12 dpi of 22 dpi. (C, D) TgBDNF mice show a significant increase in total spine number in the apical compartment when compared to age-matched WT mice (* $p < 0.05$, ** < 0.01 unpaired t-test).

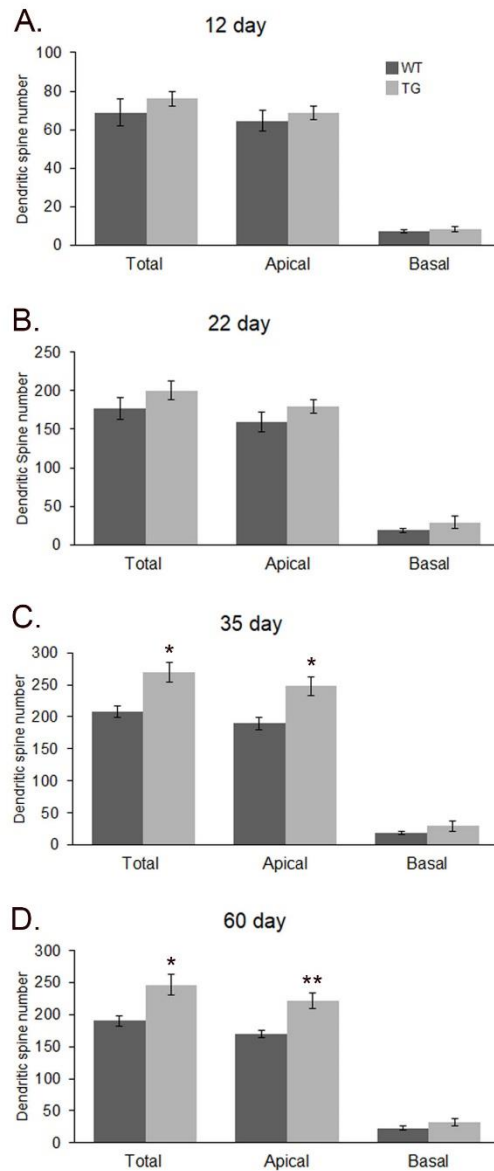


Figure 24. AbGC total spine numbers

Figure 25. Bars indicate group mean values \pm SEM (unpaired t-tests). (A) No significant difference was seen in headed spine number at 12 dpi. (B, C, D) TgBDNF mice show a significant increase in headed spine number in the apical compartment when compared to age-matched WT mice at 22 dpi, 35 dpi, and 60 dpi (* $p < 0.05$, ** $p < 0.01$, unpaired, t-test).

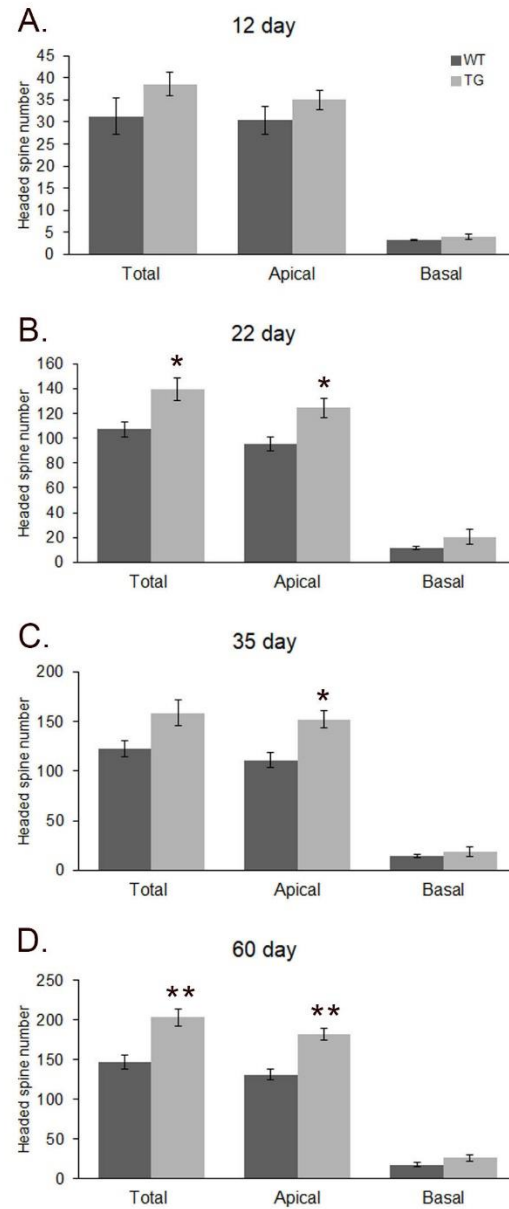


Figure 25. AbGC headed spine numbers

Figure 26. Bars indicate group mean values \pm SEM. (A-D) TgBDNF mice show increased total spine density at all time points compared to WT mice. (A, B, and D) TgBDNF mice show increased spine density in apical dendrites compared to WT mice at 12 dpi, 35dpi, and 60dpi. (* $p < 0.05$, ** $p < 0.01$, t-tests).

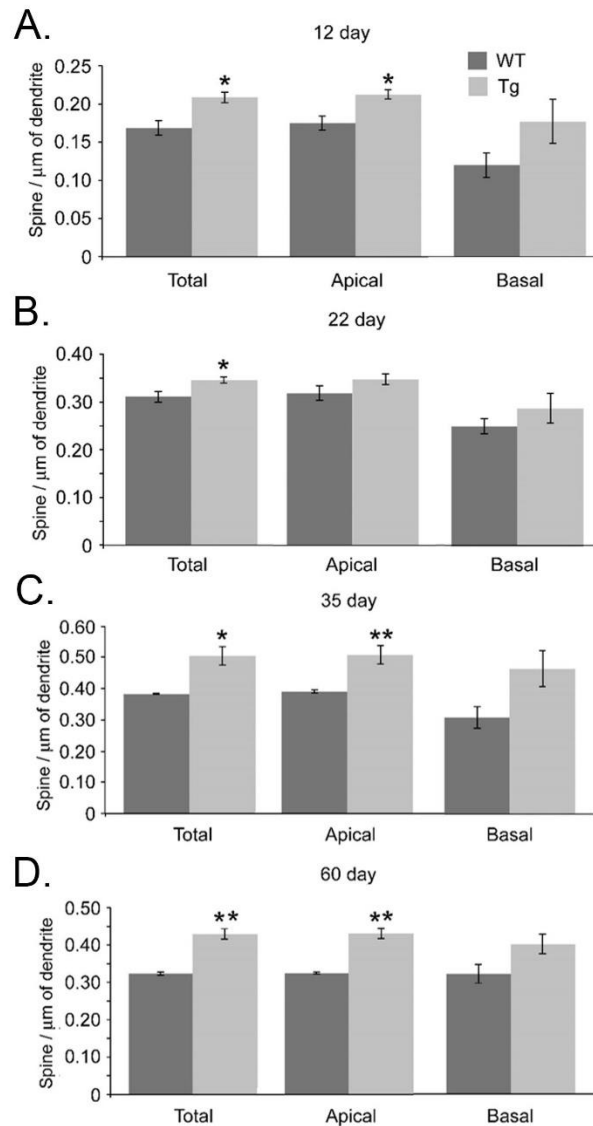


Figure 26. Analysis of total spine density on abGCs

Figure 27. Bars indicate group mean values \pm SEM. (A-D) TgBDNF mice show increased apical headed spine density at all time points. (A and D) TgBDNF mice show increased basal headed spine density at 12 dpi and 60 dpi (* $p < 0.05$, ** $p < 0.01$, t-tests).

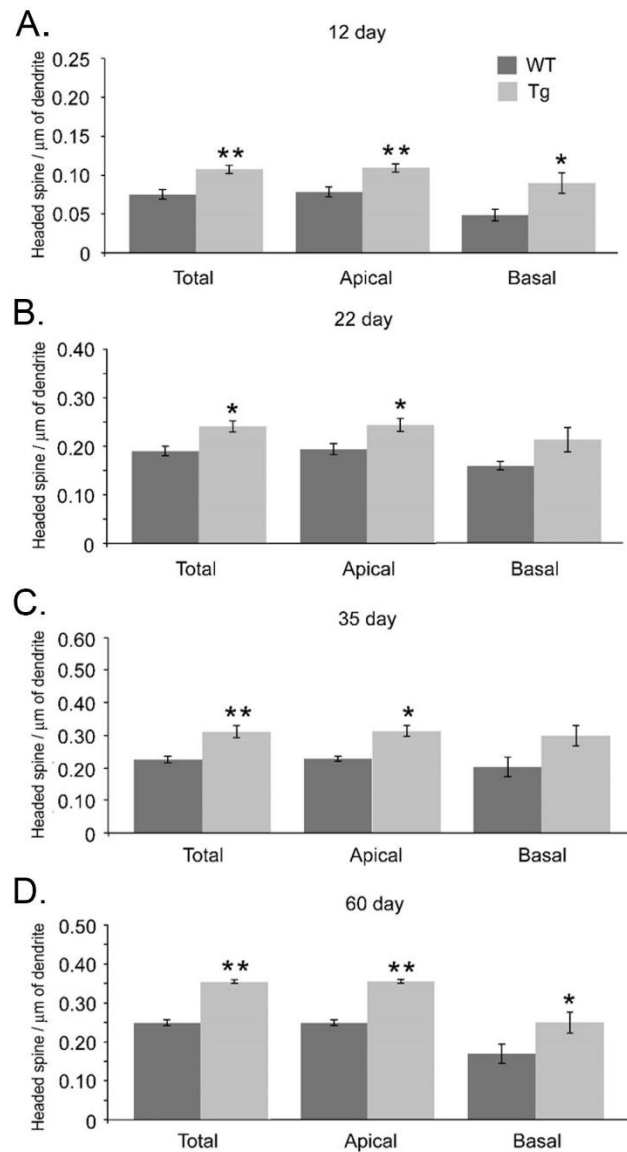


Figure 27. Analysis of headed spine density on abGCs

Figure 28. Bars indicate group mean values \pm SEM. Measures of apical spine density in the proximal (first 50 μ m), middle (second 50 μ m) and distal (dendrite beyond the first 100 μ m). (A) Middle spine densities were significantly increased in TgBDNF mice compared to WT mice at 12 dpi. (C and D) Distal spine densities were significantly increased in TgBDNF mice compared to WT mice at 35 dpi and 60 dpi. (* $p < 0.05$, t-tests).

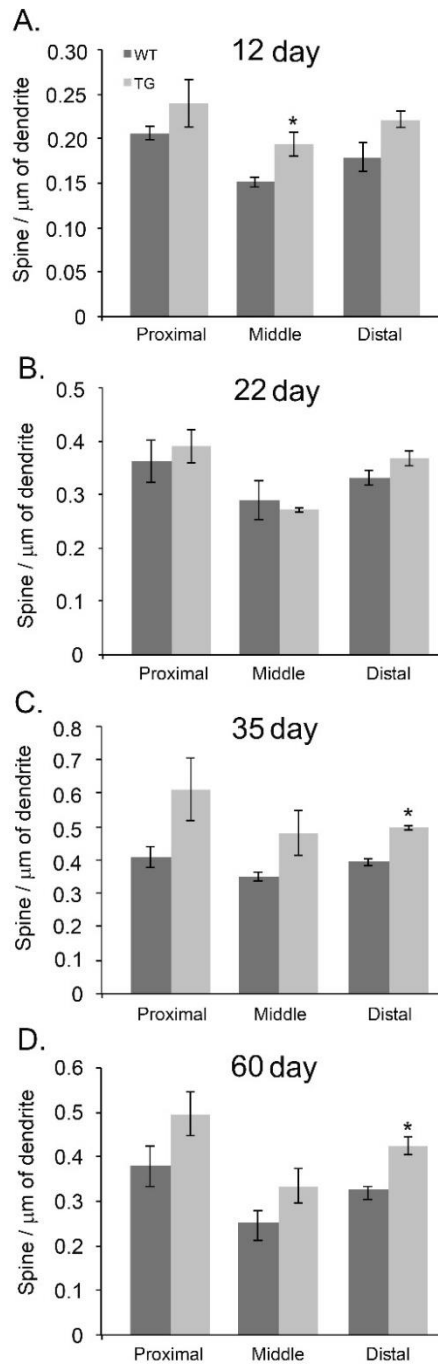


Figure 28. Segment analysis of total dendritic spines

Figure 29. Bars indicate group mean values \pm SEM. Measures of apical spine density in the proximal (first 50 μ m), middle (second 50 μ m) and distal (dendrite beyond the first 100 μ m). (A) Middle spine densities were significantly increased in TgBDNF mice compared to WT mice at 12 dpi. (A, C, and D) Distal spine densities were significantly increased in TgBDNF mice compared to WT mice at 12 dpi, 35 dpi, and 60 dpi. (* $p < 0.05$, t-tests).

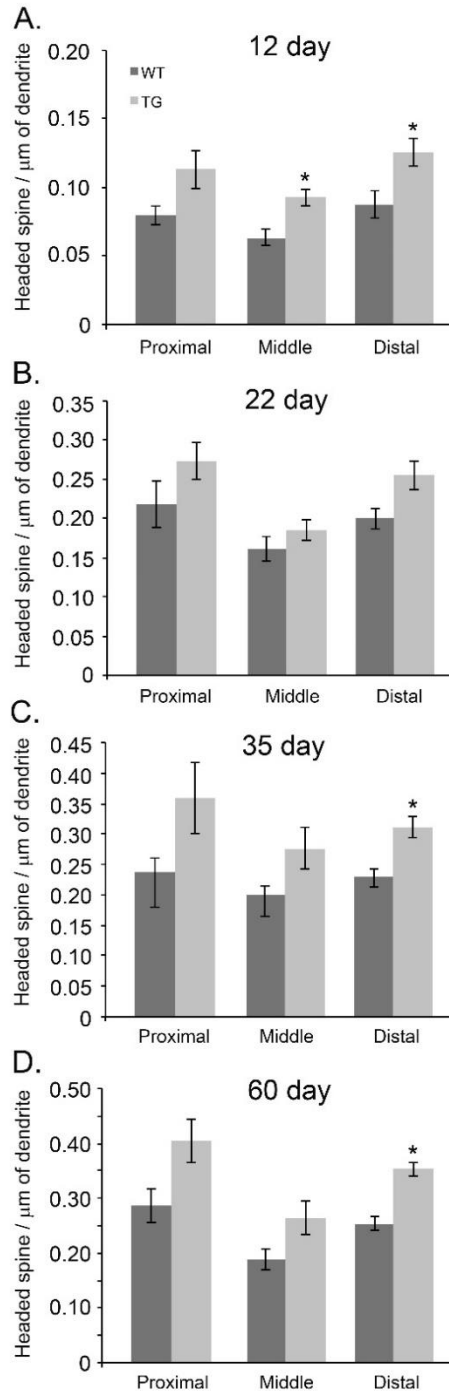


Figure 29. Segment analysis of headed dendritic spines

Figure 30. Bar graphs representing the proportions of different spine types comprising the total densities for each age and genotype. Group mean values were used.

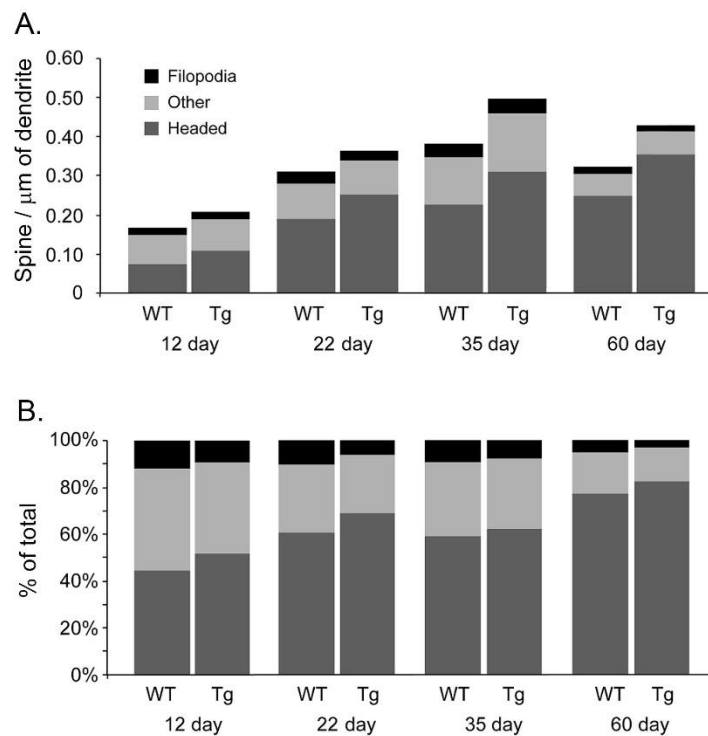


Figure 30. Spine type proportion in abGCs

PART VI- REFERENCES

- Abraham, N. M. *et al.* (2010) ‘Synaptic Inhibition in the Olfactory Bulb Accelerates Odor Discrimination in Mice’, *Neuron*. Elsevier Ltd, 65(3), pp. 399–411. doi: 10.1016/j.neuron.2010.01.009.
- Adipietro, K. A., Mainland, J. D. and Matsunami, H. (2012) ‘Functional evolution of mammalian odorant receptors’, *PLoS Genetics*, 8(7). doi: 10.1371/journal.pgen.1002821.
- Aid, T. *et al.* (2007) ‘Mouse and ratBDNF gene structure and expression revisited’, *Journal of Neuroscience Research*, 85(3), pp. 525–535. doi: 10.1002/jnr.21139.
- Alonso, M. *et al.* (2006) ‘Olfactory Discrimination Learning Increases the Survival of Adult-Born Neurons in the Olfactory Bulb’, *Journal of Neuroscience*, 26(41), pp. 10508–10513. doi: 10.1523/JNEUROSCI.2633-06.2006.
- Alonso, M. *et al.* (2012) ‘Activation of adult-born neurons facilitates learning and memory’, *Nature Neuroscience*, 15(6), pp. 897–904. doi: 10.1038/nn.3108.
- Altman, J. and Das, G. D. (1965) ‘Autoradiographic and histologicalevidence of postnatal hippocampal neurogenesis in rats’, *The Journal of Comparative Neurology*, 124(3), pp. 319–335.
- Alvarez-Buylla, A. and García-Verdugo, J. M. (2002) ‘Neurogenesis in adult subventricular zone’, *The Journal of neuroscience*, 22(3), pp. 629–634. doi: 0270-6474/02/220629-06.
- An, J. J. *et al.* (2008) ‘Distinct Role of Long 3' UTR BDNF mRNA in Spine Morphology and Synaptic Plasticity in Hippocampal Neurons’, *Cell*, 134(1), pp. 175–187. doi: 10.1016/j.cell.2008.05.045.
- Anacker, C. and Hen, R. (2017) ‘Adult hippocampal neurogenesis and cognitive flexibility-linking memory and mood’, *Nature Reviews Neuroscience*. Nature Publishing Group, 18(6), pp. 335–346. doi: 10.1038/nrn.2017.45.
- Anthony, T. E. *et al.* (2004) ‘Radial glia serve as neuronal progenitors in all regions of the central nervous system’, *Neuron*, 41(6), pp. 881–890. doi: 10.1016/S0896-6273(04)00140-0.
- Arruda-Carvalho, M. *et al.* (2014) ‘Posttraining Ablation of Adult-Generated Olfactory Granule Cells Degrades Odor – Reward Memories’, 34(47), pp. 15793–15803. doi: 10.1523/JNEUROSCI.2336-13.2014.

- Bagley, J. A. and Belluscio, L. (2010) 'Dynamic imaging reveals that brain-derived neurotrophic factor can independently regulate motility and direction of neuroblasts within the rostral migratory stream', *Neuroscience*. Elsevier Inc., 169(3), pp. 1449–1461. doi: 10.1016/j.neuroscience.2010.05.075.
- Balu, R., Pressler, R. T. and Strowbridge, B. W. (2007) 'Multiple Modes of Synaptic Excitation of Olfactory Bulb Granule Cells', *Journal of Neuroscience*, 27(21), pp. 5621–5632. doi: 10.1523/JNEUROSCI.4630-06.2007.
- Baquet, Z. C. (2004) 'Early Striatal Dendrite Deficits followed by Neuron Loss with Advanced Age in the Absence of Anterograde Cortical Brain-Derived Neurotrophic Factor', *Journal of Neuroscience*, 24(17), pp. 4250–4258. doi: 10.1523/JNEUROSCI.3920-03.2004.
- Bartel, D. L. *et al.* (2015) 'Dendrodendritic synapses in the mouse olfactory bulb external plexiform layer', *Journal of Comparative Neurology*, 523(8), pp. 1145–1161. doi: 10.1002/cne.23714.
- Bastien-Dionne, P. O. *et al.* (2010) 'Role of sensory activity on chemospecific populations of interneurons in the adult olfactory bulb', *Journal of Comparative Neurology*, 518(10), pp. 1847–1861. doi: 10.1002/cne.22307.
- Bath, K. G. *et al.* (2008) 'Variant Brain-Derived Neurotrophic Factor (Val66Met) Alters Adult Olfactory Bulb Neurogenesis and Spontaneous Olfactory Discrimination', *Journal of Neuroscience*, 28(10), pp. 2383–2393. doi: 10.1523/JNEUROSCI.4387-07.2008.
- Bath, K. G., Akins, M. R. and Lee, F. S. (2012) 'BDNF control of adult SVZ neurogenesis', *Developmental Psychobiology*, 54(6), pp. 578–589. doi: 10.1002/dev.20546.
- Bedos, M., Portillo, W. and Paredes, R. G. (2018) 'Neurogenesis and sexual behavior', *Frontiers in Neuroendocrinology*. Elsevier, (February), pp. 1–12. doi: 10.1016/j.yfrne.2018.02.004.
- Benraiss, a *et al.* (2001) 'Adenoviral brain-derived neurotrophic factor induces both neostriatal and olfactory neuronal recruitment from endogenous progenitor cells in the adult forebrain.', *The Journal of neuroscience: the official journal of the Society for Neuroscience*, 21(17), pp. 6718–6731. doi: 10.1523/JNEUROSCI.2117-01.2001 [pii].
- Benraiss, A. *et al.* (2012) 'Sustained induction of neuronal addition to the adult rat neostriatum by AAV4-delivered noggin and BDNF', *Gene Therapy*, 19(5), pp. 483–493. doi: 10.1038/gt.2011.114.
- Bergami, M. *et al.* (2008) 'Deletion of TrkB in adult progenitors alters newborn neuron integration into hippocampal circuits and increases anxiety-like behavior', *Proceedings of the National Academy of Sciences*, 105(40), pp. 15570–15575. doi: 10.1073/pnas.0803702105.

- Bergami, M. *et al.* (2013) 'TrkB Signaling Directs the Incorporation of Newly Generated Periglomerular Cells in the Adult Olfactory Bulb', *Journal of Neuroscience*, 33(28), pp. 11464–11478. doi: 10.1523/JNEUROSCI.4812-12.2013.
- Bergami, M., Berninger, B. and Canossa, M. (2009) 'Conditional deletion of TrkB alters adult hippocampal neurogenesis and anxiety-related behavior', *Communicative and Integrative Biology*, 2(1), pp. 14–16. doi: 10.4161/cib.2.1.7349.
- Berghuis, P. *et al.* (2006) 'Brain-derived neurotrophic factor selectively regulates dendritogenesis of parvalbumin-containing interneurons in the main olfactory bulb through the PLC γ pathway', *Journal of Neurobiology*, 66(13), pp. 1437–1451. doi: 10.1002/neu.20319.
- Berry, K. P. and Nedivi, E. (2017) 'Spine Dynamics: Are They All the Same?', *Neuron*. Elsevier Inc., 96(1), pp. 43–55. doi: 10.1016/j.neuron.2017.08.008.
- von Bohlen Und Halbach, O. and von Bohlen Und Halbach, V. (2018) 'BDNF effects on dendritic spine morphology and hippocampal function', *Cell and Tissue Research*. Cell and Tissue Research, pp. 1–13. doi: 10.1007/s00441-017-2782-x.
- Bond, A. M., Ming, G. L. and Song, H. (2015) 'Adult Mammalian Neural Stem Cells and Neurogenesis: Five Decades Later', *Cell Stem Cell*. Elsevier Inc., 17(4), pp. 385–395. doi: 10.1016/j.stem.2015.09.003.
- Bosch, M. and Hayashi, Y. (2012) 'Structural plasticity of dendritic spines', *Current Opinion in Neurobiology*. Elsevier Ltd, 22(3), pp. 383–388. doi: 10.1016/j.conb.2011.09.002.
- Breton-Provencher, V. *et al.* (2016) 'Principal cell activity induces spine relocation of adult-born interneurons in the olfactory bulb', *Nature Communications*, 7. doi: 10.1038/ncomms12659.
- Breton-Provencher, V., Cote, D. and Saghatelian, A. (2014) 'Activity of the Principal Cells of the Olfactory Bulb Promotes a Structural Dynamic on the Distal Dendrites of Immature Adult-Born Granule Cells via Activation of NMDA Receptors', *Journal of Neuroscience*, 34(5), pp. 1748–1759. doi: 10.1523/JNEUROSCI.3013-13.2014.
- Breton-Provencher, V. and Saghatelian, A. (2012) 'Newborn neurons in the adult olfactory bulb: Unique properties for specific odor behavior', *Behavioural Brain Research*. Elsevier B.V., 227(2), pp. 480–489. doi: 10.1016/j.bbr.2011.08.001.
- Brunjes, P. C. and Armstrong, A. M. (1996) 'Apoptosis in the rostral migratory stream of the developing rat', *Developmental Brain Research*, 92(2), pp. 219–222. doi: 10.1016/0165-3806(96)00006-5.
- Burton, S. D. (2017) 'Inhibitory circuits of the mammalian main olfactory bulb', *Journal of Neurophysiology*, 84112, p. jn.00109.2017. doi: 10.1152/jn.00109.2017.

- Burton, S. D. and Urban, N. N. (2015) 'Rapid Feedforward Inhibition and Asynchronous Excitation Regulate Granule Cell Activity in the Mammalian Main Olfactory Bulb', *Journal of Neuroscience*, 35(42), pp. 14103–14122. doi: 10.1523/JNEUROSCI.0746-15.2015.
- Calabrese, B., Wilson, M. S. and Halpain, S. (2006) 'Development and Regulation of Dendritic Spine Synapses', *Physiology*, 21(1), pp. 38–47. doi: 10.1152/physiol.00042.2005.
- Carlén, M. *et al.* (2002) 'Functional integration of adult-born neurons', *Current Biology*, 12(7), pp. 606–608. doi: 10.1016/S0960-9822(02)00771-6.
- Carleton, A. *et al.* (2003) 'Becoming a new neuron in the adult olfactory bulb', *Nature Neuroscience*, 6(5), pp. 507–518. doi: 10.1038/nn1048.
- Cauthron, J. L. and Stripling, J. S. (2014) 'Long-Term Plasticity in the Regulation of Olfactory Bulb Activity by Centrifugal Fibers from Piriform Cortex', *Journal of Neuroscience*, 34(29), pp. 9677–9687. doi: 10.1523/JNEUROSCI.1314-14.2014.
- Chan, J. P. *et al.* (2008) 'Depletion of central BDNF in mice impedes terminal differentiation of new granule neurons in the adult hippocampus', *Molecular and Cellular Neuroscience*. Elsevier Inc., 39(3), pp. 372–383. doi: 10.1016/j.mcn.2008.07.017.
- Chapleau, C. A. and Pozzo-Miller, L. (2012) 'Divergent roles of p75NTR and Trk receptors in BDNF's effects on dendritic spine density and morphology', *Neural Plasticity*, 2012. doi: 10.1155/2012/578057.
- Chiamarello, S. *et al.* (2007) 'BDNF/TrkB interaction regulates migration of SVZ precursor cells via PI3-K and MAP-K signalling pathways', *European Journal of Neuroscience*, 26(7), pp. 1780–1790. doi: 10.1111/j.1460-9568.2007.05818.x.
- Choi, S. H. *et al.* (2009) 'Regulation of hippocampal progenitor cell survival, proliferation and dendritic development by BDNF', *Molecular Neurodegeneration*, 4(1), pp. 1–12. doi: 10.1186/1750-1326-4-52.
- Clevenger, A. C. *et al.* (2008) 'BDNF promoter-mediated β -Galactosidase expression in the olfactory epithelium and bulb', *Chemical Senses*, 33(6), pp. 531–539. doi: 10.1093/chemse/bjn021.
- Cohen, M. S. *et al.* (2011) 'Neurotrophin-mediated dendrite-to-nucleus signaling revealed by microfluidic compartmentalization of dendrites', *Proceedings of the National Academy of Sciences*, 108(27), pp. 11246–11251. doi: 10.1073/pnas.1012401108.
- Conner, J. M. *et al.* (1997) 'Distribution of Brain-Derived Neurotrophic Factor (BDNF) Protein and mRNA in the Normal Adult Rat CNS: Evidence for Anterograde Axonal Transport', *The Journal of Neuroscience*, 17(7), pp. 2295–2313. doi: 10.1523/JNEUROSCI.17-07-02295.1997.

- Cunha, C., Brambilla, R. and Thomas, K. L. (2010) 'A simple role for BDNF in learning and memory?', *Frontiers in Molecular Neuroscience*, 3(February), pp. 1–14. doi: 10.3389/neuro.02.001.2010.
- Dahlen, J. E. *et al.* (2011) 'Morphological analysis of activity-reduced adult-born neurons in the mouse olfactory bulb', *Frontiers in Neuroscience*, 5(MAY), pp. 1–8. doi: 10.3389/fnins.2011.00066.
- Dean, C. *et al.* (2012) 'Distinct Subsets of Syt-IV/BDNF Vesicles Are Sorted to Axons versus Dendrites and Recruited to Synapses by Activity', *Journal of Neuroscience*, 32(16), pp. 5398–5413. doi: 10.1523/JNEUROSCI.4515-11.2012.
- Deckner, M.-L. *et al.* (1993) 'Localization of neurotrophin receptors in olfactory epithelium and bulb', *NeuroReport*, 5(3), pp. 301–304. doi: 10.1097/00001756-199312000-00030.
- Degano, A. L. *et al.* (2014) 'MeCP2 is required for activity-dependent refinement of olfactory circuits', *Molecular and Cellular Neuroscience*. Elsevier Inc., 59, pp. 63–75. doi: 10.1016/j.mcn.2014.01.005.
- Delgado, A. C. *et al.* (2014) 'Endothelial NT-3 Delivered by Vasculature and CSF Promotes Quiescence of Subependymal Neural Stem Cells through Nitric Oxide Induction', *Neuron*, 83(3), pp. 572–585. doi: 10.1016/j.neuron.2014.06.015.
- Deprez, F. *et al.* (2015) 'Postsynaptic gephyrin clustering controls the development of adult-born granule cells in the olfactory bulb', *Journal of Comparative Neurology*, 523(13), pp. 1998–2016. doi: 10.1002/cne.23776.
- Deshpande, A. *et al.* (2013) 'Retrograde monosynaptic tracing reveals the temporal evolution of inputs onto new neurons in the adult dentate gyrus and olfactory bulb', *Proceedings of the National Academy of Sciences*, 110(12), pp. E1152–E1161. doi: 10.1073/pnas.1218991110.
- Dieni, S. *et al.* (2012) 'BDNF and its pro-peptide are stored in presynaptic dense core vesicles in brain neurons', *Journal of Cell Biology*, 196(6), pp. 775–788. doi: 10.1083/jcb.201201038.
- Ebrahimi, S. and Okabe, S. (2014) 'Structural dynamics of dendritic spines: Molecular composition, geometry and functional regulation', *Biochimica et Biophysica Acta - Biomembranes*. Elsevier B.V., 1838(10), pp. 2391–2398. doi: 10.1016/j.bbamem.2014.06.002.
- Edelmann, E., Leßmann, V. and Brigadski, T. (2014) 'Pre- and postsynaptic twists in BDNF secretion and action in synaptic plasticity', *Neuropharmacology*. Elsevier Ltd, 76(PART C), pp. 610–627. doi: 10.1016/j.neuropharm.2013.05.043.
- Egger, V. and Urban, N. N. (2006) 'Dynamic connectivity in the mitral cell-granule cell microcircuit', *Seminars in Cell and Developmental Biology*, 17(4), pp. 424–432. doi: 10.1016/j.semcdb.2006.04.006.

- English, C. (2012) 'Genetic evidence that brain-derived neurotrophic factor mediates competitive interactions between individual cortical neurons', *Proceedings of the* doi: 10.1073/pnas.1206492109/-
/DCSupplemental.www.pnas.org/cgi/doi/10.1073/pnas.1206492109.
- Ennis, M., Hamilton, K. A. and Hayer, A. (2007) *Handbook of neurochemistry and molecular neurobiology: Sensory neurochemistry, Handbook of Neurochemistry and Molecular Neurobiology: Sensory Neurochemistry*. doi: 10.1007/978-0-387-30374-1.
- Eyre, M. D., Antal, M. and Nusser, Z. (2008) 'Distinct Deep Short-Axon Cell Subtypes of the Main Olfactory Bulb Provide Novel Intrabulbar and Extrabulbar GABAergic Connections', *Journal of Neuroscience*, 28(33), pp. 8217–8229. doi: 10.1523/JNEUROSCI.2490-08.2008.
- Frazier-Cierpial, L. L. and Brunjes, P. C. (1989) 'Early postnatal differentiation of granule cell dendrites in the olfactory bulbs of normal and unilaterally odor-deprived rats', *Developmental Brain Research*, 47(1), pp. 129–136. doi: 10.1016/0165-3806(89)90115-6.
- Friedman, W. J. and Greene, L. A. (1999) 'Neurotrophin signaling via Trks and p75', *Experimental Cell Research*, 253(1), pp. 131–142. doi: 10.1006/excr.1999.4705.
- Fu, A. K. and Ip, N. Y. (2017) 'Regulation of postsynaptic signaling in structural synaptic plasticity', *Current Opinion in Neurobiology*. Elsevier Ltd, 45, pp. 148–155. doi: 10.1016/j.conb.2017.05.016.
- Galvao, R. P., Garcia-Verdugo, J. M. and Alvarez-Buylla, A. (2008) 'Brain-Derived Neurotrophic Factor Signaling Does Not Stimulate Subventricular Zone Neurogenesis in Adult Mice and Rats', *Journal of Neuroscience*, 28(50), pp. 13368–13383. doi: 10.1523/JNEUROSCI.2918-08.2008.
- Gao, X., Smith, G. M. and Chen, J. (2009) 'Impaired dendritic development and synaptic formation of postnatal-born dentate gyrus granular neurons in the absence of brain-derived neurotrophic factor signaling', *Experimental Neurology*. Elsevier Inc., 215(1), pp. 178–190. doi: 10.1016/j.expneurol.2008.10.009.
- Gao, Y. and Strowbridge, B. W. (2009) 'Long-term plasticity of excitatory inputs to granule cells in the rat olfactory bulb', *Nature Neuroscience*, 12(6), pp. 731–733. doi: 10.1038/nn.2319.
- Garcia-Verdugo, J. M. *et al.* (1998) 'Architecture and cell types of the adult subventricular zone: In search of the stem cells. José Manuel García-Verdugo. 1999; Journal of Neurobiology - Wiley InterScience'. Available at: <http://www3.interscience.wiley.com/journal/75910/abstract>.
- Gascon, E. *et al.* (2005) 'Sequential activation of p75 and TrkB is involved in dendritic development of subventricular zone-derived neuronal progenitors in vitro', *European Journal of Neuroscience*, 21(1), pp. 69–80. doi: 10.1111/j.1460-9568.2004.03849.x.

- Gharami, K. *et al.* (2008) 'Brain-derived neurotrophic factor over-expression in the forebrain ameliorates Huntington's disease phenotypes in mice', *Journal of Neurochemistry*, 105(2), pp. 369–379. doi: 10.1111/j.1471-4159.2007.05137.x.
- Gheusi, G. and Lledo, P. M. (2014) *Adult neurogenesis in the olfactory system shapes odor memory and perception*. 1st edn, *Progress in Brain Research*. 1st edn. Elsevier B.V. doi: 10.1016/B978-0-444-63350-7.00006-1.
- Glaser, E. M. and Van der Loos, H. (1981) 'Analysis of thick brain sections by obverse-Reverse computer microscopy: Application of a new, high clarity Golgi-Nissl stain', *Journal of Neuroscience Methods*, 4(2), pp. 117–125. doi: 10.1016/0165-0270(81)90045-5.
- Gomez-Gaviro, M. V. *et al.* (2012) 'Betacellulin promotes cell proliferation in the neural stem cell niche and stimulates neurogenesis', *Proceedings of the National Academy of Sciences*, 109(4), pp. 1317–1322. doi: 10.1073/pnas.1016199109.
- Gong, Q. *et al.* (1994) 'Localization and regulation of low affinity nerve growth factor receptor expression in the rat olfactory system during development and regeneration', *J Comp Neurol*, 344(3), pp. 336–348. doi: 10.1002/cne.903440303.
- Gorski, J. a *et al.* (2003) 'Brain-derived neurotrophic factor is required for the maintenance of cortical dendrites.', *The Journal of neuroscience : the official journal of the Society for Neuroscience*, 23(17), pp. 6856–6865. doi: 10.3410/f.1004415.195300.
- Gottmann, K., Mittmann, T. and Lessmann, V. (2009) 'BDNF signaling in the formation, maturation and plasticity of glutamatergic and GABAergic synapses', *Experimental Brain Research*, 199(3–4), pp. 203–234. doi: 10.1007/s00221-009-1994-z.
- Gracia-Llanes, F. J. *et al.* (2010) 'GABAergic basal forebrain afferents innervate selectively GABAergic targets in the main olfactory bulb', *Neuroscience*. Elsevier Inc., 170(3), pp. 913–922. doi: 10.1016/j.neuroscience.2010.07.046.
- Greer, C. A. (1987) 'Golgi analyses of dendritic organization among denervated olfactory bulb granule cells', *Journal of Comparative Neurology*, 257(3), pp. 442–452. doi: 10.1002/cne.902570311.
- Grelat, A. *et al.* (2018) 'Adult-born neurons boost odor–reward association', *Proceedings of the National Academy of Sciences*, p. 201716400. doi: 10.1073/pnas.1716400115.
- Gritti, A. *et al.* (1999) 'Epidermal and fibroblast growth factors behave as mitogenic regulators for a single multipotent stem cell-like population from the subventricular region of the adult mouse forebrain.', *The Journal of neuroscience : the official journal of the Society for Neuroscience*, 19(9), pp. 3287–3297. doi: 10.1523/JNEUROSCI.19-09-03287.1999.
- Gritti, A., Vescovi, A. L. and Galli, R. (2002) 'Adult neural stem cells: plasticity and developmental potential', *Journal of Physiology-Paris*, 96(1–2), pp. 81–90. doi: 10.1016/S0928-4257(01)00083-3.

- Guo, W., Nagappan, G. and Lu, B. (2018) 'Differential effects of transient and sustained activation of BDNF-TrkB signaling', *Developmental Neurobiology*, pp. 1–13. doi: 10.1002/dneu.22592.
- Guthrie, K. M. and Gall, C. M. (1991) 'Differential expression of mRNAs for the NGF family of neurotrophic factors in the adult rat central olfactory system', *The Journal of Comparative Neurology*, 313(1), pp. 95–102. doi: 10.1002/cne.903130107.
- Harris, K. M. and Stevens, J. K. (1989) 'Dendritic spines of CA 1 pyramidal cells in the rat hippocampus: serial electron microscopy with reference to their biophysical characteristics.', *The Journal of neuroscience: the official journal of the Society for Neuroscience*, 9(8), pp. 2982–2997. doi: 10.1523/jneurosci.6130-10.2011.
- Hartmann, D. *et al.* (2012) 'Multiple approaches to investigate the transport and activity-dependent release of BDNF and their application in neurogenetic disorders', *Neural Plasticity*, 2012. doi: 10.1155/2012/203734.
- Harward, S. *et al.* (2016) 'Autocrine BDNF-TrkB signaling within a single dendritic spine', *Nature*, 538(538), pp. 99–103. doi: 10.1038/nature19766.Autocrine.
- Henry, R. A., Hughes, S. M. and Connor, B. (2007) 'AAV-mediated delivery of BDNF augments neurogenesis in the normal and quinolinic acid-lesioned adult rat brain', *European Journal of Neuroscience*, 25(12), pp. 3513–3525. doi: 10.1111/j.1460-9568.2007.05625.x.
- Hering, H. and Sheng, M. (2001) 'Dendritic spines: structure, dynamics and regulation', *Nature Reviews Neuroscience*, 2(12), pp. 880–888. doi: 10.1038/35104061.
- Hinds, J. W. and Hinds, P. L. (1976) 'Synapse formation in the mouse olfactory bulb. I. Quantitative studies.', *The Journal of comparative neurology*, 169(1), pp. 15–40. doi: 10.1002/cne.901690103.
- Hofer, M. *et al.* (1990) 'Regional distribution of brain-derived neurotrophic factor mRNA in the adult mouse brain-derived neurotrophic factor/hippocampus/ in situ hybridization/nerve growth factor/trophic interactions', *The EMBO Journal*, 9(8), pp. 2459–2464.
- Holtmaat, A. J. G. D. *et al.* (2005) 'Transient and persistent dendritic spines in the neocortex in vivo', *Neuron*, 45(2), pp. 279–291. doi: 10.1016/j.neuron.2005.01.003.
- Horch, H. W. and Katz, L. C. (2002) 'BDNF release from single cells elicits local dendritic growth in nearby neurons', *Nature Neuroscience*, 5(11), pp. 1177–1184. doi: 10.1038/nn927.
- Hruska, M. *et al.* (2018) 'Synaptic nanomodules underlie the organization and plasticity of spine synapses', *Nature Neuroscience*. Springer US, 21(5), pp. 671–682. doi: 10.1038/s41593-018-0138-9.

- Huang, E. J. and Reichardt, L. F. (2003) 'Trk Receptors: Roles in Neuronal Signal Transduction', *Annual Review of Biochemistry*, 72(1), pp. 609–642. doi: 10.1146/annurev.biochem.72.121801.161629.
- Huang, Z. J. *et al.* (1999) 'BDNF regulates the maturation of inhibition and the critical period of plasticity in mouse visual cortex', *Cell*, 98(6), pp. 739–755. doi: 10.1016/S0092-8674(00)81509-3.
- Ieraci, A. *et al.* (2016) 'Brain-Derived Neurotrophic Factor Val66Met Human Polymorphism Impairs the Beneficial Exercise-Induced Neurobiological Changes in Mice', *Neuropsychopharmacology*. Nature Publishing Group, 41(13), pp. 3070–3079. doi: 10.1038/npp.2016.120.
- Ihrle, R. A. and Alvarez-Buylla, A. (2008) 'Cells in the astroglial lineage are neural stem cells', *Cell and Tissue Research*, 331(1), pp. 179–191. doi: 10.1007/s00441-007-0461-z.
- Imai, T. (2014) 'Construction of functional neuronal circuitry in the olfactory bulb', *Seminars in Cell and Developmental Biology*. Elsevier Ltd, 35, pp. 180–188. doi: 10.1016/j.semcdb.2014.07.012.
- Imamura, F. and Greer, C. A. (2009) 'Dendritic branching of olfactory bulb mitral and tufted cells: Regulation by TrkB', *PLoS ONE*, 4(8). doi: 10.1371/journal.pone.0006729.
- Imayoshi, I. *et al.* (2008) 'Roles of continuous neurogenesis in the structural and functional integrity of the adult forebrain', *Nature Neuroscience*, 11(10), pp. 1153–1161. doi: 10.1038/nn.2185.
- Imayoshi, I. *et al.* (2009) 'Continuous neurogenesis in the adult brain', *Development, Growth & Differentiation*, 51(3), pp. 379–386. doi: 10.1111/j.1440-169X.2009.01094.x.
- Isaacson, J. S. and Strowbridge, B. W. (1998) 'Olfactory reciprocal synapses: Dendritic signaling in the CNS', *Neuron*, 20(4), pp. 749–761. doi: 10.1016/S0896-6273(00)81013-2.
- Isgor, C. and Sengelaub, D. R. (2003) 'Effects of neonatal gonadal steroids on adult CA3 pyramidal neuron dendritic morphology and spatial memory in rats', *Journal of Neurobiology*, 55(2), pp. 179–190. doi: 10.1002/neu.10200.
- Ji, Y. *et al.* (2010) 'Acute and gradual increases in BDNF concentration elicit distinct signaling and functions in neurons', *Nature Neuroscience*. Nature Publishing Group, 13(3), pp. 302–309. doi: 10.1038/nn.2505.
- Jiao, Y. *et al.* (2011) 'A key mechanism underlying sensory experience-dependent maturation of neocortical GABAergic circuits in vivo', *Proceedings of the National Academy of Sciences*, 108(29), pp. 12131–12136. doi: 10.1073/pnas.1105296108.
- Jin, K. *et al.* (2002) 'Vascular endothelial growth factor (VEGF) stimulates neurogenesis in vitro and in vivo', *Proc Natl Acad Sci U S A*, 99(18), pp. 11946–11950. doi: 10.1073/pnas.182296499.

- Jin, X. *et al.* (2003) 'Brain-derived neurotrophic factor mediates activity-dependent dendritic growth in nonpyramidal neocortical interneurons in developing organotypic cultures.', *The Journal of neuroscience: the official journal of the Society for Neuroscience*, 23(13), pp. 5662–5673. doi: 23/13/5662 [pii].
- Kaneko, M. *et al.* (2012) 'Dendritic BDNF Synthesis Is Required for Late-Phase Spine Maturation and Recovery of Cortical Responses Following Sensory Deprivation', *Journal of Neuroscience*, 32(14), pp. 4790–4802. doi: 10.1523/JNEUROSCI.4462-11.2012.
- Kellner, Y. *et al.* (2014) 'The BDNF effects on dendritic spines of mature hippocampal neurons depend on neuronal activity', *Frontiers in Synaptic Neuroscience*, 6(MAR), pp. 1–17. doi: 10.3389/fnsyn.2014.00005.
- Kelsch, W. *et al.* (2009) 'A Critical Period for Activity-Dependent Synaptic Development during Olfactory Bulb Adult Neurogenesis', *Journal of Neuroscience*, 29(38), pp. 11852–11858. doi: 10.1523/JNEUROSCI.2406-09.2009.
- Kelsch, W. *et al.* (2012) 'GluN2B-Containing NMDA Receptors Promote Wiring of Adult-Born Neurons into Olfactory Bulb Circuits', *Journal of Neuroscience*, 32(36), pp. 12603–12611. doi: 10.1523/JNEUROSCI.1459-12.2012.
- Kelsch, W., Lin, C.-W. and Lois, C. (2008) 'Sequential development of synapses in dendritic domains during adult neurogenesis', *Proceedings of the National Academy of Sciences*, 105(43), pp. 16803–16808. doi: 10.1073/pnas.0807970105.
- Khodosevich, K. *et al.* (2013) 'Connective Tissue Growth Factor Regulates Interneuron Survival and Information Processing in the Olfactory Bulb', *Neuron*, 79(6), pp. 1136–1151. doi: 10.1016/j.neuron.2013.07.011.
- Kirschenbaum, B. and Goldman, S. a (1995) 'Brain-derived neurotrophic factor promotes the survival of neurons arising from the adult rat forebrain subependymal zone.', *Proceedings of the National Academy of Sciences of the United States of America*, 92(1), pp. 210–214.
- Knott, G. and Holtmaat, A. (2008) 'Dendritic spine plasticity-Current understanding from in vivo studies', *Brain Research Reviews*, 58(2), pp. 282–289. doi: 10.1016/j.brainresrev.2008.01.002.
- Knott, G. W. *et al.* (2006) 'Spine growth precedes synapse formation in the adult neocortex in vivo', *Nature Neuroscience*, 9(9), pp. 1117–1124. doi: 10.1038/nn1747.
- Kobilo, T. *et al.* (2011) 'Running is the neurogenic and neurotrophic stimulus in environmental enrichment.', *Learning & memory (Cold Spring Harbor, N.Y.)*, 18(9), pp. 605–609. doi: 10.1101/lm.2283011.
- Kohara, K. *et al.* (2007) 'A Local Reduction in Cortical GABAergic Synapses after a Loss of Endogenous Brain-Derived Neurotrophic Factor, as Revealed by Single-Cell Gene Knock-Out Method', *Journal of Neuroscience*, 27(27), pp. 7234–7244. doi: 10.1523/JNEUROSCI.1943-07.2007.

- Kolarow, R., Brigadski, T. and Lessmann, V. (2007) 'Postsynaptic Secretion of BDNF and NT-3 from Hippocampal Neurons Depends on Calcium Calmodulin Kinase II Signaling and Proceeds via Delayed Fusion Pore Opening', *Journal of Neuroscience*, 27(39), pp. 10350–10364. doi: 10.1523/JNEUROSCI.0692-07.2007.
- Kolbeck, R. *et al.* (1999) 'Brain-derived neurotrophic factor levels in the nervous system of wild-type and neurotrophin gene mutant mice.', *Journal of neurochemistry*, 72(5), pp. 1930–1938. doi: 10.1046/j.1471-4159.1999.0721930.x.
- Kosaka, T. and Kosaka, K. (2008) 'Heterogeneity of parvalbumin-containing neurons in the mouse main olfactory bulb, with special reference to short-axon cells and β IV-spectrin positive dendritic segments', *Neuroscience Research*, 60(1), pp. 56–72. doi: 10.1016/j.neures.2007.09.008.
- Kowiański, P. *et al.* (2018) 'BDNF: A Key Factor with Multipotent Impact on Brain Signaling and Synaptic Plasticity', *Cellular and Molecular Neurobiology*, 38(3), pp. 579–593. doi: 10.1007/s10571-017-0510-4.
- Kuczewski, N. *et al.* (2009) 'Activity-dependent dendritic release of BDNF and biological consequences', *Molecular Neurobiology*, 39(1), pp. 37–49. doi: 10.1007/s12035-009-8050-7.
- Kuczewski, N., Porcher, C. and Gaiarsa, J. L. (2010) 'Activity-dependent dendritic secretion of brain-derived neurotrophic factor modulates synaptic plasticity', *European Journal of Neuroscience*, 32(8), pp. 1239–1244. doi: 10.1111/j.1460-9568.2010.07378.x.
- Kunze, W. A. A. *et al.* (1992) 'Intracellular responses of olfactory bulb granule cells to stimulating the horizontal diagonal band nucleus', *Neuroscience*, 48(2), pp. 363–369. doi: 10.1016/0306-4522(92)90496-O.
- Laaris, N., Puche, A. and Ennis, M. (2007) 'Complementary postsynaptic activity patterns elicited in olfactory bulb by stimulation of mitral/tufted and centrifugal fiber inputs to granule cells.', *Journal of neurophysiology*, 97(1), pp. 296–306. doi: 10.1152/jn.00823.2006.
- Lazarini, F. *et al.* (2009) 'Cellular and behavioral effects of cranial irradiation of the subventricular zone in adult mice', *PLoS ONE*, 4(9), pp. 1–11. doi: 10.1371/journal.pone.0007017.
- Lazarini, F. *et al.* (2014) 'Adult Neurogenesis Restores Dopaminergic Neuronal Loss in the Olfactory Bulb', *Journal of Neuroscience*, 34(43), pp. 14430–14442. doi: 10.1523/JNEUROSCI.5366-13.2014.
- Lemasson, M. *et al.* (2005) 'Neonatal and Adult Neurogenesis Provide Two Distinct Populations of Newborn Neurons to the Mouse Olfactory Bulb', *Journal of Neuroscience*, 25(29), pp. 6816–6825. doi: 10.1523/JNEUROSCI.1114-05.2005.

- Lepousez, G., Valley, M. T. and Lledo, P.-M. (2013) 'The Impact of Adult Neurogenesis on Olfactory Bulb Circuits and Computations', *Annual Review of Physiology*, 75(1), pp. 339–363. doi: 10.1146/annurev-physiol-030212-183731.
- Lessmann, V. and Brigadski, T. (2009) 'Mechanisms, locations, and kinetics of synaptic BDNF secretion: An update', *Neuroscience Research*, 65(1), pp. 11–22. doi: 10.1016/j.neures.2009.06.004.
- Li, W. L. *et al.* (2018) 'Adult-born neurons facilitate olfactory bulb pattern separation during task engagement', *eLife*, 7, pp. 1–26. doi: 10.7554/eLife.33006.
- Li, Y. *et al.* (2008) 'TrkB Regulates Hippocampal Neurogenesis and Governs Sensitivity to Antidepressive Treatment', *Neuron*, 59(3), pp. 399–412. doi: 10.1016/j.neuron.2008.06.023.
- Li, Y. *et al.* (2012) 'Conditional ablation of brain-derived neurotrophic factor-TrkB signaling impairs striatal neuron development', *Proceedings of the National Academy of Sciences*, 109(38), pp. 15491–15496. doi: 10.1073/pnas.1212899109.
- Lim, D. A. and Alvarez-buylla, A. (2016) 'The Adult Ventricular – Subventricular Zone', *Cold Spring Harbor perspectives in biology*, pp. 1–34.
- Lin, C. W. *et al.* (2010) 'Genetically Increased Cell-Intrinsic Excitability Enhances Neuronal Integration into Adult Brain Circuits', *Neuron*. Elsevier Ltd, 65(1), pp. 32–39. doi: 10.1016/j.neuron.2009.12.001.
- Lindberg, O. R. *et al.* (2012) 'EGF-Induced Expansion of Migratory Cells in the Rostral Migratory Stream', *PLoS ONE*, 7(9). doi: 10.1371/journal.pone.0046380.
- Liu, H. and Guthrie, K. M. (2011) 'Neuronal replacement in the injured olfactory bulb', *Experimental Neurology*. Elsevier Inc., 228(2), pp. 270–282. doi: 10.1016/j.expneurol.2011.01.021.
- Liu, P. Z. and Nusslock, R. (2018) 'Exercise-mediated neurogenesis in the hippocampus via BDNF', *Frontiers in Neuroscience*, 12(FEB), pp. 1–6. doi: 10.3389/fnins.2018.00052.
- Livneh, Y. *et al.* (2009) 'Sensory Input Enhances Synaptogenesis of Adult-Born Neurons', *Journal of Neuroscience*, 29(1), pp. 86–97. doi: 10.1523/JNEUROSCI.4105-08.2009.
- Livneh, Y., Adam, Y. and Mizrahi, A. (2014) 'Odor processing by adult-born neurons', *Neuron*. Elsevier Inc., 81(5), pp. 1097–1110. doi: 10.1016/j.neuron.2014.01.007.
- Livneh, Y. and Mizrahi, A. (2011) 'Long-term changes in the morphology and synaptic distributions of adult-born neurons', *Journal of Comparative Neurology*, 519(11), pp. 2212–2224. doi: 10.1002/cne.22625.
- Livneh, Y. and Mizrahi, A. (2012) 'Experience-dependent plasticity of mature adult-born neurons', *Nature Neuroscience*. Nature Publishing Group, 15(1), pp. 26–28. doi: 10.1038/nn.2980.

- Lledo, P.-M., Saghatelian, A. and Lemasson, M. (2004) 'Inhibitory Interneurons in the Olfactory Bulb: From Development to Function', *The Neuroscientist*, 10(4), pp. 292–303. doi: 10.1177/1073858404263460.
- Lledo, P. M., Alonso, M. and Grubb, M. S. (2006) 'Adult neurogenesis and functional plasticity in neuronal circuits', *Nature Reviews Neuroscience*, 7(3), pp. 179–193. doi: 10.1038/nrn1867.
- Lledo, P. M., Merkle, F. T. and Alvarez-Buylla, A. (2008) 'Origin and function of olfactory bulb interneuron diversity', *Trends in Neurosciences*, 31(8), pp. 392–400. doi: 10.1016/j.tins.2008.05.006.
- Lledo, P. M. and Saghatelian, A. (2005) 'Integrating new neurons into the adult olfactory bulb: Joining the network, life-death decisions, and the effects of sensory experience', *Trends in Neurosciences*, 28(5), pp. 248–254. doi: 10.1016/j.tins.2005.03.005.
- Lodovichi, C. and Belluscio, L. (2012) 'Odorant Receptors in the Formation of the Olfactory Bulb Circuitry', *Physiology*, 27(4), pp. 200–212. doi: 10.1152/physiol.00015.2012.
- Lois, C. and Alvarez-Buylla, A. (1993) 'Proliferating subventricular zone cells in the adult mammalian forebrain can differentiate into neurons and glia.', *Proceedings of the National Academy of Sciences of the United States of America*, 90(5), pp. 2074–2077. doi: 10.1073/pnas.90.5.2074.
- Lois, C. and Alvarez-Buylla, A. (1996) 'Chain Migration of Neuronal Precursors', 271(February).
- Luskin, M. B. (1993) 'Restricted proliferation and migration of postnatally generated neurons derived from the forebrain subventricular zone', *Neuron*, 11(1), pp. 173–189. doi: 10.1016/0896-6273(93)90281-U.
- Ma, D. K. *et al.* (2009) 'Adult neural stem cells in the mammalian central nervous system', *Cell Research*, 19(6), pp. 672–682. doi: 10.1038/cr.2009.56.
- Maisonpierre, P. C. *et al.* (1990) 'NT-3, BDNF, and NGF in the developing rat nervous system: Parallel as well as reciprocal patterns of expression', *Neuron*, 5(4), pp. 501–509. doi: 10.1016/0896-6273(90)90089-X.
- Malvaut, S. and Saghatelian, A. (2016) 'The role of adult-born neurons in the constantly changing olfactory bulb network', *Neural Plasticity*, 2016. doi: 10.1155/2016/1614329.
- Mandairon, N. *et al.* (2006) 'Long-term fate and distribution of newborn cells in the adult mouse olfactory bulb: Influences of olfactory deprivation', *Neuroscience*, 141(1), pp. 443–451. doi: 10.1016/j.neuroscience.2006.03.066.
- Mandairon, N. *et al.* (2018) 'Opposite regulation of inhibition by adult-born granule cells during implicit versus explicit olfactory learning', *eLife*, 7, pp. 1–14. doi: 10.7554/eLife.34976.

- Marlatt, M. W. *et al.* (2012) 'Running throughout middle-age improves memory function, hippocampal neurogenesis, and BDNF levels in female C57BL/6J mice', *Developmental Neurobiology*, 72(6), pp. 943–952. doi: 10.1002/dneu.22009.
- Masana, Y. *et al.* (1993) 'Localization of trkB mRNA in postnatal brain development', *Journal of Neuroscience Research*, 35(5), pp. 468–479. doi: 10.1002/jnr.490350503.
- Matsuda, N. *et al.* (2009) 'Differential Activity-Dependent Secretion of Brain-Derived Neurotrophic Factor from Axon and Dendrite', *Journal of Neuroscience*, 29(45), pp. 14185–14198. doi: 10.1523/JNEUROSCI.1863-09.2009.
- Matsutani, S. and Yamamoto, N. (2004) 'Brain-derived neurotrophic factor induces rapid morphological changes in dendritic spines of olfactory bulb granule cells in cultured slices through the modulation of glutamatergic signaling', *Neuroscience*, 123(3), pp. 695–702. doi: 10.1016/j.neuroscience.2003.10.030.
- Matsutani, S. and Yamamoto, N. (2004) 'Postnatal development of dendritic spines on olfactory bulb granule cells in rats.', *The Journal of comparative neurology*, 473(4), pp. 553–61. doi: 10.1002/cne.20107.
- Matsutani, S. and Yamamoto, N. (2008) 'Centrifugal innervation of the mammalian olfactory bulb', *Anatomical Science International*, 83(4), pp. 218–227. doi: 10.1111/j.1447-073x.2007.00223.x.
- Matsuzaki, M. *et al.* (2004) 'Structural basis of long-term potentiation in single dendritic spines', *Nature*, 429(6993), pp. 761–766. doi: 10.1038/nature02617.
- Maynard, K. R. *et al.* (2017) 'Bdnf mRNA splice variants differentially impact CA1 and CA3 dendrite complexity and spine morphology in the hippocampus', *Brain Structure and Function*. Springer Berlin Heidelberg, 222(7), pp. 3295–3307. doi: 10.1007/s00429-017-1405-3.
- McDole, B. *et al.* (2015) 'BDNF over-expression increases olfactory bulb granule cell dendritic spine density in vivo', *Neuroscience*. IBRO, 304, pp. 146–160. doi: 10.1016/j.neuroscience.2015.07.056.
- McLean, J. H., Darby-King, A. and Bonnell, W. S. (2001) 'Neonatal olfactory sensory deprivation decreases BDNF in the olfactory bulb of the rat', *Developmental Brain Research*, 128(1), pp. 17–24. doi: 10.1016/S0165-3806(01)00144-4.
- Mizoguchi, Y. *et al.* (2003) 'A rapid increase in the total number of cell surface functional GABAA receptors induced by brain-derived neurotrophic factor in rat visual cortex.', *The Journal of biological chemistry*, 278(45), pp. 44097–102. doi: 10.1074/jbc.M305872200.
- Mizrahi, A. (2007) 'Dendritic development and plasticity of adult-born neurons in the mouse olfactory bulb', *Nature Neuroscience*, 10(4), pp. 444–452. doi: 10.1038/nn1875.
- Moreno, M. *et al.* (2014) 'Alteration of olfactory perceptual learning and its cellular basis in aged mice', *Neurobiology of Aging*. Elsevier Ltd, 35(3), pp. 680–691. doi: 10.1016/j.neurobiolaging.2013.08.034.

- Mori, B. Y. K., Nowycky, M. C. and Shepherd, G. M. (1981) 'Analysis of Synaptic Potentials in Mitral Cells in the Isolated Turtle Olfactory Bulb', 50, pp. 295–309.
- Mori, K., Nagao, H. and Yoshihara, Y. (1999) 'The Olfactory Bulb: Coding and Processing of Odor Molecule Information', *Science*, 286(5440), pp. 711–715. doi: 10.1126/science.286.5440.711.
- Mori, K., Nagao, H. and Yoshihara, Y. (2007) 'The Olfactory Bulb : Coding and Processing of Odor Molecule Information', 286(October 1999), pp. 711–715.
- Murata, K. *et al.* (2011) 'Compensation of Depleted Neuronal Subsets by New Neurons in a Local Area of the Adult Olfactory Bulb', *Journal of Neuroscience*, 31(29), pp. 10540–10557. doi: 10.1523/JNEUROSCI.1285-11.2011.
- Nagayama, S., Homma, R. and Imamura, F. (2014) 'Neuronal organization of olfactory bulb circuits', *Frontiers in Neural Circuits*, 8(September), pp. 1–19. doi: 10.3389/fncir.2014.00098.
- Naritsuka, H. *et al.* (2009) 'Perisomatic-targeting granule cells in the mouse olfactory bulb', *Journal of Comparative Neurology*, 515(4), pp. 409–426. doi: 10.1002/cne.22063.
- Nef, S. *et al.* (2001) 'Neurotrophins are not required for normal embryonic development of olfactory neurons', *Developmental Biology*, 234(1), pp. 80–92. doi: 10.1006/dbio.2001.0240.
- Neve, R. L. and Beart, M. F. (1989) 'Visual experience regulates gene expression in the developing striate cortex GAP43/calcium/calmodulin-dependent protein kinase α /glutamic', *Neurobiology*, 86(June), pp. 4781–4784.
- Nissant, A. and Pallotto, M. (2011) 'Integration and maturation of newborn neurons in the adult olfactory bulb - from synapses to function', *European Journal of Neuroscience*, 33(6), pp. 1069–1077. doi: 10.1111/j.1460-9568.2011.07605.x.
- Nowycky, M. C., Mori, K. and Shepherd, G. M. (1981) 'GABAergic mechanisms of dendrodendritic synapses in isolated turtle olfactory bulb', *Journal of Neurophysiology (Bethesda)*, 46(3), pp. 639–648. doi: 10.1152/jn.1981.46.3.639.
- Nunes, D. and Kuner, T. (2015) 'Disinhibition of olfactory bulb granule cells accelerates odour discrimination in mice', *Nature Communications*. Nature Publishing Group, 6, pp. 1–13. doi: 10.1038/ncomms9950.
- Nusser, Z. *et al.* (2001) 'Disruption of GABA(A) receptors on GABAergic interneurons leads to increased oscillatory power in the olfactory bulb network', *Journal of Neurophysiology*, 86(6), p. 2823–2833. doi: 0022-3077/01.
- Orefice, L. L. *et al.* (2013) 'Distinct Roles for Somatic and Dendritically Synthesized Brain-Derived Neurotrophic Factor in Morphogenesis of Dendritic Spines', *Journal of Neuroscience*, 33(28), pp. 11618–11632. doi: 10.1523/JNEUROSCI.0012-13.2013.

- Pallotto, M. *et al.* (2012) 'Early Formation of GABAergic Synapses Governs the Development of Adult-Born Neurons in the Olfactory Bulb', *Journal of Neuroscience*, 32(26), pp. 9103–9115. doi: 10.1523/JNEUROSCI.0214-12.2012.
- Panja, D. and Bramham, C. R. (2014) 'BDNF mechanisms in late LTP formation: A synthesis and breakdown', *Neuropharmacology*. Elsevier Ltd, 76(PART C), pp. 664–676. doi: 10.1016/j.neuropharm.2013.06.024.
- Panzanelli, P. *et al.* (2009) 'Early Synapse Formation in Developing Interneurons of the Adult Olfactory Bulb', *Journal of Neuroscience*, 29(48), pp. 15039–15052. doi: 10.1523/JNEUROSCI.3034-09.2009.
- Park, H. and Poo, M. (2013) 'Neurotrophin regulation of neural circuit development and function', *Nature Reviews Neuroscience*. Nature Publishing Group, 14(1), pp. 7–23. doi: 10.1038/nrn3379.
- Parnass, Z., Tashiro, A. and Yuste, R. (2000) 'Analysis of spine morphological plasticity in developing hippocampal pyramidal neurons', *Hippocampus*, 10(5), pp. 561–568. Available at: [http://www.ncbi.nlm.nih.gov/entrez/query.fcgi?cmd=Retrieve&db=PubMed&dopt=Citation&list_uids=11075826%5Cn\(null\)](http://www.ncbi.nlm.nih.gov/entrez/query.fcgi?cmd=Retrieve&db=PubMed&dopt=Citation&list_uids=11075826%5Cn(null)).
- Patapoutian, A. and Reichardt, L. F. (2001) 'Trk receptors: Mediators of neurotrophin action', *Current Opinion in Neurobiology*, 11(3), pp. 272–280. doi: 10.1016/S0959-4388(00)00208-7.
- Petreanu, L. and Alvarez-Buylla, A. (2002) 'Maturation and death of adult-born olfactory bulb granule neurons: role of olfaction', *Journal of Neuroscience*, 22(14), pp. 6106–6113. doi: 10.1523/JNEUROSCI.22/14/6106 [pii].
- Phillips, H. *et al.* (1990) 'Widespread expression of BDNF but not NT3 by target areas of basal forebrain cholinergic neurons', *Science*, 250(4978), pp. 290–294. doi: 10.1126/science.1688328.
- Ponti, G. *et al.* (2013) 'Cell cycle and lineage progression of neural progenitors in the ventricular-subventricular zones of adult mice', *Proceedings of the National Academy of Sciences*, 110(11), pp. E1045–E1054. doi: 10.1073/pnas.1219563110.
- Price, J. L. and Powell, T. P. (1970) 'An electron-microscopic study of the termination of the afferent fibres to the olfactory bulb from the cerebral hemisphere.', *Journal of cell science*, 7(1), pp. 157–187.
- Rall, W. *et al.* (1966) 'Dendrodendritic synaptic pathway for inhibition in the olfactory bulb', *Experimental Neurology*, 14(1), pp. 44–56. doi: 10.1016/0014-4886(66)90023-9.
- Rauskolb, S. *et al.* (2010) 'Global Deprivation of Brain-Derived Neurotrophic Factor in the CNS Reveals an Area-Specific Requirement for Dendritic Growth', *Journal of Neuroscience*, 30(5), pp. 1739–1749. doi: 10.1523/JNEUROSCI.5100-09.2010.

- Sakamoto, M., Kageyama, R. and Imayoshi, I. (2014) 'The functional significance of newly born neurons integrated into olfactory bulb circuits', *Frontiers in Neuroscience*, 8(8 MAY), pp. 1–9. doi: 10.3389/fnins.2014.00121.
- Saneyoshi, T., Fortin, D. A. and Soderling, T. R. (2010) 'Regulation of spine and synapse formation by activity-dependent intracellular signaling pathways', *Current Opinion in Neurobiology*, 20(1), pp. 108–115. doi: 10.1016/j.conb.2009.09.013.
- Scharfman, H. *et al.* (2005) 'Increased neurogenesis and the ectopic granule cells after intrahippocampal BDNF infusion in adult rats', *Experimental Neurology*, 192(2), pp. 348–356. doi: 10.1016/j.expneurol.2004.11.016.
- Schikorski, T. and Stevens, C. F. (1999) 'Quantitative fine-structural analysis of olfactory cortical synapses', *Proc Natl Acad Sci U S A*, 96(7), pp. 4107–4112. doi: 10.1073/pnas.96.7.4107.
- Shepherd, G. M. *et al.* (2007) 'The olfactory granule cell: From classical enigma to central role in olfactory processing', *Brain Research Reviews*, 55(2 SPEC. ISS.), pp. 373–382. doi: 10.1016/j.brainresrev.2007.03.005.
- Shieh, P. B. and Ghosh, A. (1999) 'Molecular Mechanisms Underlying Activity-Dependent Regulation of BDNF Expression'.
- Smail, S. *et al.* (2016) 'Increased olfactory bulb BDNF expression does not rescue deficits in olfactory neurogenesis in the huntington's disease R6/2 mouse', *Chemical Senses*, 41(3), pp. 221–232. doi: 10.1093/chemse/bjv076.
- Snappyan, M. *et al.* (2009) 'Vasculature Guides Migrating Neuronal Precursors in the Adult Mammalian Forebrain via Brain-Derived Neurotrophic Factor Signaling', *Journal of Neuroscience*, 29(13), pp. 4172–4188. doi: 10.1523/JNEUROSCI.4956-08.2009.
- Snider, W. D. (1994) 'Functions of the Neurotrophins What the Knockouts Are Teaching Us NT-3', *Cell*, 77, pp. 627–638. doi: 10.1016/0092-8674(94)90048-5.
- Stranahan, A. M. *et al.* (2009) 'Voluntary exercise and caloric restriction enhance hippocampal dendritic spine density and BDNF levels in diabetic mice', *Hippocampus*, 19(10), pp. 951–961. doi: 10.1002/hipo.20577.
- Strowbridge, B. W. (2010) 'Linking Local Circuit Inhibition to Olfactory Behavior: A Critical Role for Granule Cells in Olfactory Discrimination', *Neuron*. Elsevier Inc., 65(3), pp. 295–297. doi: 10.1016/j.neuron.2010.01.029.
- Sultan, S. *et al.* (2010) 'Learning-dependent neurogenesis in the olfactory bulb determines long-term olfactory memory', *The FASEB Journal*, 24(7), pp. 2355–2363. doi: 10.1096/fj.09-151456.
- Sun, W., Kim, H. and Moon, Y. (2010) 'Control of neuronal migration through rostral migration stream in mice', *Anatomy & Cell Biology*, 43(4), p. 269. doi: 10.5115/acb.2010.43.4.269.

- Sun, Y. *et al.* (2006) 'Vascular endothelial growth factor-B (VEGFB) stimulates neurogenesis: Evidence from knockout mice and growth factor administration', *Developmental Biology*, 289(2), pp. 329–335. doi: 10.1016/j.ydbio.2005.10.016.
- Tada, T. and Sheng, M. (2006) 'Molecular mechanisms of dendritic spine morphogenesis', *Current Opinion in Neurobiology*, 16(1), pp. 95–101. doi: 10.1016/j.conb.2005.12.001.
- Taliaz, D. *et al.* (2010) 'Knockdown of brain-derived neurotrophic factor in specific brain sites precipitates behaviors associated with depression and reduces neurogenesis', *Molecular Psychiatry*. Nature Publishing Group, 15(1), pp. 80–92. doi: 10.1038/mp.2009.67.
- Tanaka, J. *et al.* (2008) 'Protein Synthesis and Neurotrophin-Dependent Structural Plasticity of Single Dendritic Spines', *Science*, 319(September), pp. 1683–1688.
- Toda, T. and Gage, F. H. (2017) 'Review: adult neurogenesis contributes to hippocampal plasticity', *Cell and Tissue Research*. Cell and Tissue Research, pp. 1–17. doi: 10.1007/s00441-017-2735-4.
- Urban, N. N. (2002) 'Lateral inhibition in the olfactory bulb and in olfaction', *Physiology and Behavior*, 77(4–5), pp. 607–612. doi: 10.1016/S0031-9384(02)00895-8.
- Urban, N. N. and Arevian, A. C. (2009) 'Computing with dendrodendritic synapses in the olfactory bulb', *Annals of the New York Academy of Sciences*, 1170, pp. 264–269. doi: 10.1111/j.1749-6632.2009.03899.x.
- Valley, M. T. *et al.* (2009) 'Ablation of mouse adult neurogenesis alters olfactory bulb structure and olfactory fear conditioning', *Frontiers in Neuroscience*, 3(NOV), pp. 1–13. doi: 10.3389/neuro.22.003.2009.
- Vigers, A. J. *et al.* (2012) 'Sustained expression of brain-derived neurotrophic factor is required for maintenance of dendritic spines and normal behavior', *Neuroscience*, 212, pp. 1–18. doi: 10.1016/j.neuroscience.2012.03.031.
- Vilar, M. and Mira, H. (2016) 'Regulation of neurogenesis by neurotrophins during adulthood: Expected and unexpected roles', *Frontiers in Neuroscience*, 10(FEB), pp. 1–9. doi: 10.3389/fnins.2016.00026.
- Vivar, C., Potter, M. C. and van Praag, H. (2012) 'All About Running: Synaptic Plasticity, Growth Factors and Adult Hippocampal Neurogenesis', in *Brain Imaging in Behavioral Neuroscience*, pp. 189–210. doi: 10.1007/7854_2012_220.
- Wallace, J. L. *et al.* (2017) 'Development and Refinement of Functional Properties of Adult-Born Neurons', *Neuron*. Elsevier Inc., 96(4), pp. 1–14. doi: 10.1016/j.neuron.2017.09.039.
- Wang, L. *et al.* (2015) 'Autocrine Action of BDNF on Dendrite Development of Adult-Born Hippocampal Neurons', *Journal of Neuroscience*. doi: 10.1523/JNEUROSCI.4682-14.2015.

- Waterhouse, E. G. *et al.* (2012a) 'BDNF Promotes Differentiation and Maturation of Adult-born Neurons through GABAergic Transmission', *Journal of Neuroscience*, 32(41), pp. 14318–14330. doi: 10.1523/JNEUROSCI.0709-12.2012.
- Waterhouse, E. G. *et al.* (2012b) 'BDNF Promotes Differentiation and Maturation of Adult-born Neurons through GABAergic Transmission', *Journal of Neuroscience*, 32(41), pp. 14318–14330. doi: 10.1523/JNEUROSCI.0709-12.2012.
- Waterhouse, E. G. and Xu, B. (2009) 'New insights into the role of brain-derived neurotrophic factor in synaptic plasticity', *Molecular and Cellular Neuroscience*. Elsevier Inc., 42(2), pp. 81–89. doi: 10.1016/j.mcn.2009.06.009.
- Wetmore, C. *et al.* (1990) 'Localization of brain-derived neurotrophic factor mRNA to neurons in the brain by in situ hybridization', *Exp.Neurol.*, 109(0014–4886 (Print)), pp. 141–152.
- Whitman, M. C. and Greer, C. A. (2007) 'Adult-generated neurons exhibit diverse developmental fates', *Developmental Neurobiology*, 67(8), pp. 1079–1093. doi: 10.1002/dneu.20389.
- Whitman, M. C. and Greer, C. A. (2007) 'Synaptic Integration of Adult-Generated Olfactory Bulb Granule Cells: Basal Axodendritic Centrifugal Input Precedes Apical Dendrodendritic Local Circuits', *Journal of Neuroscience*, 27(37), pp. 9951–9961. doi: 10.1523/JNEUROSCI.1633-07.2007.
- Whitman, M. C. and Greer, C. A. (2009) 'Adult neurogenesis and the olfactory system', *Progress in Neurobiology*, 89(2), pp. 162–175. doi: 10.1016/j.pneurobio.2009.07.003.
- Winner, B. *et al.* (2002) 'Long-term survival and cell death of newly generated neurons in the adult rat olfactory bulb', *European Journal of Neuroscience*, 16(9), pp. 1681–1689. doi: 10.1046/j.1460-9568.2002.02238.x.
- Woolf, T. B., Shepherd, G. M. and Greer, C. A. (1991) 'Serial reconstructions of granule cell spines in the mammalian olfactory bulb', *Synapse*, 7(3), pp. 181–192. doi: 10.1002/syn.890070303.
- Wu, Y. C. *et al.* (2011) 'Dendritic trafficking of brain-derived neurotrophic factor mRNA: Regulation by translin-dependent and -independent mechanisms', *Journal of Neurochemistry*, 116(6), pp. 1112–1121. doi: 10.1111/j.1471-4159.2010.07166.x.
- Wyatt, R. M., Tring, E. and Trachtenberg, J. T. (2012) 'Pattern and not magnitude of neural activity determines dendritic spine stability in awake mice', *Nature Neuroscience*. Nature Publishing Group, 15(7), pp. 949–951. doi: 10.1038/nn.3134.
- Xie, Y., Hayden, M. R. and Xu, B. (2010) 'BDNF Overexpression in the Forebrain Rescues Huntington's Disease Phenotypes in YAC128 Mice', *Journal of Neuroscience*, 30(44), pp. 14708–14718. doi: 10.1523/JNEUROSCI.1637-10.2010.

- Yamaguchi, M. and Mori, K. (2005) 'Critical period for sensory experience-dependent survival of newly generated granule cells in the adult mouse olfactory bulb.', *Proceedings of the National Academy of Sciences of the United States of America*, 102(27), pp. 9697–9702. doi: 10.1073/pnas.0406082102.
- Yokoi, M., Mori, K. and Nakanishi, S. (1995) 'Refinement of odor molecule tuning by dendrodendritic synaptic inhibition in the olfactory bulb.', *Proceedings of the National Academy of Sciences*, 92(8), pp. 3371–3375. doi: 10.1073/pnas.92.8.3371.
- Yoshihara, Y., De Roo, M. and Muller, D. (2009) 'Dendritic spine formation and stabilization', *Current Opinion in Neurobiology*, 19(2), pp. 146–153. doi: 10.1016/j.conb.2009.05.013.
- Young, K. M. *et al.* (2007) 'Subventricular Zone Stem Cells Are Heterogeneous with Respect to Their Embryonic Origins and Neurogenic Fates in the Adult Olfactory Bulb', *Journal of Neuroscience*, 27(31), pp. 8286–8296. doi: 10.1523/JNEUROSCI.0476-07.2007.
- Yuste, R. and Bonhoeffer, T. (2004) 'Genesis of dendritic spines: Insights from ultrastructural and imaging studies', *Nature Reviews Neuroscience*, 5(1), pp. 24–34. doi: 10.1038/nrn1300.
- Zagrebelsky, M. and Korte, M. (2014) 'Form follows function: BDNF and its involvement in sculpting the function and structure of synapses', *Neuropharmacology*. Elsevier Ltd, 76(PART C), pp. 628–638. doi: 10.1016/j.neuropharm.2013.05.029.
- Zheng, F. *et al.* (2011) 'Regulation of brain-derived neurotrophic factor exon IV transcription through calcium responsive elements in cortical neurons', *PLoS ONE*, 6(12). doi: 10.1371/journal.pone.0028441.
- Zheng, F. *et al.* (2012) 'Regulation of brain-derived neurotrophic factor expression in neurons', *Journal of neurochemistry*, 4(1), pp. 735–41. doi: 10.1016/j.nbd.2007.06.007.
- Zigova, T. *et al.* (1998) 'Intraventricular Administration of BDNF Increases the Number of Newly Generated Neurons in the Adult Olfactory Bulb', *Molecular and Cellular Neuroscience*, 245, pp. 234–245.
- Zou, D. J., Greer, C. A. and Firestein, S. (2002) 'Expression pattern of α CaMKII in the mouse main olfactory bulb', *Journal of Comparative Neurology*, 443(3), pp. 226–236. doi: 10.1002/cne.10125.